ISSN 2658-3518

LIMNOLOGY & FRESHWATER BIOLOGY

2019, № 1

> abiotic and biotic water components;
> ecosystem-level studies;
> systematics and aquatic ecology;
> paleolimnology and environmental histories;
> laboratory experiments and modeling

Original Article

ISSN 2658-3518
LIMNOLOGY FRESHWATER BIOLOGY
www.limnolfwbiol.com

Hidden diversity of micro-eukaryotes in Lake Baikal: a metagenomic approach

Mincheva E.V.[1]*, Peretolchina T.E.[1], Kravtsova L.S.[1], Tupikin A.E.[2], Pudovkina T.A.[1], Ananyeva I.A.[3], Triboy T.I.[1], Voylo M.A.[1], Bukin Yu.S.[1,3]

[1] *Limnological Institute, Siberian Branch of the Russian Academy of Sciences, Ulan-Batorskaya Str., 3, Irkutsk, 664033, Russia*
[2] *Institute of Chemical Biology and Fundamental Medicine, Siberian Branch of the Russian Academy of Sciences, Lavrentiev Ave., 8, Novosibirsk, 630090,Russia*
[3] *Irkutsk State University, Karl Marx Str., 1, Irkutsk, 664003, Russia*

ABSTRACT. We have studied the diversity and composition of communities of micro-eukaryotes from two localities: area under anthropogenic impact near the town of Baikalsk and reference area, Irinda Bay, based on high-throughput ITS2 rDNA region sequencing. High taxonomic diversity of micro-eukaryotes has been revealed in both localities studied. However, micro-eukaryotic community from the area under anthropogenic impact is depressed, compared to reference area. Analysis of taxonomic diversity has revealed that community from the area under anthropogenic impact has a trend towards a decrease in diversity. Among the detected taxa, Alveolata, Stramenopiles and Fungi prevailed. Sörensen index of OTUs was 65%, which indicates the similarity of communities studied by taxonomic composition. The spectrum of Alveolata and Stramenopiles taxa identified in the area under the anthropogenic impact and the reference area was similar. The main differences were revealed in spectrum of Fungi taxa.

Keywords: micro-eukaryotes, metagenome, ITS2 rDNA, algae, Lake Baikal

1. Introduction

Although micro-eukaryotes have been investigated since the 17th century, they still remain understudied, especially in freshwater ecosystems (Debroas et al., 2017). Protists, Stramenopiles, Chromista, Cryptophyta and Fungi comprise micro-eukaryotes. Knowledge about the diversity of the micro-eukaryotic community in freshwater reservoirs is essential for predicting the ecosystem functioning.

The taxonomically and functionally diverse micro-eukaryotes communities have remained vastly unexplored due to the complexity of their identification, peculiarities of the life cycle, the presence of cryptic species, etc.

Currently, the development of high-throughput sequencing has allowed for a more full assessment of taxonomic diversity of communities, including even their hardly detectable members (Mueller et al., 2011; Debroas et al., 2017). Thus, using high-throughput sequencing methods, a large variety of micro-eukaryotes was discovered in freshwater ecosystems (Kammerlander et al., 2015).

Different fragments of 18S rDNA and internal transcribed spacer ITS1 are the most used molecular genetic markers for metabarcoding studies of eukaryotic communities (Bokulich and Mills, 2013; Charvet et al., 2014; Kammerlander et al., 2015). However, recently it has been shown that ITS2 compared to ITS1 is more informative, especially, for a description of the taxonomic composition of fungal communities (Bazzicalupo et al., 2013; Banchi et al., 2018a; 2018b).

Recently, high-throughput sequencing of 18S rDNA was performed for analysis of micro-eukaryote diversity in Lake Baikal, and allowed to investigate the communities of the water column, bottom sediments, as well as green algae communities and their associated organisms (Yi et al., 2017; Mikhailov et al., 2019). These studies provided data on the presence of Fungi from various taxa: zygomycetes, glomeromycetes, chytridyomycetes, asco- and basidiomycetes, as well as allowed to describe the diversity of the SAR group (Stramenopiles, Alveolata, Rhizaria) in Lake Baikal.

During the past decade, researchers recorded the massive blooming of filamentous algae in Lake Baikal. In some parts of the lake, the changes in the dominant phytobenthos species were observed (Kravtsova et al., 2012). In this regard, the study of micro-eukaryotes would be useful to identify species that may play an important role in these processes.

*Corresponding author.
E-mail address: elenakuznetsova01@gmail.com (E.V. Mincheva)

The aim of this study was to explore the taxonomic diversity of aquatic fungi and protists from the reference area and the area under anthropogenic impact at Lake Baikal using ITS2 marker.

2. Material and methods

The samples were collected in summer, 2018 from two localities of Lake Baikal: reference area, Irinda Bay (54°50'N; 109°40'E; the temperature of water was 12 °C, water transparency by Secchi disc was 6 m), and area with strong anthropogenic impact, near Baikalsk town (51°30'N; 104°15'E; the temperature of water was 11 °C, water transparency by Secchi disc was 3 m). The samples were collected at three depths according to vertical zonality (Izhboldina, 2007) of green alga distribution: 0 – 2 m, 2 – 5 m and 6 – 10 m.

DNA was extracted from the algae, their substrate and filtered water (free from invertebrates) according to the modified protocol described by Doyle and Dickson (1987). For each locality, 60 DNA samples were extracted and mixed for subsequent PCR.

ITS2 rDNA was amplified in PCR using the primers: ITS3_KYO2 F: 5'-GAT GAA GAA CGY AGY RAA-3' (Asemaninejad et al., 2016) and ITS4 R: 5'-TCC TCC GCT TAT TGA TAT GC-3' (White et al., 1990).

PCR and Illumina MiSeq paired-end sequencing were performed in the SB RAS Genomics Core Facility (ICBFM SB RAS, Novosibirsk).

The UPARSE pipeline (Edgar, 2013) was used to cluster contigs of all samples. Contigs with 97% similarity were classified into one operational taxonomic unit (OTU).

The representativeness OTUs (number of sequences per OTU) of species rank were used to calculate Shannon indices of community biodiversity (Shannon, 1948). Underestimated α-diversity was evaluated using Chao1 (Chiu et al., 2014). Calculations were performed using the R packages «vegan» (Dixon, 2003).

3. Results and Discussion

After stitching, trimming and chimera removing, total dataset consisted of 89134 reads, where micro-eukaryotes were represented by 9966 reads (3778 reads for Irinda Bay (reference area) and 6188 reads for Baikalsk city (area under anthropogenic impact)). The average length of the reads was 340 bp.

Sequence dataset was clustered into 144 OTUs of species rang, 123 OTUs of them occurred in Irinda Bay and 90 OTUs were found in Baikalsk (Supplementary Table can be found online at https://github.com/barnsys/microeukaryoticcommunity), both communities shared 69 OTUs. The index Chao1 showed that the taxonomic diversity of communities observed and predicted differed by < 10% (Table 1). This means that the amount of input data was sufficient to fully characterize taxonomic diversity (species richness) in each of the two communities studied.

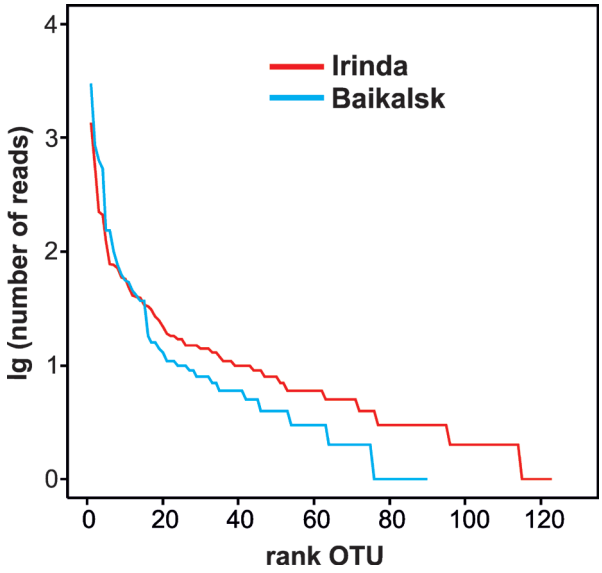

Fig. 1. Species abundance curves of the communities studied.

Previous studies of micro-eukaryotic communities in Lake Baikal were performed using 454-sequencing, which allowed produce from several hundreds to 30000 reads per sample in average (Mikhailov et al., 2019). The total amount of reads included not only micro-eukaryotes but also the dominant phytoplankton and metazoa OTUs. Due to a relatively small number of reads, the number of underestimated OTUs of species rank in these studies was 10% or more. In our study, the Illumina MiSeq technology allowed production of a greater number of reads, due to which we obtained reliable estimates of species richness even for rare components of communities.

Shannon's and Evenness diversity indices of micro-eukaryotes communities from Irinda Bay were higher than for those near Baikalsk town (Table 1). The species abundance curve for the communities near Baikalsk town is significantly sharper than that of the Irinda Bay community. The analysis has indicated that micro-eukaryotic community from the area under anthropogenic impact near Baikalsk town is depressed compared to the reference area, Irinda Bay (Fig. 1).

Table 1. The diversity indices estimated for the communities studied

Sampling locations	Number of species	Chao1 index	Shannon index	Evenness
Irinda	123	124	2.88	0.59
Baikalsk	90	98	2.04	0.45

Sörensen similarity index of OTUs detected in the studied communities was 65%. In both micro-eukaryotic communities studied, Alveolata was the most numerous group (83–97%) (Fig. 2A). The diversity of Alveolata taxa from both localities was approximately equal, but their abundance was different (Fig. 2A). Among Alveolata, the representatives of Oligohymenophorea, in particular, Ciliata (*Vorticella*, *Pseudovorticella*), were the most abundant. Stramenopiles comprised 20% and 9% in communities from Irinda Bay and Baikalsk town, respectively (Fig. 2B). Stramenopiles from both communities were mostly presented by diatom alga Bacillariophyceae (*Gomphonema* sp., *Didymosphenia geminata*, *Amphiprora* sp., *Fragilariopsis* sp.) and were more abundant in the community from the reference area of Irinda Bay (Fig. 2D). *D. geminata* was more representative in the reference area, whereas *Gomphonema* sp. was more abundant in the area with anthropogenic impact. Representatives of both genera are typical for the stony littoral zone of open Lake Baikal. Alveolata and Stramenopiles are key components of aquatic food webs both as a food source (e.g. diatoms) and as major consumers of bacterial biomass (e.g. ciliates) (Šlapeta et al., 2005).

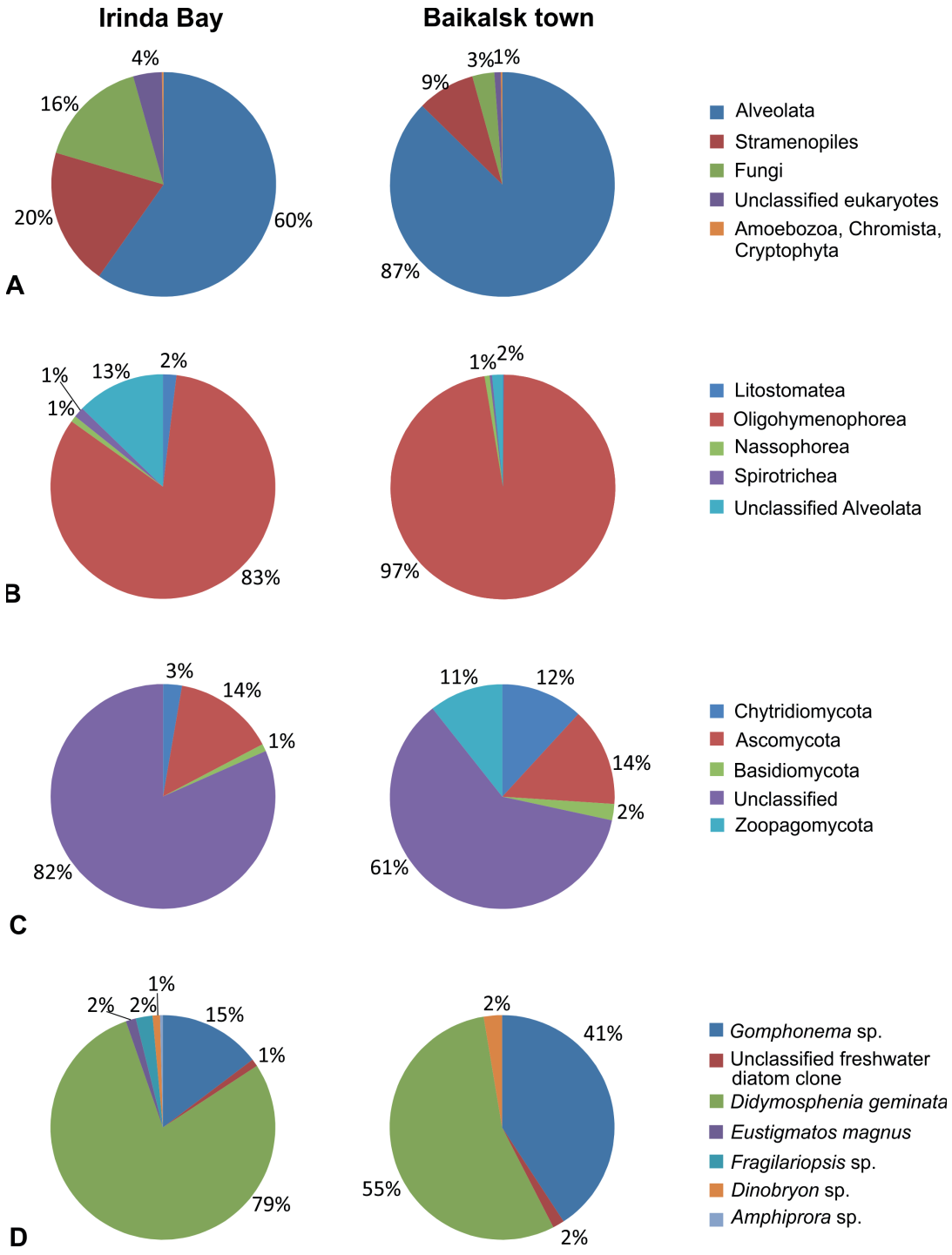

Fig. 2. Community structure of micro-eukaryotes from two localities of Lake Baikal. A – total micro-eukaryotic diversity from Irinda Bay and Baikalsk town; B – diversity of Alveolata from Irinda Bay and Baikalsk town; C – diversity of Fungi from Irinda Bay and Baikalsk town; D – diversity of Stramenopiles from Irinda Bay and Baikalsk town.

Fungi comprised 3–16% of the communities studied (Fig. 2A). Fungi contribute significantly to the organic matter decomposition and food web; they affect water quality and taxonomic composition of communities (Zhang et al., 2015; 2018). Fungi from Irinda Bay were more abundant. The bulk of the sequences obtained belonged to unclassified freshwater fungi, probably, due to a small number of ITS2 sequences for identified species of Fungi available through GenBank. The composition of communities from two localities was different. Among Ascomycota, saprotrophs or alga parasites, *Alternaria* sp. and *Cladosporium flocossum* were more abundant in the reference area. Representatives of phylum Zoopagomycota, which in general are parasites of micro-metazoan, were observed only in Baikalsk (Fig. 2C). Members of the Chytridiomycota are known to be widespread in freshwater ecosystems, where they act as parasites and decomposers (Johnson et al., 2006; Kagami et al., 2012). Chytridiomycota were more abundant in the area under anthropogenic impact and were mostly represented by *Rhizophidium*, members of which are phytopathogens and alga parasites (Letcher et al., 2004).

Conclusions

Taxonomic diversity of micro-eukaryotes in the reference area of Irinda Bay was higher than that in the area under anthropogenic impact. Taxonomic composition of Alveolata and Stramenopiles from the communities studied was similar, and the main differences were related with the abundance of their taxa. Communities from different areas mostly differed in taxonomic composition of Fungi. The community from the reference area lacked representatives of Zoopagomycota, whereas they are abundant in the region under anthropogenic impact. In addition, in the latter locality Chytridiomycota were mostly represented by *Rhizophidium*, members of which are phytopathogens and alga parasites. Representatives of this genus may be recommended as markers for monitoring of the stability of freshwater alga community.

Acknowledgements

We thank I.V. Khanaev and V.I. Chernykh for their assistance in sampling.

This study was supported by project No. 0345–2016–0004 (AAAA-A16-116122110060-9) funded by the Government, and by project No. 17-44-388071r_a funded by RFBR and the Government of the Irkutsk Region.

References

Asemaninejad A., Weerasuriya N., Gloor G.B. et al. 2016. New primers for discovering fungal diversity using nuclear large ribosomal DNA. PloS one 11. DOI: 10.1371/journal.pone.0159043

Banchi E., Ametrano C.G., Stanković D. et al. 2018a. DNA metabarcoding uncovers fungal diversity of mixed airborne samples in Italy. PloS one 13. DOI: 10.1371/journal.pone.0194489

Banchi E., Stankovic D., Fernández-Mendoza F. et al. 2018b. ITS2 metabarcoding analysis complements lichen mycobiome diversity data. Mycological Progress 17: 1049–1066. DOI: 10.1007/s11557-018-1415-4

Bazzicalupo A.L., Bálint M., Schmitt I. 2013. Comparison of ITS1 and ITS2 rDNA in 454 sequencing of hyperdiverse fungal communities. Fungal Ecology 6: 102–109. DOI: 10.1016/j.funeco.2012.09.00

Bokulich N.A., Mills D.A. 2013. Improved selection of internal transcribed spacer-specific primers enables quantitative, ultra-high-throughput profiling of fungal communities. Applied and Environmental Microbiology 79: 2519–2526. DOI: 10.1128/AEM.03870-12

Charvet S., Vincent W.F., Lovejoy C. 2014. Effects of light and prey availability on Arctic freshwater protist communities examined by high-throughput DNA and RNA sequencing. FEMS Microbiology Ecology 88: 550–564. DOI: 10.1111/1574-6941.12324

Chiu C.H., Wang Y.T., Walther B.A. et al. 2014. An improved nonparametric lower bound of species richness via a modified good–turing frequency formula. Biometrics 70: 671–682. DOI: 10.1111/biom.12200

Debroas D., Domaizon I., Humbert J.F. et al. 2017. Overview of freshwater microbial eukaryotes diversity: a first analysis of publicly available metabarcoding data. FEMS Microbiology Ecology 93: 1–14. DOI: 10.1093/femsec/fix023

Dixon P. 2003. VEGAN, a package of R functions for community ecology. Journal of Vegetation Science 14: 927–930. DOI: 10.1111/j.1654-1103.2003.tb02228.x

Doyle J.J., Dickson E.E. 1987. Preservation of plant samples for DNA restriction endonuclease analysis. Taxon 36: 715–722. DOI: 10.2307/1221122

Edgar R.C. 2013. UPARSE: highly accurate OTU sequences from microbial amplicon reads. Nature Methods 10: 996. DOI: 10.1038/nmeth.2604

Izhboldina L.A. 2007. Guide and key to benthonic and periphyton algae of Lake Baikal (meio – and macrophytes) with short information about their ecology. Novosibirsk: Nauka-Center. (in Russian)

Johnson P.T., Longcore J.E., Stanton D.E. et al. 2006. Chytrid infections of *Daphnia pulicaria*: development, ecology, pathology and phylogeny of *Polycaryum laeve*. Freshwater Biology51:634–648.DOI:10.1111/j.1365-2427.2006.01517.x

Kagami M., Amano Y., Ishii N. 2012. Community structure of planktonic fungi and the impact of parasitic chytrids on phytoplankton in Lake Inba, Japan. Microbial Ecology 63: 358–368. DOI: 10.1007/s00248-011-9913-9

Kammerlander B., Breiner H.W., Filker S. et al. 2015. High diversity of protistan plankton communities in remote high mountain lakes in the European Alps and the Himalayan mountains. FEMS Microbiology Ecology 91. DOI: 10.1093/femsec/fiv010

Kravtsova L.S., Izhboldina L.A., Khanaev I.V. et al. 2012. Disturbances of the vertical zoning of green algae in the coastal part of the Listvennichnyi gulf of Lake Baikal. Doklady Biological Sciences 447: 350–352. DOI: 10.1134/S0012496612060026

Letcher P.M., Powell M.J., Chambers J.G. et al. 2004. Phylogenetic relationships among Rhizophydium isolates from North America and Australia. Mycologia 96: 1339–1351. DOI: 10.1080/15572536.2005.11832883

Mikhailov I.S., Zakharova Y.R., Bukin Y.S. et al. 2019. Co-occurrence networks among bacteria and microbial eukaryotes of Lake Baikal during a spring phytoplankton bloom. Microbial Ecology 77: 96–109. DOI: 10.1007/s00248-018-1212-2

Mueller G.M., Foster M.S., Bills G.F. 2011. Biodiversity of fungi: inventory and monitoring methods. New York: Academic.

Shannon C.E. 1948. A mathematical theory of communication. Bell Labs Technical Journal 27: 379–423. DOI: 10.1002/j.1538-7305.1948.tb01338.x

Šlapeta J., Moreira D., López-García P. 2005. The extent of protist diversity: insights from molecular ecology of freshwater eukaryotes. Proceedings of the Royal Society B: Biological Sciences 272: 2073–2081. DOI: 10.1098/rspb.2005.3195

White T.J., Bruns T.D., Lee S.B. et al. 1990. Amplification and direct sequencing of fungal ribosomal RNA genes for phylogenetics. In: Innis M.A., Gelfand D.H., Sninsky J.J. et al. (Eds.), PCR protocols: a guide to methods and applications. New York, pp. 315–322.

Yi Z., Berney C., Hartikainen H. et al. 2017. High-throughput sequencing of microbial eukaryotes in Lake Baikal reveals ecologically differentiated communities and novel evolutionary radiations. FEMS Microbiology Ecology 93. DOI: 10.1093/femsec/fix073

Zhang H., Huang T., Chen S. 2015. Ignored sediment fungal populations in water supply reservoirs are revealed by quantitative PCR and 454 pyrosequencing. BMC Microbiology 15: 44. DOI: 10.1186/s12866-015-0379-7

Zhang H., Jia J., Chen S. et al. 2018. Dynamics of bacterial and fungal communities during the outbreak and decline of an algal bloom in a drinking water reservoir. International Journal of Environmental Research and Public Health 15: 361. DOI: 10.3390/ijerph15020361

Limnology and Freshwater Biology 2019 (1): 155-162 DOI:10.31951/2658-3518-2019-A-1-155

Original Article

ISSN 2658-3518
LIMNOLOGY FRESHWATER BIOLOGY
www.limnolfwbiol.com

Metagenomic analysis of viral communities in diseased Baikal sponge *Lubomirskia baikalensis*

Butina T.V.[1,*], Bukin Yu.S.[1,2], Khanaev I.V.[1], Kravtsova L.S.[1], Maikova O.O.[1], Tupikin A.E.[3], Kabilov M.R.[3], Belikov S.I.[1]

[1] *Limnological Institute, Siberian Branch of the Russian Academy of Sciences, Ulan-Batorskaya Str., 3, Irkutsk, 664033, Russia*
[2] *Irkutsk National Research Technical University, Lermontov Str., 83, Irkutsk, 664074, Russia*
[3] *Institute of Chemical Biology and Fundamental Medicine, Siberian Branch of the Russian Academy of Sciences, Lavrentiev Ave., 8, Novosibirsk, 630090, Russia*

ABSTRACT. Sponges are an ecologically important component of marine and freshwater bodies. Sponge community includes a variety of microorganisms: fungi, algae, archaea, bacteria and viruses. Despite active research in the field of aquatic virology, biodiversity and the role of viruses in sponges are poorly studied. The relevance of research in this area is also related to the worldwide problem of sponge diseases. The aim of this study was to elucidate the genetic diversity of viruses in the associated community of diseased endemic Baikal sponge *Lubomirskia baikalensis* using metagenomic analysis. As a result, we have shown for the first time a high genetic and taxonomic diversity of DNA viruses in the Baikal sponge community. Identified sequences belonged to 16 viral families that infect a wide range of organisms. Moreover, our analysis indicated the differences in viral communities of visually healthy and diseased branches of the sponge. The approach used in this study is promising for further studies of viral communities in sponges, obtaining more complete information about the taxonomic and functional diversity of viruses in holobionts and entire Lake Baikal, and identifying the role of viruses in sponge diseases.

Keywords: metagenomic analysis, virome, viral diversity, viral communities, sponges, Lake Baikal

1. Introduction

Viruses are the most ubiquitous, abundant and diverse biological objects on Earth. They are of particular importance in the water environments, where their concentration reaches 10^{11} particles/ml (Wilhelm and Matteson, 2008). They regulate the abundance, composition and biodiversity of numerous aquatic microorganisms and other hydrobionts, participate in biochemical processes and, in general, influence significantly on the functioning and ecological state of water bodies (Wommack and Colwell, 2000; Suttle, 2007; Jacquet et al., 2015). Despite the considerable advances in the field of aquatic virology in recent decades, we lack knowledge about viruses of marine and, especially, freshwater invertebrates including symbiotic organisms, or it is incomplete.

Sponges are the oldest multicellular invertebrates (phylum Porifera) that represent complex symbioses in marine and freshwater ecosystems and have unusual properties: high diversity, abundance and biomass; contribution to primary production and nitrification though symbioses; high chemical and physical adaptation; competitiveness; biomineralization; production of the secondary metabolites, etc. (Diaz and Ruetzler, 2001; Bell, 2008). The sponge community includes various microorganisms: fungi, dinoflagellates, small algae, archaea, bacteria, and viruses. The abundance and diversity of viruses can be very significant, considering a great number of their potential hosts in the sponge community. However, the diversity and importance of viruses have been little studied compared to other sponge-associated microorganisms, and the role of viruses in the sponges remains largely unknown. Previously, virus-like particles (VLPs) morphologically similar to adenoviruses, picornaviruses and mimiviruses were rarely found in some sponges (Vacelet and Gallissian, 1978; Johnson, 1984; Claverie et al., 2009). Recently, the first comprehensive morphological assessment of sponge-associated viruses by transmission electron microscopy has revealed diverse communities of viral-like particles in the different marine sponge species (Pascelli et al, 2018). Moreover, the first metaviromic studies provided new molecular data on the composition, function of viruses inhabiting reef sponges, and showed a high diversity of sponge viral communities (Laffy et al., 2016; 2018).

*Corresponding author.
E-mail address: tvbutina@mail.ru (T.V. Butina)

As natural filter feeders, sponges play a great role in the existence of any water body, which is especially relevant for Lake Baikal as a unique natural object characterized by a huge freshwater supply, ancient origin, a rich diversity of endemic flora and fauna, etc. (Kozhova and Izmesteva, 1998). According to the current taxonomy, two families represent the Baikal sponges: endemic Lubomirskiidae (includes 4 genera and 14 species) and cosmopolitan Spongillidae (3 genera and 5 species) (Efremova, 2001; 2004; Itskovich et al., 2017). Endemic species inhabit almost all depths of the lake (from 1 m to maximum depths), but the bulk of their abundance and species diversity is concentrated at depths of 5-30 m (Khanaev et al., 2018), where their biomass mostly exceeds the biomass of all zoobenthic groups (Kozhov, 1970). The most mass species *Lubomirskia baikalensis* is the only branching sponge in Lake Baikal, which colonies reach up to 1.5 m in height.

The first investigations of viruses associated with the Baikal sponges *Lubomirskia baikalensis* were based on the analysis of marker genes. We identified a high diversity of *g20* gene of cyanophages (Butina et al., 2015) and *g23* genes of T4-like bacteriophages (Butina T.V., unpublished data) in the community of *L. baikalensis*. The analysis revealed specific groups of cyanophages different from those inhabiting the lake water, which is natural and corresponds to the hologenome concept. Holobiont is a united complex of the host organism (sponge, coral, etc.) and associated microorganisms (Rohwer et al., 2002). The genetic material of holobiont (hologenome) changes faster than the genome of the host organism, which increases the potential and adaptability of the complex organism in unfavourable and changing conditions (Rosenberg et al., 2007). Sponges are one of the most diverse and complex aquatic holobionts (Webster and Thomas, 2016; Pita et al., 2018).

Over the past decades, Lake Baikal has experienced an increasing anthropogenic load. Global climate change (Shimaraev and Domysheva, 2013) and anthropogenic impact on the Baikal ecosystem in recent years have contributed to the obvious changes in the structure of benthic communities from the coastal zone: abundant growth of filamentous algae, especially in places with high anthropogenic load; the mass development of cosmopolitan small-cell algae that are untypical for the lake and inhabit eutrophic water bodies; and, at the same time, a decrease in the number of endemic phytoplankton species (Kravtsova et al., 2012; 2014; Timoshkin et al., 2016; Bondarenko and Logacheva, 2017). In addition, since 2011 there has been a mass disease and mortality of sponges (Bormotov, 2012). Several types of disease in the Baikal sponges were described, all of which are characteristic of *Lubomirskia baikalensis*: bleaching, necrosis, violet cyanobacterial biofilm, and brown spots (Timoshkin et al., 2016; Khanaev et al., 2018). Notably, sponge disease is a well-known worldwide problem, and since 1983 the sponge disease outbreaks have been reported in a wide range of geographic locations, however, no diseases have been reported in freshwater sponge populations before (Webster, 2007). The understanding of the origin and causative agents of sponge disease is still insufficient. Some works indicated potential bacterial pathogens in sponges, however, most studies showed only shift in the microbial community of diseased sponges (dysbiosis) in comparison with healthy individuals (Webster, 2007; Belikov et al., 2018). To our knowledge, no viral putative pathogens have been found in diseased sponges.

The aim of this work was the study of the genetic diversity of DNA viruses in the associated community of the endemic Baikal sponge *Lubomirskia baikalensis* with signs of disease using metagenomic analysis. Viruses do not have universal genes, like the ribosomal genes of pro- and eukaryotes; therefore, the metagenomic analysis is still the most informative way to study the diversity of viral communities in natural samples. As far as we know, metagenomic studies of viruses in freshwater sponges have not been carried out previously.

2. Materials and methods

Sampling, obtaining the viral fraction and DNA extraction

The *Lubomirskia baikalensis* sponges were sampled using lightweight diving equipment in March 2015 in the Maloye More Strait of Lake Baikal, near the Malye Olkhonskiye Vorota Strait. Two branches of 2-3 cm^3 in volume were collected from the same sponge. One branch looked healthy (sample Sv3h), and another had lesions in the form of brown spots (sample Sv3d) (Fig. 1). The sponge samples were washed twice in sterile water, frozen and transported to the laboratory. To obtain the fraction of virus-like particles, the samples were homogenized and centrifuged (3000 rpm, 30 min); the aqueous fraction was passed through a syringe filter with a pore size of 0.2 μm (Sartorius). Then, the samples were treated with DNase I and RNase A enzymes (Thermo Fisher Scientific) to remove contaminating nucleic acids. Viral DNA was extracted by the method with proteinase K, SDS and phenol-chloroform extraction (Sambrook et al., 1989).

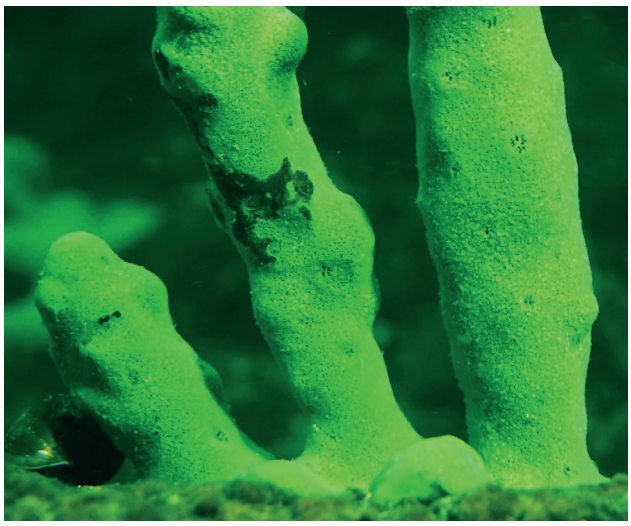

Fig. 1. Diseased sponge *L. baikalensis* with brown spots lesions

Library preparation and sequencing

The total viral DNA was sheared in a microTUBE AFA Fiber Snap-cap using a Covaris S2 instrument (Covaris) with a medium size distribution of fragments of about 500 bp. The paired-end libraries were prepared using a NEBNext Ultra DNA library prep kit for Illumina (NEB). Sequencing of the virome was conducted on a MiSeq genome sequencer (2x300cycles, Illumina) in SB RAS Genomics Core Facility (ICBFM SB RAS, Novosibirsk, Russia).

Analysis of virome datasets

The primary processing of the received data (paired reads of 2x300 bp) was performed using the R package "ShortReads" (Morgan et al., 2009). The sequences of less than 100 nucleotides were excluded before the next analysis.

Taxonomic identification of viral sequences was performed using the BLASTn algorithm (Altschul et al., 1990) against NCBI RefSeq complete viral genomes database (September 2018 release) (Pruitt et al., 2005). The BLASTn parameters used were as follows: cost to open a gap, two; cost to extend a gap, one; word size for word finder algorithm, twelve; penalty for a nucleotide mismatch, one; reward for a nucleotide match, one. The sequence reads were considered 'identified' if it had a relative in the reference database with an e-value of $< 10^{-5}$ and bit score ≥ 50. The results of BLASTn analysis were saved as a hit table. BLAST hits corresponding to the same viral genome subject ID were considered to belong to one virotype. Each subject ID from the BLASTn hit table was converted to a taxonomic annotation of the virus for a tabulated representation of the various virotypes in the sample. For further analysis, data on the representativeness of virotypes (number of reads per virotype in a sample) were normalized to the average number of reads per sample.

Rarefaction analysis was performed to assess the species richness in the samples (Heck et al., 1975). The representativeness of virotypes was used to calculate Shannon and Simpson indices of community biodiversity (Hill, 1973). Comparison of samples was carried out by cluster UPGMA method using the Bray-Curtis (Faith et al., 1987) and the Gower distances (Gower and Legendre, 1986). The clustering accuracy was estimated using the bootstrap method (1000 replicas). Before clustering, the representativeness of virotypes in samples was transformed into relative values (number of reads per virotype in a sample divided by total viral reads). The reliability of the difference between the distributions of virotypes representativeness in the compared communities was estimated using the chi square test. Statistical calculations were performed using the R packages "vegan" (Dixon, 2003) and "pvclust" (Suzuki and Shimodaira, 2006).

For a comparative analysis, other metaviromic datasets were used in this study: from the marine sponge *Rhopaloeides odorabile* (Great Barrier Reef (GBR), Davis Reef, sampled in January 2014; Laffy et al., 2016), from corals *Acropora millepora* (GBR, Orpheus Island Reef, sampled in March 2013) and *Pocillopora damicornis* (GBR, Trunk Reef, November 2012; Weynberg et al., 2014). The reference data sets were also processed and analyzed according to the procedure described above.

3. Results

Identification of viral sequences in sponge viromes

After processing and filtering of raw paired reads, 310 080 high-quality sequences remained for the sample Sv3h and 327 901 – for the sample Sv3d. The total number of sequences similar to the genomes of viruses in the RefSeq database for the samples of the sponge *Lubomirskia baikalensis* Sv3h and Sv3d was 6903 and 13432, respectively. This averaged to 2.23% and 4.1% of the total data sets, which is comparable with the analysis of reference metagenomic data sets (2.79%, 3.35% and 4.18% for samples of *P. damicornis*, *R. odorabile* and *A. millepora*, respectively).

The majority of the sequences in virome datasets from *L. baikalensis* were similar to double-stranded DNA (dsDNA) viruses, which is attributed to the method for preparing libraries for the MiSeq platform (Illumina), in which dsDNA has a significant advantage at the amplification stage (Kim and Bae, 2011). Thus, the proportion of single-stranded DNA (ssDNA) viruses did not exceed 0.8%. We also detected a small number of RNA viruses (0.16% and 0.54% in the Sv3h and Sv3d samples, respectively), among which there were not only reverse-transcribing viruses of the *Retroviridae* but also those from other families. We cannot explain the presence of reads similar to viral RNA, since we constructed and sequenced the libraries of total viral DNA. Further, we did not consider the sequences similar to RNA viruses.

Taxonomic diversity of viral communities

In this study, we have identified 259 and 293 virotypes in samples from the Baikal sponge *Lubomirskia baikalensis* (for the samples Sv3h and Sv3d, respectively), which belong to sixteen viral families (Fig. 2). The families *Siphoviridae*, *Myoviridae*, *Podoviridae*, *Phycodnaviridae*, *Poxviridae*, and *Mimiviridae* were the most numerous (represented by more than 1% of the sequences and accounted for approximately 97% of virome reads). The significant parts of viromes (19.1% and 15.1% in the samples Sv3h and Sv3d, respectively) were unclassified to the family rank viruses (Fig. 2).

Bacteriophages (the families *Siphoviridae, Myoviridae* and *Podoviridae*) had the largest proportion in viromes of *L. baikalensis*, which was expectable considering the large abundance of bacteria in the sponge holobionts (up to 35% of the total sponge biomass at densities exceeding 10^9 microbial cells per cubic centimetre of sponge tissue) (Hentschel et al., 2012). In the list of potential hosts for detected bacteriophages, the representatives of the phyla *Proteobacteria* prevailed (data not shown). As known, the members of the phyla *Proteobacteria* (especially, of the classes *Alpha-*, *Gamma-* and *Deltaproteobacteria*) are well-represented in the highly diverse sponge microbial

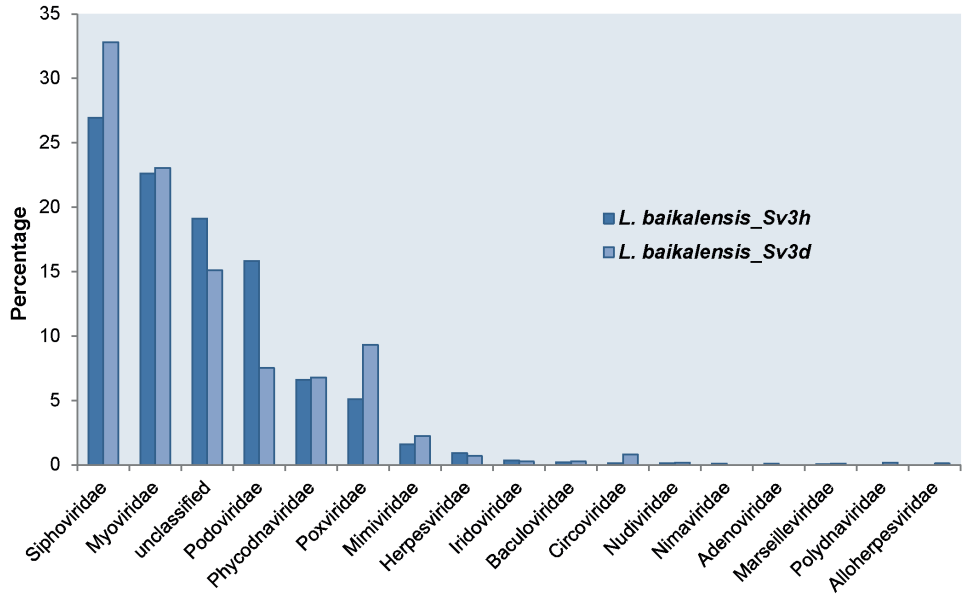

Fig. 2. Percentage of different viral families in viromes of *Lubomirskia baikalensis*

communities (Hentschel et al., 2012). In our study, the *Alphaproteobacteria virus phiJl001*, which infects a novel marine bacterium isolated from the marine sponge *Ircinia strobilina* (Lohr et al., 2005), has been detected among the identified virotypes. In addition, a great number of sequences were unexpectedly related to unclassified *Idiomarinaceae phage 1N2-2*. The *Idiomarinaceae* is a family within the order *Alteromonadales* of the class *Gammaproteobacteria*. Members of this family have been isolated from saline habitats, such as coastal and oceanic waters, solar salterns, submarine hydrothermal fluids and inland hypersaline wetlands (Albuquerque and da Costa, 2014). The *Synechococcus phage S-CBP4* and *Prochlorococcus phage P-SSM2* (*Podoviridae* and *Myoviridae* families, respectively) were also ones of the dominant (more than 1% of reads) putative bacteriophages in the Baikal sponge viromes.

Among the most abundant virotypes, there were also some eukaryotic viruses: viruses of microalgae *Chrysochromulina ericina virus* and *Emiliania huxleyi virus 86* (the family *Phycodnaviridae*), the viruses of protozoa *Yellowstone lake mimivirus*, *Megavirus chiliensis* (*Mimiviridae/Megaviridae*) and *Cedratvirus A11* (unclassified, putative *Pithoviridae* family), as well as *BeAn 58058 virus (Poxviridae)*, and *Yellowstone Lake virophage 5* (unclassified).

A comparative analysis of the diseased and the visually healthy sponge branches of *L. baikalensis* revealed that the composition of the most numerous families in two samples of the sponge was the same, but their percentage differed (Fig. 2). For example, the families *Siphoviridae*, *Myoviridae*, *Phycodnaviridae*, *Poxviridae*, and *Mimiviridae* were more abundant in the sample from the diseased branch of the sponge, and the families *Podoviridae*, *Iridoviridae* and *Herpesviridae* prevailed in the healthy one. Representatives of the families *Nimaviridae* and *Adenoviridae* were found only in the sample Sv3h, while *Polydnaviridae* and *Alloherpesviridae* were found only in Sv3d, but the number of reads for these families was low (less than 22). In general, the viromes of the visually healthy and diseased branches of *L. baikalensis* were significantly different (P value < 0.01).

It should be noted that the number of reads was insufficient to estimate the total viral diversity in the samples of *L. baikalensis*, since the rarefaction curves in our analysis did not reach the plateau (data not shown). Thus, we estimated mainly only dominant sponge-associated viruses. In the future, it is necessary to carry out a deeper sequencing of virome libraries from the existing and/or new samples of the Baikal sponges.

Comparative analysis of sponge and coral viromes

Figure 3 shows the proportions of viral families and unclassified at the rank of family viruses in the metagenomes of the Baikal sponge, marine sponge and corals. Tailed bacteriophages of the order Caudovirales (*Myoviridae*, *Siphoviridae* and *Podoviridae* families) dominated all datasets, but the distribution of these taxa differed between holobionts. Viral metagenome of *Rhopaloeides odorabile* was obvious for a greater number of the *Myoviridae* and vice versa – for a less number of the *Siphoviridae* in comparison with other metagenomes. The *Podoviridae* were the most numerous in the health branch of *Lubomirskia baikalensis (*Sv3h), as well as in corals *Acropora millepora* and *Pocillopora damicornis*. The families *Phycodnaviridae, Poxviridae, Mimiviridae*, and *Herpesviridae* also dominated all datasets, comprising 95-98% of reads together with tailed bacteriophages and unclassified viruses. The viromes of sponges differed from corals by a greater number of *Phycodnaviridae* and *Mimiviridae*. Unclassified viruses prevailed in *L. baikalensis* (Sv3h) and in *A. millepora*. The *Herpesviridae* were the most abundant in the sponge *R. odorabile*. The ssDNA viruses of the family *Microviridae* lacked in *L. baikalensis* while in the coral *P. damicornis* they accounted for 2.8%. Variation between holobionts was also observed in composition and percentage of less numerous families (Fig. 3). The highest number of families (thirty) was detected in the marine sponge *R. odorabile*, which is most likely due to

the largest number of reads.

UPGMA cluster analysis (considering the dominant virotypes, accounted for 95% of data sets) revealed two reliable clusters both, by using the Bray-Curtis and the Gower distances. One cluster consisted of viral metagenomes from Baikal sponge, and other – from the marine sponge and corals (Fig. 4).

4. Discussion and conclusions

In this study, we investigated viral communities of diseased sponge *L. baikalensis* through metagenomics. Despite the small number of reads, diversity indices of viruses in the *L. baikalensis* sponge were comparable to those in marine holobionts (Table 1), where the number of reads was much higher. Thus, we were able to identify a high diversity of viruses in samples of the Baikal sponge, and our analysis indicates the appropriateness of the chosen protocols for the isolation of VLPs and preparation of sponge viral DNA libraries for further studies of viral communities in the Baikal sponges.

Three bacteriophage families of the order *Caudovirales*: *Siphoviridae*, *Myoviridae* and *Podoviridae* mostly represented the *L. baikalensis* virome. This was expectable considering the high abundance and diversity of their bacterial hosts in associated communities. These viruses normally predominate in viromes of the aquatic biomes. Metagenomic studies of marine sponges also indicated the dominance of tailed bacteriophages (Laffy et al., 2016; 2018). The families *Phycodnaviridae*, *Mimiviridae* and *Poxviridae* were also numerous. Members of *Phycodnaviridae* infect microalgae; *Mimiviridae* are the largest viruses that infect amoeba and other protozoa. The dominance of viruses of these families in the sponge hologenome is also expectable considering the presence of their hosts in the communities of the Baikal sponges. At the same time, Claverie et al. (2009) show circumstantial

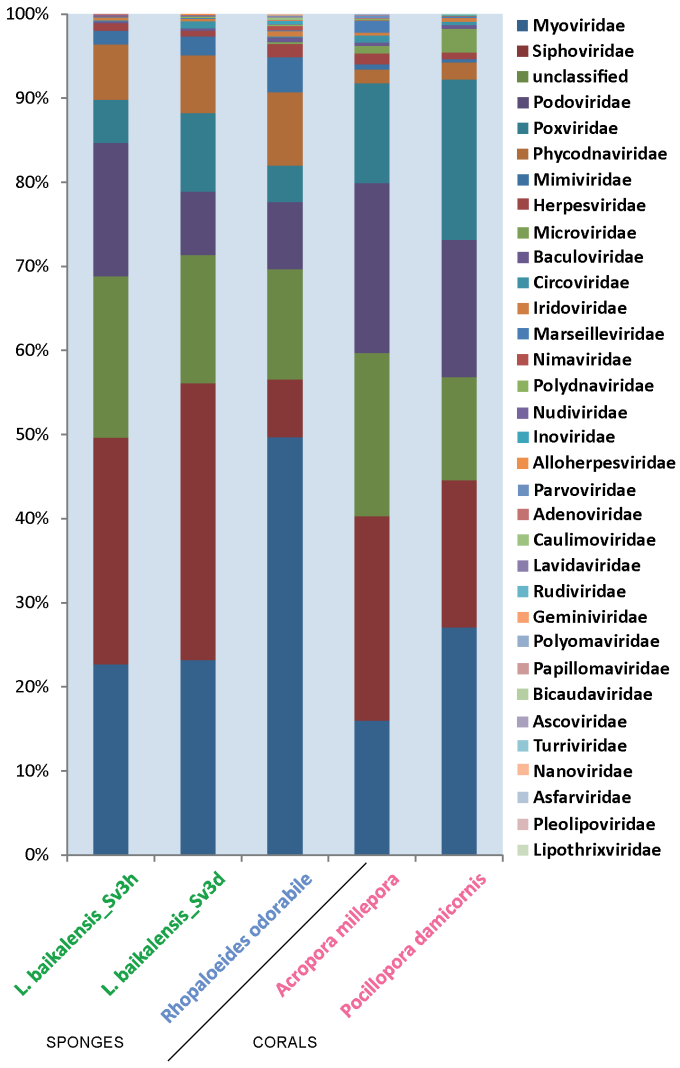

Fig. 3. The proportions of viral families and unclassified viruses in metaviromes of sponges and corals

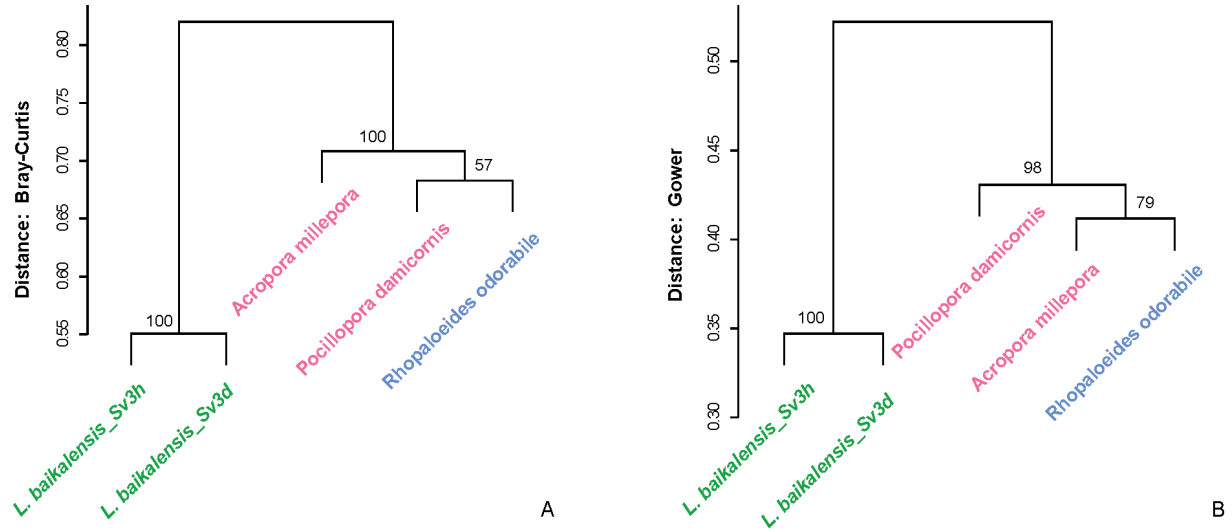

Fig. 4. UPGMA cluster analysis estimating the differences in diversity and composition of viromes performed using the Bray-Curtis (A) and the Gower (B) distances. The samples from the Baikal sponge are marked in green, and those from marine sponge and corals – in blue and pink, respectively

Table 1. Diversity indexes for the samples from sponges *L. baikalensis* and reference viromes

Samples	Alpha diversity	Shannon index	Simpson index
L. baikalensis_Sv3h	259	4,699	0,981
L. baikalensis_Sv3d	293	4,348	0,965
R. odorabile	697	4,378	0,955
A. millepora	520	4,588	0,973
P. damicornis	813	5,028	0,959

evidence of the possible mimivirus infection of some marine sponges (and corals).

It is worth noting that many viral families have a wide range of taxonomically distant hosts, and the list of species for the known viral families is constantly increasing. For example, known representatives of the heavily investigated family *Poxviridae* infect the widest host range among vertebrate and invertebrate taxa (Haller et al., 2014; Oliveira et al., 2017). Recently, new Salmon gill poxvirus (SGPV) has been found in the marine inhabitants (Gjessing et al., 2015). Like in our study, the sequences affiliated to *Poxviridae* were also detected in marine sponges *Amphimedon queenslandica* and *Ianthella basta* (Laffy et al., 2018). Therefore, it is most likely that the sequences of the sponge viromes similar to the known poxviruses of the terrestrial animals as well as other viruses of eukaryotes actually belong to unknown viruses that infect the aquatic invertebrates.

Despite the diversity of aquatic invertebrates, our knowledge of viral pathogens of this animal group including sponges is limited. Virus-like particles have been often identified without isolation of viruses and study of their pathogenesis in different species of invertebrates (Johnson, 1984; Munn, 2006). To date, several tens of aquatic invertebrates (mainly mollusks and crustaceans) viruses are known, and they are tentatively or more accurately assigned to the different families, including those found in the *L. baikalensis* sponge and other viromes: *Herpesviridae*, *Baculoviridae*, *Iridoviridae*, *Adenoviridae*, *Nimaviridae*, and *Coronaviridae*. In fact, previous studies have shown that herpes-like viruses are commonly observed in cnidarian viromes (Vega Thurber et al., 2008). It is suggested that herpes-like viruses infect all corals. Moreover, the sequences similar to *Herpesviridae* dominated samples of healthy corals but were less abundant in stressed or diseased coral tissues (Vega Thurber et al., 2008; Soffer et al., 2014). Thus, herpes-like viruses, as well as the abovementioned viruses of other families, may be a part of stable health sponge holobionts. The sponges provide food and habitat for many small invertebrates (mollusks, polychaetes, crustaceans and others) (Wulff, 2006), and those viruses could also be present in sponge viromes.

The diversity of a number of viral families belonging to the Nucleo-cytoplasmic large DNA viruses (NCLDVs) group was found in the sponge *L. baikalensis* and reference viromes, as well as in other studies of marine sponges (Laffy et al., 2016; 2018). NCLDVs is a monophyletic group of eukaryotic viruses with a large double-stranded DNA genome ranging from 100 kb to 1.26 Mb (Yutin and Koonin, 2012). This group consists of seven families, five of which were found in the viromes *L. baikalensis*: *Iridoviridae*, *Marseilleviridae*, *Mimiviridae*, *Phycodnaviridae*, and *Poxviridae*. NCLDVs are known to have important roles in marine ecosystems (Hingamp et al., 2013) and most likely no less significant in sponges and other holobionts (Vega Thurber et al., 2008). Sequences similar to NCLDVs, including members of the *Phycodnaviridae*, *Poxviridae* and *Mimiviridae* were relatively more abundant in bleached coral tissues than in non-bleached ones (Soffer et al., 2014).

Mass disease of the Baikal sponges, throughout the entire water area of the lake, covering not only in the recreational but also in relatively favourable areas (Khanaev et al., 2018), indicates the infectious nature of the disease. However, the bacterial pathogens in the Baikal sponges have not been detected yet. As noted above, the viral pathogens of worldwide marine sponge diseases are also unknown and, unfortunately, the number of investigations in this field is the fewest. On the contrary, some viruses are known to be potential causative agents of coral diseases. It was suggested that eukaryotic circular Rep-encoding single-stranded DNA (CRESS-DNA) viruses (particularly *Circoviridae* and *Nanoviridae*), and their associated satellites may be responsible for white plague-like diseases of tropical corals (Soffer et al., 2014). Some sequences similar to circoviruses were also detected in the Baikal sponge viromes, but as mentioned above these ssDNA viruses were, probably, underestimated in our study. Therefore, the role of CRESS-DNA, as well as NCLDVs viruses in sponge holobionts, remains to be revealed in further examination of DNA-viruses (including ssDNA) in a number of diseased and healthy (without signs of disease) sponges.

Diseases of sponge and other holobionts are a result of stress due to the environmental perturbations and are accompanied by dysbiosis that is the substantial shifts in taxonomic and functional diversity of microbial communities (Pita et al., 2018). In this study, we analyzed the sponge with the signs of disease and, most likely, this individual also had dysbiosis and corresponding changes in abundances and composition of viral communities especially in the affected branch. This may explain a significant difference of viromes from the affected and visually healthy tissues of the *L. baikalensis* sponge. As a rule, the diversity of microbiota including viruses in diseased sponges is higher in

comparison with the stable healthy holobiont (Pita et al., 2018), and in our study the number of virotypes in the diseased branch was a little more than in the visually healthy one.

All sponge- and coral-associated viral communities were significantly different in our analysis (P value <0.01); in addition, the freshwater viromes were distant from the marine ones (Fig. 4). This is consistent with the data reported previously, where the viruses associated with sponges were species specific (Laffy et al., 2018), and the environmental conditions affected the formation of viral communities (Batista et al., 2018). It should be noted that the methods of sample preparation influence on the results of metagenomic analysis; hence, some proportion of differences between the viromes from the Baikal and marine holobionts may be a consequence of this fact.

Therefore, the metagenomic analysis of the viral community from the Baikal sponges have revealed for the first time a high genetic and taxonomic diversity of viruses in the associated communities of the *L. baikalensis* sponges, and demonstrated the differences in viral communities of visually healthy and diseased branches of the sponge. In general, our study broadens the understanding of the nature of symbiotic communities in freshwater organisms. Future investigations are necessary to assess the diversity and functions of viral communities in different species of the Baikal sponges; understand the role of viruses in mass disease and mortality of sponges; and trace the dynamics of viral communities in the course of the disease until adaptation of sponge holobionts and the onset of a new stable equilibrium state.

Acknowledgments

The study was carried out within the framework of the state task No. 0345–2019–0002 and supported by the funding of RFBR and the Government of the Irkutsk Region, project No. 17-44-388080.

References

Albuquerque L., da Costa M.S. 2014. The family Idiomarinaceae. In: Rosenberg E., DeLong E.F., Lory S. et al. (Eds.), The Prokaryotes. Heidelberg, pp. 361–385. DOI: 10.1007/978-3-642-38922-1_232

Altschul S.F., Gish W., Miller W. et al. 1990. Basic local alignment search tool. Journal of Molecular Biology 215: 403–410. DOI: 10.1016/S0022-2836(05)80360-2

Batista D., Costa R., Carvalho A.P. et al. 2018. Environmental conditions affect activity and associated microorganisms of marine sponges. Marine Environmental Research 142: 59–68. DOI: 10.1016/j.marenvres.2018.09.020

Belikov S.I., Feranchuk S.I., Butina T.V. et al. 2018. Mass disease and mortality of Baikal sponges. Limnology and Freshwater Biology 1: 36–42. DOI: 10.31951/2658-3518-2018-A-1-36

Bell J.J. 2008. The functional roles of marine sponges. Estuarine, Coastal and Shelf Science 79: 341–353. DOI: 10.1016/j.ecss.2008.05.002

Bondarenko N.A., Logacheva N.F. 2017. Structural changes in phytoplankton of the littoral zone of Lake Baikal. Hydrobiological Journal 53: 16–24. DOI: 10.1615/HydrobJ.v53.i2.20

Bormotov A.E. 2012. What has happened to Baikal sponges? Science First Hand 32: 20–23.

Butina T.V., Potapov S.A., Belykh O.I. et al. 2015. Genetic diversity of cyanophages of the myoviridae family as a constituent of the associated community of the Baikal sponge *Lubomirskia baicalensis*. Russian Journal of Genetics 51: 313–317. DOI: 10.1134/S1022795415030011

Claverie J.M., Grzela R., Lartigue A. et al. 2009. Mimivirus and Mimiviridae: giant viruses with an increasing number of potential hosts, including corals and sponges. Journal of Invertebrate Pathology 101: 172–180. DOI: 10.1016/j.jip.2009.03.011

Diaz M.C., Rützler K., 2001. Sponges: an essential component of Caribbean coral reefs. Bulletin of Marine Science 69: 535–546.

Dixon P. 2003. VEGAN, a package of R functions for community ecology. Journal of Vegetation Science 14: 927–930. DOI:10.1658/1100-9233(2003)014[0927:vaporf]2.0.co;2

Efremova S.M. 2001. Sponges (Porifera). In: Timoshkin O.A. (Ed.), Index of animal species inhabiting Lake Baikal and its catchment area. Novosibirsk, pp. 182–192. (in Russian)

Efremova S.M. 2004. New genus and new species of sponges from family Lubomirskiidae Rezvoj, 1936. In: Timoshkin O.A. (Ed.), Index of animal species inhabiting Lake Baikal and its catchment area. Novosibirsk, pp. 1261–1278. (in Russian)

Faith D.P., Minchin P.R., Belbin L. 1987. Compositional dissimilarity as a robust measure of ecological distance. Vegetatio 69: 57–68. DOI: 10.1007/BF00038687

Gjessing M.C., Yutin N., Tengs T. et al. 2015. Salmon gill poxvirus, the deepest representative of the Chordopoxvirinae. Journal of Virology 89: 9348–9367. DOI: 10.1128/JVI.01174-15

Gower J.C., Legendre P. 1986. Metric and Euclidean properties of dissimilarity coefficients. Journal of Classification 3: 5–48. DOI: 10.1007/BF01896809

Haller S.L., Peng C., McFadden G. et al. 2014. Poxviruses and the evolution of host range and virulence. Infection, Genetics and Evolution 21: 15–40. DOI: 10.1016/j.meegid.2013.10.014

Heck Jr. K.L., van Belle G., Simberloff D. 1975. Explicit calculation of the rarefaction diversity measurement and the determination of sufficient sample size. Ecology 56: 1459–1461. DOI: 10.2307/1934716

Hentschel U., Piel J., Degnan S.M. et al. 2012. Genomic insights into the marine sponge microbiome. Nature Reviews Microbiology 10: 641–654. DOI: 10.1038/nrmicro2839

Hill M.O. 1973. Diversity and evenness: a unifying notation and its consequences. Ecology 54: 427–432. DOI: 10.2307/1934352

Hingamp P., Grimsley N., Acinas S.G. et al. 2013. Exploring nucleo-cytoplasmic large DNA viruses in Tara Oceans microbial metagenomes. The ISME Journal 7: 1678–1695. DOI: 10.1038/ismej.2013.59

Itskovich V., Kaluzhnaya O., Veynberg Y. et al. 2017. Endemic Lake Baikal sponges from deep water. 2: Study of the taxonomy and distribution of deep-water sponges of Lake Baikal. Zootaxa 4236: 335–342. DOI: 10.11646/zootaxa.4236.2.8

Jacquet S., Miki T., Noble R. et al. 2010. Viruses in aquatic ecosystems: important advancements of the last 20 years and prospects for the future in the field of microbial oceanography and limnology. Advances in Oceanography and Limnology 1: 97–141. DOI: 10.1080/19475721003743843

Johnson P.T. 1984. Viral diseases of marine invertebrates. Helgoländer Meeresuntersuchungen [Heligoland Marine Surveys] 37: 65–98.

Khanaev I.V., Kravtsova L.S., Maikova O.O. et al. 2018. Current state of the sponge fauna (Porifera: Lubomirskiidae) of Lake Baikal: sponge disease and the problem of conservation of diversity. Journal of Great Lakes Research 44: 77–85. DOI:10.1016/j.jglr.2017.10.004

Kim K.H., Bae J.W. 2011. Amplification methods bias metagenomic libraries of uncultured single-stranded and double-stranded DNA viruses. Applied and Environmental Microbiology 77: 7663–7668. DOI: 10.1128/AEM.00289-11

Kozhov M.M. 1970. About the benthos of south Baikal. Izvestiya BGNII pri IGU [Bulletin of the Biological and Geographical Research Institute at the Irkutsk State University] 23: 3–12. (in Russian)

Kozhova O.M., Izmesteva L.R. 1998. Lake Baikal: Evolution and biodiversity. Leiden: Backhuys Publisher.

Kravtsova L.S., Izhboldina L.A., Khanaev I.V. et al. 2012. Disturbances of the vertical zoning of green algae in the coastal part of the Listvennichnyi Gulf of Lake Baikal. Doklady Biological Sciences 448: 227–229. DOI: 10.1134/S0012496612060026

Kravtsova L.S., Izhboldina L.A., Khanaev I.V. et al. 2014. Nearshore benthic blooms of filamentous green algae in Lake Baikal. Journal of Great Lakes Research 40: 441–448. DOI: 10.1016/j.jglr.2014.02.019

Laffy P.W., Wood-Charlson E.M., Turaev D. et al. 2016. HoloVir: a workflow for investigating the diversity and function of viruses in invertebrate holobionts. Frontiers in Microbiology 7: 822. DOI: 10.3389/fmicb.2016.00822

Laffy P.W., Wood-Charlson E.M., Turaev D. et al. 2018. Reef invertebrate viromics: diversity, host specificity and functional capacity. Environmental Microbiology 20: 2125–2141. DOI: 10.1111/1462-2920.14110

Lohr J.E., Chen F., Hill R.T. 2005. Genomic analysis of bacteriophage ΦJL001: insights into its interaction with a sponge-associated alpha-proteobacterium. Applied and Environmental Microbiology 71: 1598–1609. DOI: 10.1128/AEM.71.3.1598-1609.2005

Morgan M., Anders S., Lawrence M. et al. 2009. ShortRead: a bioconductor package for input, quality assessment and exploration of high-throughput sequence data. Bioinformatics 25: 2607–2608. DOI: 10.1093/bioinformatics/btp450

Munn C.B. 2006. Viruses as pathogens of marine organisms – from bacteria to whales. Journal of the Marine Biological Association of the United Kingdom 86: 453–467. DOI: 10.1017/S002531540601335X

Oliveira G.P., Rodrigues R., Lima M.T. et al. 2017. Poxvirus host range genes and virus–host spectrum: a critical review. Viruses 9: 331. DOI:10.3390/v9110331

Pascelli C., Laffy P.W., Kupresanin M. et al. 2018. Morphological characterization of virus-like particles in coral reef sponges. PeerJ 6. DOI:10.7717/peerj.5625

Pita L., Rix L., Slaby B.M. et al. 2018. The sponge holobiont in a changing ocean: from microbes to ecosystems. Microbiome 6: 46. DOI:10.1186/s40168-018-0428-1

Rohwer F., Seguritan V., Azam F. et al. 2002. Diversity and distribution of coral-associated bacteria. Marine Ecology Progress Series 243: 1–10. DOI: 10.3354/meps243001

Rosenberg E., Koren O., Reshef L. et al. 2007. The role of microorganisms in coral health, disease and evolution. Nature Reviews Microbiology 5: 355–362. DOI: 10.1038/nrmicro1635

Pruitt K.D., Tatusova T., Maglott D.R. 2005. NCBI Reference Sequence (RefSeq): a curated non-redundant sequence database of genomes, transcripts and proteins. Nucleic Acids Research 33. DOI: 10.1093/nar/gki025

Sambrook J., Fritsch E.F., Maniatis T. 1989. Molecular cloning: a laboratory manual (Ed. 2). New York: Cold spring harbor laboratory press.

Shimaraev M.N., Domysheva V.M. 2013. Trends in hydrological and hydrochemical processes in Lake Baikal under conditions of modern climate change. In: Goldman C.R., Kumagai M., Robarts R.D. (Eds.), Climatic change and global warming of inland waters. Impacts and mitigation for ecosystems and societies. Chichester, pp. 43–66. DOI 10.1002/9781118470596.ch3

Soffer N., Brandt M.E., Correa A.M. et al. 2014. Potential role of viruses in white plague coral disease. The ISME Journal 8: 271–283. DOI: 10.1038/ismej.2013.137

Suttle C.A. 2007. Marine viruses – major players in the global ecosystem. Nature Reviews Microbiology 5: 801–812. DOI: 10.1038/nrmicro1750

Suzuki R., Shimodaira H. 2006. Pvclust: an R package for assessing the uncertainty in hierarchical clustering. Bioinformatics 22: 1540–1542. DOI: 10.1093/bioinformatics/btl117

Timoshkin O.A., Samsonov D.P., Yamamuro M. et al. 2016. Rapid ecological change in the coastal zone of Lake Baikal (East Siberia): is the site of the world's greatest freshwater biodiversity in danger? Journal of Great Lakes Research 42: 487–497. DOI:10.1016/j.jglr.2016.02.011

Vacelet J., Gallissian M.F. 1978. Virus-like particles in cells of the sponge Verongia cavernicola (Demospongiae, Dictyoceratida) and accompanying tissues changes. Journal of Invertebrate Pathology 31: 246–254. DOI 10.1016/0022-2011(78)90014-9

Vega Thurber R.L., Barott K.L., Hall D. et al. 2008. Metagenomic analysis indicates that stressors induce production of herpes-like viruses in the coral *Porites compressa*. Proceedings of the National Academy of Sciences of the United States of America 105: 18413–18418. DOI: 10.1073/pnas.0808985105

Webster N.S. 2007. Sponge disease: a global threat? Environmental Microbiology 9: 1363–1375. DOI: 10.1111/j.1462-2920.2007.01303.x

Webster N.S., Thomas T. 2016. The Sponge Hologenome. mBio 7. DOI:10.1128/mBio.00135-16

Weynberg K.D., Wood-Charlson E.M., Suttle C.A. et al. 2014. Generating viral metagenomes from the coral holobiont. Frontiers in Microbiology 5: 206. DOI: 10.3389/fmicb.2014.00206

Wilhelm S.W., Matteson A.R. 2008. Freshwater and marine virioplankton: a brief overview of commonalities and differences. Freshwater Biology 53: 1076–1089. DOI: 10.1111/j.1365-2427.2008.01980.x

Wommack K.E., Colwell R.R. 2000. Virioplankton: viruses in aquatic ecosystems. Microbiology and Molecular Biology Reviews 64: 69–114.

Wulff J.L. 2006. Ecological interactions of marine sponges. Canadian Journal of Zoology 84: 146–166. DOI:10.1139/Z06-019

Yutin N., Koonin E.V. 2012. Hidden evolutionary complexity of nucleo-cytoplasmic large DNA viruses of eukaryotes. Virology Journal 9: 161. DOI: 10.1186/1743-422X-9-161

Limnology and Freshwater Biology 2019 (1): 163-171 DOI:10.31951/2658-3518-2019-A-1-163

Original Article

ISSN 2658-3518
LIMNOLOGY FRESHWATER BIOLOGY
www.limnolfwbiol.com

Morphological and genetic polymorphism of new *Diacyclops* taxonomic group from Lake Baikal (Copepoda: Cyclopoida)

Mayor T.Yu., Zaidykov I.Yu.*, Kirilchik S.V.

Limnological Institute, Siberian Branch of the Russian Academy of Sciences, Ulan-Batorskaya Str., 3, Irkutsk, 664033, Russia

ABSTRACT. In this study, we have performed morphological and molecular analyses of a phylogenetic group (VIG2) in the complex of Baikal cyclopoids that are morphologically similar to *Diacyclops versutus*, *D. improcerus* and *D. galbinus*. The first internal transcribed spacer (*ITS1*) and the mitochondrial cytochrome c oxidase subunit I (*COI*) were chosen as molecular markers. We have measured 27 morphological features and obtained values of 18 morphometric characteristics. We present an illustrated description of the females VIG2. We show that representatives of VIG2 belong to the new taxonomic group *Diacyclops* in Lake Baikal. Genetic and morphometric differences in the representatives of VIG2 from four locations are comparable to the intraspecific level of differences.

Keywords: Copepoda, *Diacyclops*, morphometry, Lake Baikal, *COI*, *ITS*

1. Introduction

The Cyclopoida in Baikal represent one of the numerous and highly endemic groups of arthropods in the number of species yielding to amphipods, ostracods, and harpacticoids (Timoshkin, 2001). In the number of species, two taxonomically complex genera *Acanthocyclops* Kiefer, 1927 and *Diacyclops* Kiefer, 1927 (Mazepova, 1978; Sheveleva et al., 2012) dominate among the Baikal cyclopoids. Three endemic species from this group, *D. versutus* (Mazepova, 1962), *D. improcerus* (Mazepova, 1950), and *D. galbinus* (Mazepova, 1962), are widespread in the Baikal littoral zone, occur together during sampling and have a similar morphology, which previously suggested their close relationship (Mazepova, 1978).

The first results of the molecular phylogenetic study of Baikal cyclopoids identified a discordance between molecular and morphological data (Mayor et al., 2017; 2018). Among the analyzed specimens similar in morphology to *D. versutus*, *D. improcerus*, and *D. galbinus*, there were three phylogenetic groups with an unclear taxonomic status (VIG1-3). The acronym VIG stands for the first letters of the species name of the three species studied (V - ***v****ersutus*, I - ***i****mprocerus*, G - ***g****albinus*). The VIG1 and VIG2 phylogenetic groups included 5 and 6 nucleotide sequences of individuals morphologically determined as *D. versutus* (3 and 1 nucleotide sequences), *D. improcerus* (1 and 4), and *D. galbinus* (1 and 1), respectively. The VIG3 included 2 nucleotide sequences: 1 for *D. galbinus* and 1 for *D. improcerus*. The appearance of phylogenetic groups can be due to an insufficient description of the Baikal cyclopoids. The identified case can also be due to the presence of cryptic speciation among endemic Baikal cyclopoids or mitochondrial introgression in the group of *D. versutus / D. improcerus / D. galbinus*. A series of studies show the presence of cryptic species for Cyclopoida (Monchenko, 2000; Blaha et al., 2010; Ueda et al., 2011; Karanovic and Krajicek, 2012; Sukhikh and Alekseev, 2015). As a rule, sibling species are identified accidentally during molecular studies, and, in order to obtain their taxonomic description, it is advisable to carry out additional analysis of morphology in combination with the use of molecular methods.

The aim of this work is to assess the morphological and genetic polymorphism of cyclopoids that are similar in morphology to *D. versutus / D. improcerus / D. galbinus* constituting one phylogroup (VIG2) and inhabiting the Southern Baikal.

2. Material and methods

Samples were collected in Lake Baikal from depths of up to 15 m in April – June 2018 using a net and dredge. Collecting sites were chosen in the vicinity of the Bolshoye Goloustnoe (52˚02′N 105˚24′E), Bolshiye Koty (51˚54′N 105˚04′E), and Listvyanka (51˚51′N 104˚52′E) settlements as well as the town of Slyudyanka (51˚40′N 103˚42′E). Samples with live crustaceans were handled in the laboratory, adult females with egg sacs were fixed in 96% ethanol and stored at –20 ˚C. The taxonomic identification of cyclopoids was performed using the identification table by G.F. Mazepova (1978).

*Corresponding author.
E-mail address: igorrock11@mail.ru (I. Yu. Zaidykov)

Morphological analysis

Morphological features were measured according to the Kozminski scheme (Kozminski, 1936) using a MSP-1 stereomicroscope (LOMO, Russia), an Olympus CX 41 microscope (Olympus, Japan), a Levenhuk M 800 Plus digital camera and a LevenhukLite software (Levenhuk, Inc., USA). The length of the body was obtained by summing the lengths of cephalothorax, thorax, and abdomen. For the fourth pair of swimming legs, the length (Lenp3P4) and width (Wenp3P4) of the distal endopodite segment, the length of the same segment from the beginning to the point of attachment of the outer seta (Lo), the length of the internal apical spine(IAS), and the length of the external apical spine (EAS) on the distal segment were measured. For the fifth pair of swimming legs, the length (LP5) and width (WP5) of the distal segment, the length of the spine (LSpP5), and seta on the distal segment (LSeP5) were measured. The setae on the caudal branches were designated according to Dussart and Defaye (2006).

Statistical analyses were performed using the R v. 3.4.2 software (R Core Team, 2017). The mean error (m) was determined according to the formula (1).

$$m = SD / \sqrt{N-1}\ , \quad (1)$$

where SD is the standard deviation and N is the number of observations. Normality of the distribution of the parameter values was assessed using the Shapiro-Wilk test. For normally distributed parameter values, the comparison of sampling sets was performed using one-way analysis of variance (one-way ANOVA). Otherwise, a permutation test was used.

For confocal laser scanning microscopy (CLSM), a female was stained with Congo Red overnight and mounted on slide following the procedure described by Michels and Büntzow (2010). The material was scanned using a Carl Zeiss LSM 710 laser confocal microscope (Zeiss, Germany); lens: Plan-Apochromat 20 ×/0.8 and 63×/1.40 Oil DIC M27; filters: 570 – 670 nm; lasers: 561 nm: 3.0%. For scanning electron microscopy (SEM), specimens fixed in 96% ethanol were dehydrated in 99% ethanol, transferred into 100% hexamethyldisiloxan, dried overnight in a fume hood, mounted on stubs, coated with gold, and observed under a Quanta 200 microscope (FEI Company, USA) with accelerating voltage of 15kV (Laforsch and Tollrian, 2000; Zaidykov and Naumova, 2011).

Molecular genetic analysis

Total DNA for molecular genetic analysis was isolated from egg sacs or somatic tissue using proteinase K according to the previously described protocol (Mayor et al., 2010). For PCR, we used universal primers LCO-1490 and HCO-2198 to amplify the *COI* fragment, and KP2 (5'-AAAAAGCTTCCGTAGGTGAACCTGCG-3') and 5.8S (5'-AGCTTGGTGCGTTCTTCATCGA-3') to amplify *ITS1* (Folmer et al., 1994; Phillips et al., 2000). Amplification was carried out in a T100™ thermal cycler (BioRad, USA) using PCR reagents from Evrogen (Russia). The reaction occurred in a 1X Encyclo buffer for PCR in the presence of 3.5 mM magnesium, 5 μM of each primer, 0.2 mM of each dNTP and 0.5 units of Encyclo DNA polymerase, and 1 μl of DNA-containing mixture. The amplification program included the stage of heating the mixture to 94 ˚C for 4 min, 35-40 cycles consisting of the following steps: 94 ˚C for 15 s, 48 ˚C or 55 ˚C (for *COI* and *ITS1* fragments, respectively) for 20 s, 72 ˚C for 1 min, and the final elongation stage at 72 ˚C for 4 min. The separation and isolation of amplicons for sequencing from the agarose gel was performed according to the protocol described previously (Mayor et al., 2010). The nucleotide sequences of the target fragments were determined in an ABI 3500 8-capillary genetic analyzer (Thermo Fisher Scientific, USA) using the ABI PRISM BigDye Terminator v. 3.1 sequencing kit.

Alignment of nucleotide sequences, selection of a nucleotide substitution model, calculation of genetic distances and construction of phylogenetic schemes by the maximum likelihood (ML) method were performed with the Mega version 7.0.21 program (Kumar et al., 2017). During alignment of the rDNA nucleotide sequences, the Gblock version 0.91b program was additionally used to remove regions with high divergence (Castresana, 2000). The genetic distances for the *COI* gene fragment were calculated, taking into account all the positions of the codon. To analyze the *COI* and *ITS1* data sets, respectively, a three-parameter Tamura model supplemented by the share of stable sites (T92 + I) and a two-parameter Kimura model with the gamma distribution (K2P + G) were chosen, taking into account the Akaike information criterion (AIC) and the Bayesian information criterion (BIC). Nodal support for the resulting branches was estimated with 1000 bootstrap replications. DNA polymorphism was evaluated using the DnaSP 5.10.01 program (Rozas et al., 2003). Our previously published nucleotide sequences of Baikal cyclopoids (KT075063-65, KT075067-68, and KT075070) and two nucleotide sequences (MK217350-51) kindly provided by Yu. A. Galimova were also included in the set of the analyzed data. One nucleotide sequence (EU877959) was borrowed from the GenBank database as an outgroup.

3. Results and discussion

Morphological analysis

We collected 66 adult females of *D.* sp. in the Southern Baikal. Due to the morphometric analysis, 27 morphological features were measured and values of 18 the morphometric parameters used in Cyclopoida studies were obtained (Monchenko, 1974; Lajus and Alekseev, 2000; Blaha et al., 2010) for statistical analysis (Table 1). Some of these parameters represent the description of *D. galbinus, D. versutus,* and *D. improcerus*: LA1/Lcphth, Lf/Wf, Tl position, Lenp3P4/Wenp3P4, IAS/EAS, Tmi/Tme. Three more parameters: Te/Ti, Td/Te, Tl/Wf, which G.F. Mazepova (1950; 1962) gave for *D. galbinus, D. versutus,* and *D. improcerus,* are additionally defined (Table 2). Parameter values Te/Ti, Lf/Wf, IAS/EAS of *D. galbinus, D. versutus,* and *D. improcerus* according to the description of these

Table 1. Morphometric and quantitative morphological parameters of VIG2 from different sampling sets, the results of a single-factor ANOVA (F-criterion) and permutational test of their variability

Characteristics	Mean ± m				F	Pr
	Listvyanka	Slyudyanka	Bolshoye Goloustnoe	Bolshie Koty		
Body length, μm	830 ± 11.0 (14)	807 ± 11.82 (16)	817 ± 9.85 (11)	794 ± 9.44 (17)	1.60	0.20
LA1/Lcphth,	1.02 ± 0.01 (14)	1.00 ± 0.02 (18)	0.98 ± 0.01 (11)	1.00 ± 0.01 (19)	0.83	0.48
Lf/Wf	3.17 ± 0.08 (16)	3.19 ± 0.06 (20)	3.06 ± 0.06 (11)	3.06 ± 0.04 (19)	1.73	0.17
Tl position	0.79 ± 0.01 (13)	0.79 ± 0.01 (20)	0.80 ± 0.01 (11)	0.77 ± 0.01 (19)	0.65	0.59
Tl/Te	0.60 ± 0.02 (13)	0.63 ± 0.02 (19)	0.64 ± 0.02 (11)	0.64 ± 0.02 (19)	0.86	0.47
Tmi/Tme	1.64 ± 0.02 (13)	1.63 ± 0.02 (18)	1.65 ± 0.02 (11)	1.63 ± 0.02 (18)	0.18	0.91
Ti/Lf	0.47 ± 0.02 (13)	0.47 ± 0.01 (20)	0.47 ± 0.01 (11)	0.49 ± 0.01 (19)	0.51	0.67
Ti/Tmi	0.11 ± 0.004 (12)	0.11 ± 0.003 (18)	0.11 ± 0.003 (11)	0.11 ±0.003 (18)	0.17	0.69*
Ti/Tme	0.19 ± 0.005 (15)	0.19 ± 0.004 (20)	0.18 ± 0.004 (11)	0.19 ± 0.005 (19)	0.24	0.67*
Ti/Td	0.66 ± 0.04 (12)	0.61 ± 0.02 (19)	0.59 ± 0.01 (11)	0.58 ± 0.01 (19)	0.76	0.52*
Ti/Te	0.61 ± 0.02 (13)	0.64 ± 0.02 (20)	0.61 ± 0.01 (11)	0.64 ± 0.01 (19)	0.81	0.49
Lenp3P4/Wenp3P4	1.44 ± 0.03 (13)	1.40 ± 0.02 (19)	1.40 ± 0.02 (10)	1.45 ± 0.03 (17)	1.05	0.38
Lo/Lenp3P4	0.62 ± 0.01 (13)	0.63 ± 0.01 (19)	0.65 ± 0.01 (10)	0.64 ± 0.01 (17)	1.95	0.11*
IAS/EAS	1.60 ± 0.03 (13)	1.59 ± 0.04 (18)	1.65 ± 0.05 (10)	1.58 ± 0.02 (17)	0.06	0.63*
IAS/Wenp3P4	1.77 ± 0.07 (13)	1.71 ± 0.04 (18)	1.78 ± 0.03 (10)	1.74 ± 0.03 (17)	0.52	0.67
IAS/Lenp3P4	1.23 ± 0.05 (13)	1.22 ± 0.02 (18)	1.27 ± 0.02 (10)	1.21 ± 0.02 (17)	0.7	0.56
LSpP5/LP5	1.26 ± 0.04 (12)	1.10 ± 0.03 (18)	1.24 ± 0.13 (9)	1.24 ± 0.06 (18)	2.01	0.11*
WP5/LSpP5	0.35 ± 0.02 (12)	-	0.32 ± 0.02 (9)	0.33 ± 0.01 (18)	0.67	0.52
LSeP5/LSpP5	1.64 ± 0.05 (10)	1.85 ± 0.07 (16)	1.62 ± 0.11 (9)	1.63 ± 0.10 (18)	0.98	0.38*

LA1/Lcphth is the ratio of an antennule length to a cephalothorax length. **Lf/Wf** is the ratio of the length to the width of caudal rami. **Tl location** is the ratio of a caudal rami length from the beginning to the point of attachment of a lateral seta to the caudal rami length. The brackets indicate the number of specimens for which measurements made and the parameter defined; * - permutation test results.

Table 2. Morphometric and morphological parameters of VIG2, *D. versutus*, *D. galbinus*, and *D. improcerus*

Parameter	VIG2*	*D. versutus***	*D. galbinus***	*D. improcerus***
Body length, μm	747 – 902 (803)	620 - 920 (770)	730 - 1000 (860)	480 - 750 (610)
Lf/Wf	2.80 - 3.61 (3.08)	1.8 - 3.4 (2.5)	2.9 - 5.4 (3.7)	1.8 - 4.1 (3.0)
Te/Ti	1.36 - 1.96 (1.63)	0.5 - 1.8 (1.2)	0.6 - 1.8 (1.2)	1.0 - 2.1 (1.6)
Tmi/Tme	1.58 - 1.72 (1.64)	1.7 - 2.2 (1.8)	1.3 - 1.9 (1.6)	
Td/Te	0.97 – 1.13 (1.04)	0.9 - 1.5 (1.2)	0.8 -1.2 (1.00)	-
Tl/Wf	1.02 – 1.61 (1.39)	0.3 -0.6 (0.5)	1.4 – 2.0 (1,6)	
Lenp3P4/Wenp3P4	1.25 - 1.56 (1.39)	1.0 - 1.8 (1.4)	1.6 - 3.0 (2.0)	1.0 - 1.4 (1.2)
IAS/EAS	1.46 – 2.02 (1.63)	0.6 -1.2 (1.0)	1.1 - 1.8 (1.3)	1.0 - 1.9 (1.35)
LA1/Lcphth	0.88 – 1.22 (1.00)	short, hardly reach the middle of the cephalothorax	reach the posterior margin of the cephalothorax	short, usually reach the middle of the cephalothorax
Color	white	white	green	white, yellow, light green

* - our data of 14 specimens, for which molecular data were obtained, confirming their attribution to a single phylogenetic group;

** - data of G.F. Mazepova (1978); the brackets indicate the average value of parameters.

species may be the same. The values of the parameters Tmi/ Tme, Td /Te, Tl/Wf are shown in the description of *D. galbinus* and *D. versutus* but are unknown for *D. improcerus*. In the key to Baikal cyclopoid species, the ratio of an antennule length to a cephalothorax length (LA1/Lcphth), the width of the A1 first segment, and the body shape are used to separate *D. improcerus*, *D. galbinus*, and *D. versutus* (Mazepova, 1978).

For each of the 18 parameters, we obtained the values of the Fisher criterion (Table 1, F). The differences were considered statistically meaningful in the case when the level of significance was less than 0.05 ($Pr < 0.05$). For all of the selected parameters, specimens collected from four locations in the Southern Baikal did not reliably differ.

Specimens could be identified only up to the rank of the genus *Diacyclops*. Specimens are morphologically similar to *D. galbinus D. improcerus,* and *D. versutus* but, at the same time, have some differences from each of these three species (Table 2). The studied specimens differ from *D. improcerus* in larger body size and more elongated antennules; from *D. versutus* – in smaller values of the Tmi/Tme parameter, in larger values of the Tl/Wf and IAS/EAS parameters, and more elongated antennules; from *D galbinus* – in coloration and a lower value of Lenp3P4/Wenp3P4. The available description of these species allows comparing only six morphometric parameters (Mazepova, 1950; 1962). Unfortunately, it is impossible to compare the collected material with the type material of *D. galbinus, D. improcerus,* and *D. versutus* since they are missing in public collections. According to the morphological and molecular data (Fig. 5), we attribute the studied specimens to a single taxonomic group, named VIG2, which is new for endemic cyclopoids from Lake Baikal. The rank of this taxonomic group, as well as the groups VIG1 and VIG3, remains unclear. The use of the hybridological method in the future would clarify this issue. Probably, a new combination of features in the VIG2 specimens caused difficulties in the taxonomic identification of cyclopoids and an inconsistency between the molecular and morphological data that we described previously (Mayor et al., 2017). We provide a description of the VIG2 females. The description is based on the morphological data of 14 specimens, for which molecular data were obtained, confirming their attribution to a single phylogenetic group. These specimens were collected in each of the four sampling locations described above. The description is based on the work of Hołynska and Dimante-Deimantovica (2016).

Body length 747 - 902 μm (without caudal rami length). Chephalothorax length/width 0.9 - 1.2, cephalothorax width/genital somite width 2.0 - 3.3, prosome length/urosome length 1.2 – 1.4.

Genital double-somite longer than its greatest width, 1.1 - 1.6 (Fig. 1A, 1B). The posterior margins of the 1-st and 2-nd abdominal segments are smooth. The posterior margin of anal somite with a continuous row of spinules (Fig. 1E, 1F). Anal sinus is ornamented with two diagonal rows of minute spinules (Fig. 1C). Caudal rami length/width 2.8 - 3.6, smooth on the inner side. Lateral seta is inserted at a distance of 0.17 – 0.29 ramus length measured from the posterior end. Dorsal seta is almost as long as terminal external seta, Td/ Te 0.97 – 1.13. Terminal internal seta is shorter than terminal external seta, Ti/Te 0.51 – 0.74. Terminal median internal seta (Tmi) is the longest, it is 1.58 – 1.72 times as long as terminal median external seta (Tme). Relative lengths of caudal setae Td, Ti, Tmi, Tme, and Te are 0.7 – 0.9, 0.3 – 0.5, 4.5 – 6.2, 2.2 – 2.8, and 0.7 – 0.8 times as long as caudal rami. Caudal setae Ti, Tmi, Tme, Te are setose; dorsal seta has setae at distal part; lateral seta is naked (Fig. 1F). There is a row of short spinules above the point of lateral seta insertion (Fig. 1D).

Antennule 11-segmented, reaching posterior margin of chephalothorax shield for most individuals, 0.88 – 1.22. Length ratios of antennular segments from proximal end are 1.0, 0.3, 0.5, 0.3, 0.2, 0.3, 0.6, 0.5, 0.3, 0.4, and 0.5. Spinules present on proximo-ventral surface of segment 1 (Fig. 2A, 2B).

The antenna consists of coxobasis and three-segmented endopodite, bearing 3, 1, 9, and 7 setae, respectively. The coxobasis ornamented with two rows of spinules on the ventral surface, a row of setae on the caudal surface (Fig. 2C) armed with two subequal naked setae on the distal inner corner and exopodal seta with short setules reaching the 3-rd endopodal segment (Fig. 2B, 2D). The first endopodal segment with smooth inner seta at 0.42 length and group of setae at the distal part of the caudal margin (Fig. 2C). The second and third endopodal segments are ornamented with one and two diagonal rows of spinules on the caudal surface (Fig. 2E).

Segmentation formula of P1 – P4 exopod/ endopod: 2/2.3/2.3/3.3/3 (Fig. 3A). Ultimate exopodal segment spine formula is 3.3.3.3, and setae formula is 5.4.4.4. Table 3 shows the P1 – P4 spine and seta formula. The P1-P4 coxa ornamented with two rows of spines on the right and left side of the frontal surface (Fig. 3B, 3D, 3E). P2 – P3 coxa has notched external corner and ornamented with a row of spines on the lateral surface. P2 – P4 basis ornamented with a row of spines on the central part of the frontal margin (Fig. 3D, 3E). The P4 intercoxal sclerite has two rows of long spines in the middle and on the distal margin of the caudal surface (3C, F), and is smooth from the frontal one. P4 coxa ornamented with five groups of spines on the caudal surface. P4 endpodal segment 1.3 - 1.6 times as long as wide; inner apical spine on 3-rd endopodal segment 1.5 – 2.0 as long as outer apical spine, 1.0 – 1.4 as long as segment (Fig. 3F).

P5 (Fig. 4A, 4B) relatively small, two-segmented. First segment broad and short, armed with single slender outer seta, 41 μm. Second segment cylindrical, 2.5 times as long as wide, armed with apical outer seta and subapical inner spine. Apical seta (32 μm) 1.9 times as long as P5 distal segment, and 1.7 times as long as subapical spine.

VIG2 belongs to a taxonomically complex and rich in species composition genus *Diacyclops* that includes more than 100 species (Stoch, 2001). Along with the complex of *D. improcerus, D. versutus,* and

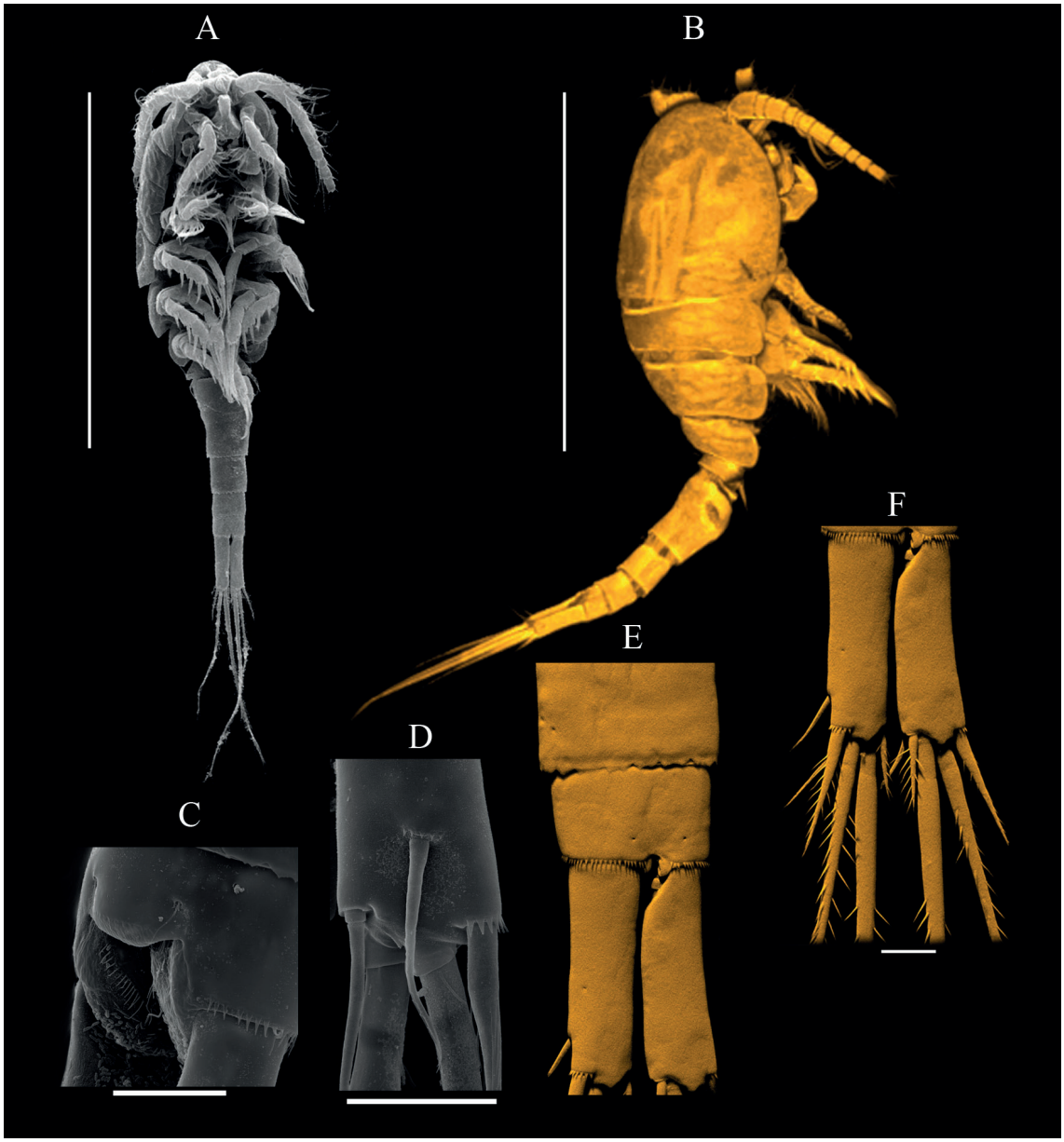

Fig. 1. Scanning electron (**A**, **C**, **D**) and confocal laser (**B**, **E**, **F**) micrographs of the taxonomic group VIG2, ♀. **A** – habitus, ventral. **B** - habitus, lateral. **C** – anal somite, lateral. **D** – lateral seta. **E** – the 2-nd abdominal segment, anal somite, caudal rami, dorsal. **F** – caudal rami, dorsal. Scale bars: **A** – **B** = 500 μm; **C** – **F** = 20 μm.

D. galbinus, a new taxonomic group morphologically belongs to the group of species *languidoides* named after the first described species of this group *Diacyclops languidoides languidoides* (Lilljeborg, 1901). Among the Baikal cyclopoids, the new taxonomic group is the closest morphologically to *D. galbinus*. V.I. Monchenko (1974) suggested that *D. galbinus* is a synonym for *D. languidoides moravicus* Sterba, 1956. Representatives of VIG2 differ from *D. languidoides moravicus* by greater body length, Te/Ti and IAS / EAS parameters, and lower value of Lenp3P4/Wenp3P4 (Sterba, 1956). We believe that they belong to different species.

In our sampling sets of cyclopoids collected from the Southern Baikal, the adult VIG2 specimens are found in large numbers from late April to June, starting from the interstitial zone. Thus, this taxonomic group can be used as an indicator in the long-term dynamics and assessing the anthropogenic pressure on Lake Baikal. Probably, VIG2 may become a biological object in the study of chromatin diminution. The latter phenomenon has been found in *D. galbinus* (Ivankina et al., 2013).

Molecular phylogenetic analysis

We obtained 15 nucleotide sequences of the mitochondrial *COI* gene fragment of 620 - 675 bp in length. The data were obtained for three to seven specimens from each sampling set. The common fragment, excluding the missing data, was 482 bp. Analysis of this fragment showed the presence of six polymorphic positions, among which one was in the first position of the codon. Transversions were found in two positions. All substitutions were synonymous.

For the first time, we have obtained the nucleotide sequences of the rDNA fragment that includes *ITS1* for the endemic Baikal cyclopoids. The rDNA nucleotide sequences with a length of 329-363 bp were determined for 10 specimens. The data were obtained for three to seven specimens from each sampling set. Upon aligning and removing regions with high divergence, the common fragment excluding the missing data was 252 bp. Analysis of this fragment showed the presence

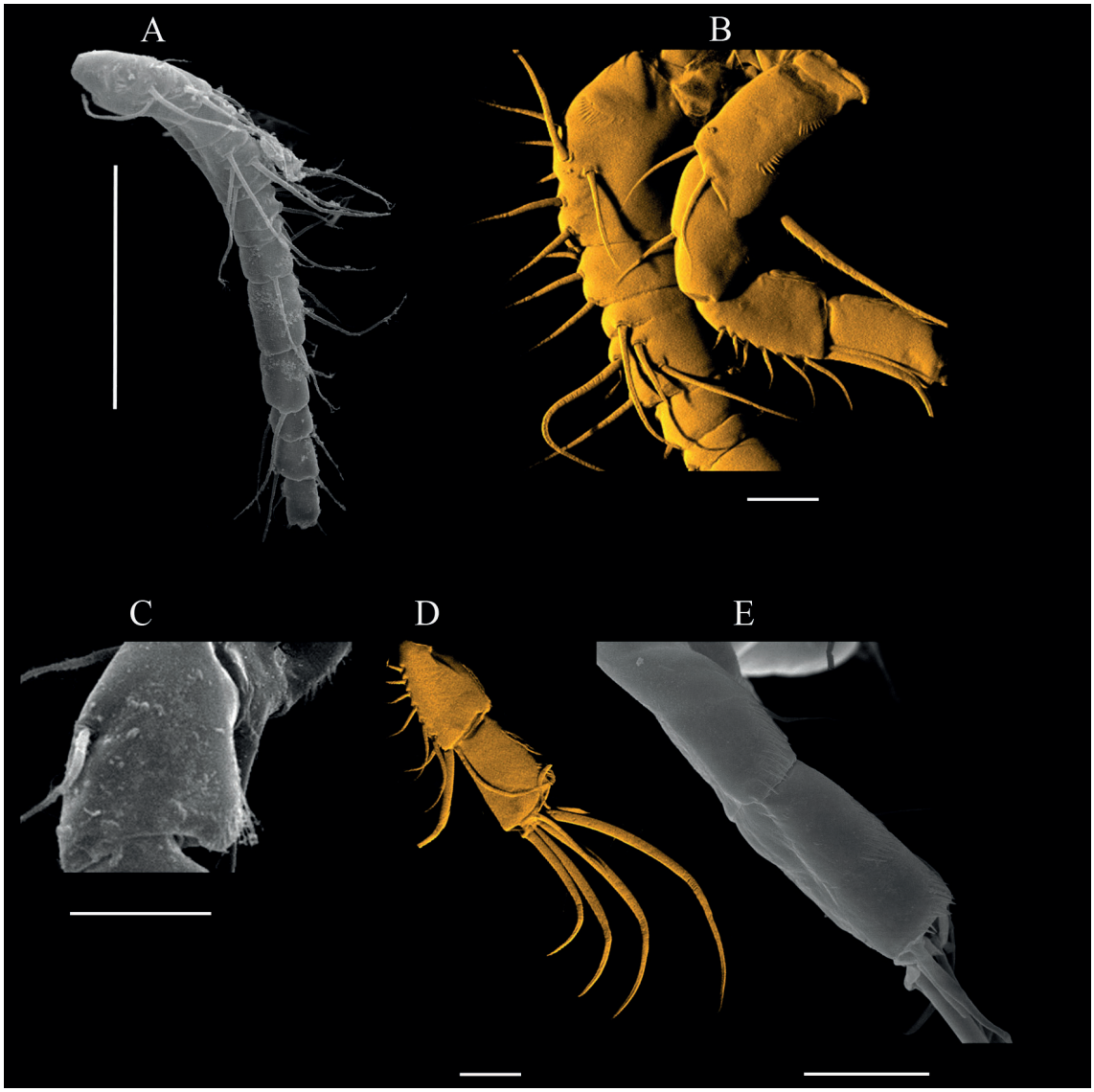

Fig. 2. Scanning electron (**A**, **C**, **E**) and confocal laser (**B**, **D**) micrographs of the taxonomic group VIG2, ♀. **A** – antennule, ventral. **B** – antennule: segments 1- 5, antenna, ventral. **C – E** – antenna. **C** – the 1-st endopodite, ventral. **D** – the 2-nd and 3-nd endopodits, ventral, lateral seta. **E** – the 2-nd and 3-nd endopodits, lateral. Scale bars: **A** = 100 μm; **B – E** = 20 μm.

of four polymorphic positions, in which only transitions were found.

Based on the obtained molecular data, phylogenetic schemes have been constructed (Fig. 5, 6). The tree topologies for the two molecular markers are consistent with each other. The nucleotide sequences of the VIG2 specimens form one monophyletic group. The values of genetic distances within this group are on average 0.005 and 0.003 according to *COI* and *ITS1*, respectively. At the same time, in the data set for the *COI* gene, the genetic distances between the nucleotide sequences belonging to the VIG2 and VIG1 phylogenetic groups are two orders of magnitude higher, averaging 0.21. In the data set for *ITS1*, the genetic distances between the nucleotide sequences of VIG2 and the endemic Baikal species *D. arenosus* (Mazepova, 1950) and *D. jasnitskii* (Mazepova, 1950) are on average 0.13 and 0.14. The obtained values of intra- and interspecies genetic distances for both molecular markers are similar to those for Cyclopoida (Wyngaard et al., 2010; Miracle et al., 2013; Zagoskin et al., 2014; Krajicek et al., 2016).

The VIG2 specimens collected in Lake Baikal near the Listvyanka and Bolshiye Koty settlements as well as the town of Slyudyanka are genetically close to each other and form a panmictic population. At the same

Table 3. The armature of legs 1 – 4 of the VIG2 taxonomic group. Spines are denoted by Roman. setae by Arabic numerals

	Coxopodite	Basipodite	Exopodite	Endopodite
Leg 1	0-1	1-1	I-1; III-2-3	0-1; 1-I-4
Leg 2	0-1	1-0	I-1; I-1; II-I.1-3	0-1; 1-I.1-4
Leg 3	0-1	1-0	I-1; I-1; II-I.1-3	0-1; 0-1; 1-I.1-3
Leg 4	0-1	1-0	I-1; I-1; II-I.1-3	0-1; 0-2; 1-II-2

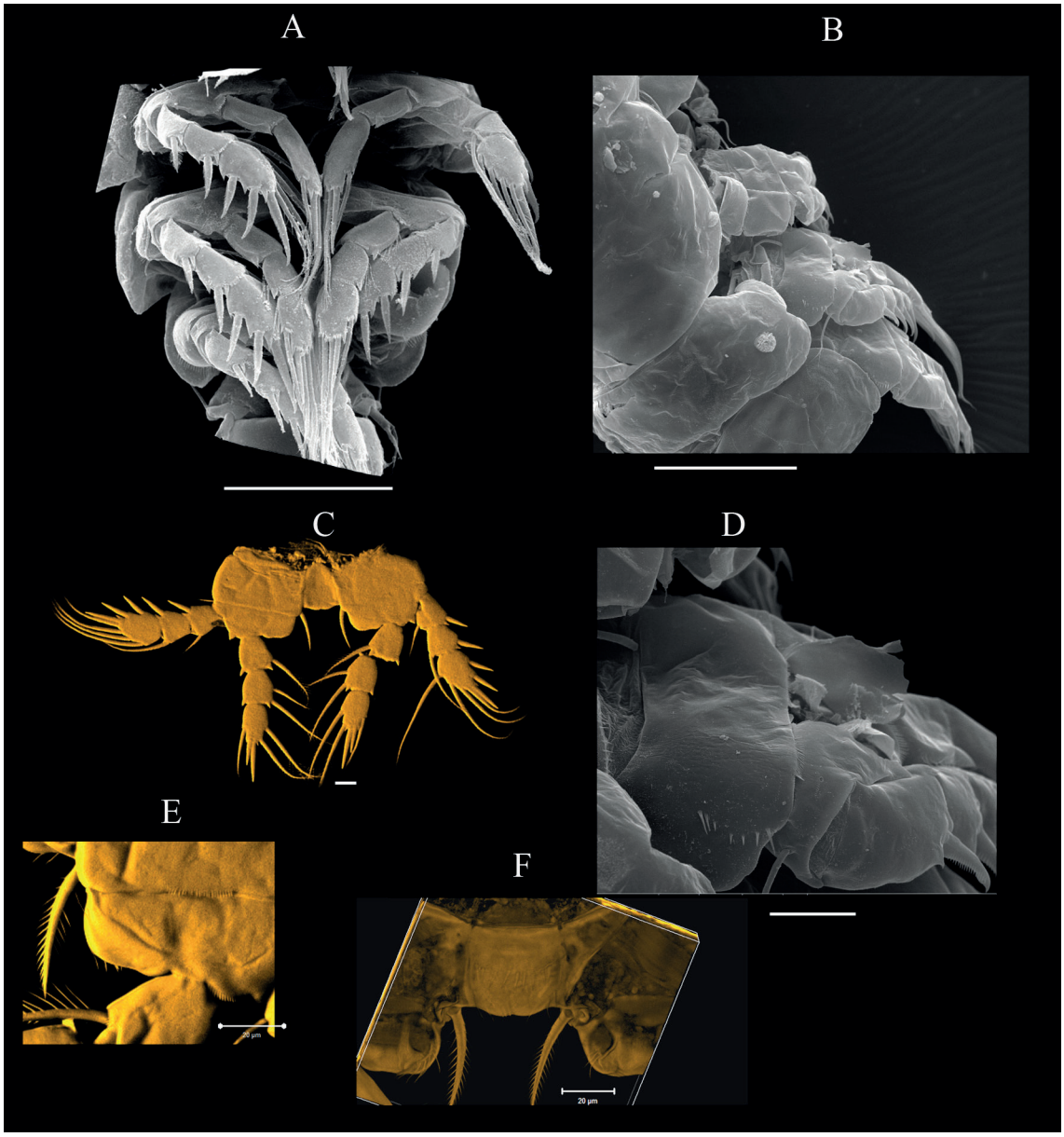

Fig. 3. Scanning electron (**A**, **B**, **D**) and confocal laser (**C**, **E**, **F**) micrographs of the taxonomic group VIG2, ♀. **A** – the 2-nd – 5-th pedigerous somites, ventral. **B** – Leg 1 – 3, lateral. **C** – leg 4, frontal. **D** – leg 2 coxopodite, lateral. **E** – leg 4, part of coxopodite, basipodite, frontal. **F** – leg 4, intercoxal sclerite, caudal. Scale bars: **A** – **B** = 100 μm; **C** – **F** = 20 μm.

time, the specimens collected near the settlement of Bolshoye Goloustnoye show some genetic isolation for the *COI* gene from other representatives of this species (Fig. 5). At the same time, specimens do not differ in 18 morphometric parameters from Bolshoye Goloustnoye, Listvyanka, Bolshiye Koty and Slyudyanka.

Conclusions

1. Genetic and morphometric differences in the representatives of VIG2 from four locations of the Southern Baikal are low and comparable to the intraspecific level of differences.
2. Representatives of VIG2 belong to the new taxonomic group of *Diacyclops* in Lake Baikal and morphologically similar to *D. galbinus, Diacyclops versutus,* and *D. improcerus* but, at the same time, have a number of differences from each of these three species.

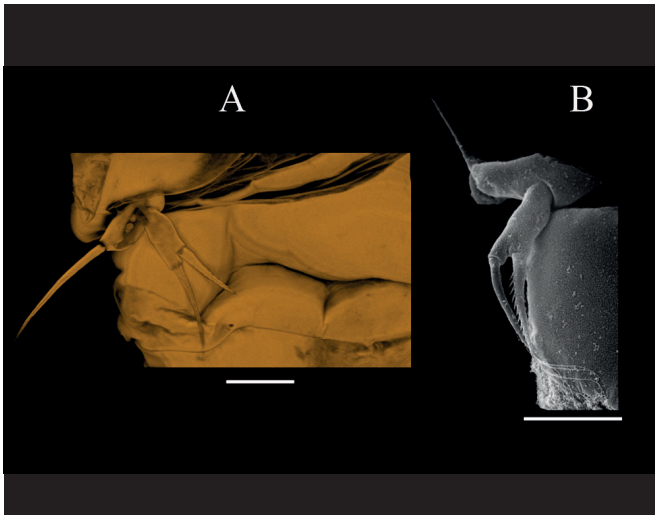

Fig. 4. Scanning electron (**B**) and confocal laser (**A**) micrographs of the taxonomic group VIG2, ♀. **A, B** – P5, frontal. Scale bars: **A** – **B** = 20 μm.

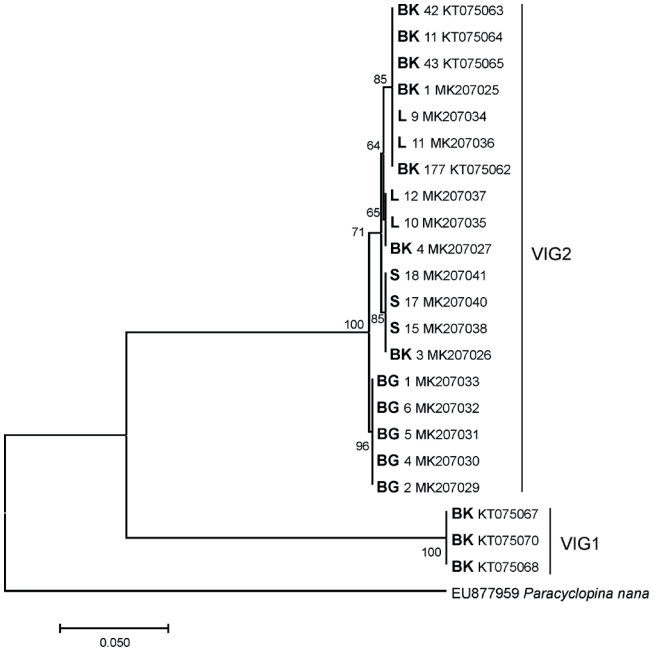

Fig. 5. Phylogenetic tree constructed based on the *COI* gene fragment by the maximum likelihood method (ML, T92 + I). The number in the node is the bootstrap value of the branching node support. The collecting site is indicated in the designation of nucleotide sequences: **BK** - Bolshiye Koty, **L** - Listvyanka, **S** – Slyudyanka, **BG** - Bolshoye Goloustnoe, specimen number and GenBank accession numbers.

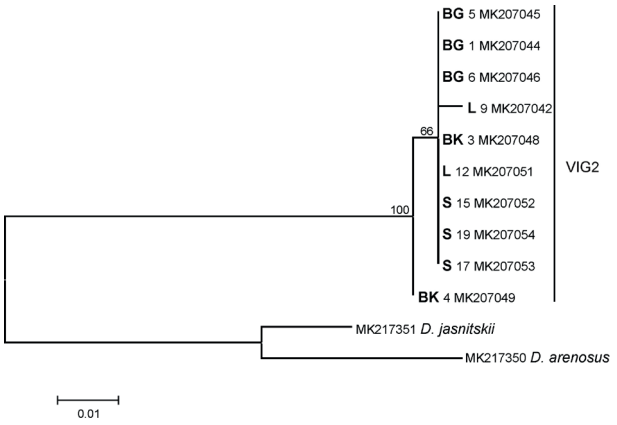

Fig. 6. Phylogenetic tree constructed based on *ITS1* by the maximum likelihood method (ML, K2P + I). The number in the node is the bootstrap value of the branching node support. The collecting site is indicated in the designation of nucleotide sequences: **BK** - Bolshiye Koty, **L** - Listvyanka, **S** – Slyudyanka, **BG** - Bolshoye Goloustnoe, specimen number and GenBank accession numbers.

Acknowledgements

We are grateful to M. Hołynska (Museum and Institute of Polish Academy of Sciences), E. Naumova, and Yu. Bukin (LIN SB RAS) for valuable comments on morphological analysis of the material and its statistical processing, and to Yu. Galimova (IMCB SB RAS) for the kindly provided nucleotide sequences. The SEM and CLSM studies were performed at the Instrumentation Center "Electronic Microscopy" of the Collective Instrumental Center "Ultramicroanalysis" (LIN SB RAS). The study was supported by the Russian Foundation for Basic research grant AAAA-A18-118032390006-1 «The study of phylogeny and morphology of *Diacyclops versutus* (Mazepova, 1962), *D. improcerus* (Mazepova, 1950), and *D. galbinus* (Mazepova, 1961) (Copepoda: Cyclopoida) from Lake Baikal» No. 18-34-00200 mol-a.

References

Blaha M., Hulak M., Sloukova J. et al. 2010. Molecular and morphological patterns across *Acanthocyclops vernalis – robustus* species complex (Copepoda, Cyclopoida). Zoologica Scripta 39: 259–268. DOI: 10.1111/j.1463-6409.2010.00422.x

Castresana J. 2000. Selection of conserved blocks from multiple alignments for their use in phylogenetic analysis. Molecular Biology and Evolution 17: 540–552.

Dussart B.H., Defaye D. 2006. World directory of Crustacea Copepoda of inland waters II, Cyclopiformes. Leiden: Backhuys Publisher.

Folmer O., Black M., Hoeh W. et al. 1994. DNA primers for amplification of mitochondrial cytochrome c oxidase subunit I from diverse metazoan invertebrates. Molecular Marine Biology and Biotechnology 3: 294–299.

Hołynska M., Dimante-Deimantovica I. 2016. Redescription and taxonomic notes on *Cyclops bohater* Kozminski, 1933 and *Cyclops lacustris* G.O. Sars, 1863 (Arthropoda, Crustacea), with an identification key to the *Cyclops* species of Fenno-Scandinavia. European Journal of Taxonomy 212: 1–31. DOI: 10.5852/ejt.2016.212

Ivankina E.A., Alekseeva A.L., Semeshin V.F. et al. 2013. Cytophotometric determination of genome size in two species of Cyclops Lake Baikal (Crustacea: Copepoda: Cyclopoida). Cell and Tissue Biology 7: 192–199. DOI: 10.1134/S1990519X13020053

Karanovic T., Krajicek M. 2012. First molecular data on the western Australian *Diacyclops* (Copepoda, Cyclopoida) confirm morpho-species but question size differentiation and monophyly of the *Alticola*-group. Crustaceana 85: 1549–1569. DOI: 10.1163/156854012X651709

Kozminski Z. 1936. Morfometrische und ökologische Untersuchungen an Cyclopiden der strenuus-Gruppe. Internationale Revue der gesamten Hydrobiologie und Hydrographie [International Review of Hydrobiology] 33: 161–240. (in German)

Krajicek M., Fott J., Miracle M.R. et al. 2016. The genus *Cyclops* (Copepoda, Cyclopoida) in Europe. Zoologica Scripta: 671–682. DOI:10.1111/zsc.12183

Kumar S., Stecher G., Tamura K. 2016. Mega7: molecular evolutionary genetic analysis version 7.0 for bigger datasets. Molecular Biolology and Evolution 33: 1870–1874. DOI: 10.1093/molbev/msw054

Laforsch C., Tollrian R. 2000. A new preparation technique of daphnids for scanning electron microscopy using hexamethyldisilazane. Archiv für Hydrobiologie [Archive for Hydrobiology] 149: 587–596.

Lajus D., Alekseev V. 2000. Components of morphological variation in Baikalian endemial cyclopid Acanthocyclops signifier complex from different localities. Hydrobiologia 417: 25–35.

Mazepova G.F. 1950. New species of Cyclopoids from Lake Baikal. Izvestiya Akademii Nauk SSSR. Seriya biologicheskaya [Bulletin of the USSR Academy of Sciences. Biological sciences] 75: 865–868. (in Russian)

Mazepova G.F. 1962. The benthic Cyclopoids of Southern Baikal. In: Bazikalova A.Y. (Ed.), Systematics and ecology of crustaceans of Baikal. Leningrad, pp. 172–195. (in Russian)

Mazepova G.F. 1978. Cyclopoids of Lake Baikal. Novosibirsk: Nauka. (in Russian)

Mayor T.Y., Sheveleva N.G., Sukhanova L.V. et al. 2010. Molecular-phylogenetic analysis of cyclopoids (Copepoda: Cyclopoida) from Lake Baikal and its water catchment. Russian Journal of Genetics 46: 1373–1380. DOI: 10.1134/S102279541011013X

Mayor T.Y., Galimova Y.A., Sheveleva N.G. et al. 2017. Molecular-phylogenetic analysis of *Diacyclops* and *Acanthocyclops* (Copepoda: Cyclopoida) from Lake Baikal based on COI gene. Russian Journal of Genetics 53: 1–7. DOI: 10.1134/S1022795417020041

Mayor T.Y., Zaidykov I.Y., Galimova Y.A. et al. 2018. Molecular phylogeny of *Diacyclops versutus* (Mazepova, 1961), *D. improcerus* (Mazepova, 1950) and *D. galbinus* (Mazepova, 1961) (Copepoda: Cyclopoida) from Lake Baikal. In: International Conference "Freshwater ecosystems – Key problems", pp. 224–225.

Michels J., Büntzow M. 2010. Assessement of Congo red as a fluorescence marker for the exoskeleton of small Crustaceans and the cuticle of Polychaetes. Journal of Microscopy 238: 95–101. DOI: 10.1111/j.1365-2818.2009.03360

Miracle M.R., Alekseev V., Monchenko V. et al. 2013. Molecular-genetic-based contribution to the taxonomy of the *Acanthocyclops robustus* group. Journal of Natural History 47: 863–888. DOI: 10.1080/00222933.2012.744432

Monchenko V.I. 1974. Gnathostoma Cyclopoida, Cyclopidae. Fauna of Ukraine. Kiev: Naukova dumka. (in Ukrainian)

Monchenko V.I. 2000. Cryptic species in *Diacyclops bicuspidatus* (Copepoda: Cyclopoida): evidence from crossbreeding studies. Hydrobiologia 417: 101–107.

Phillips R.P., Matsuoka M.P., Konon I. et al. 2000. Phylogenetic analysis of mitochondrial and nuclear sequences supports inclusion of *Acantholingua ohridana* in the genus *Salmo*. Copea 2: 546–550.

R Core Team. 2017. R: a language and environment for statistical computing. Vienna: R Foundation for Statistical Computing. https://www.R-project.org/.

Rozas J., Sanchez-DelBarrio J.C., Messeguer X. 2003. DnaSP, DNA polymorphism analyses by the coalescent and other methods. Bioinformatics 19: 2496–2497.

Sheveleva N.G., Mirabdulaev I.M., Ivankina E.A. et al. 2012. The species composition and ecology of Cyclopoids in Lake Baikal. In: International Conference "Actual problems of studying of the Crustaceans of continental waters", pp. 319–322. (in Russian)

Sterba O. 1956. Vzacni a novi korysi z nasich krasvych vod. Biologia 11: 385–403. (in Slovak)

Stoch F. 2001. How many species of Diacyclops? New taxonomic characters and species richness in a freshwater cyclopid genus (Copepoda, Cyclopoida). Hydrobiologia 453/454: 525–531.

Sukhikh N., Alekseev V. 2015. Genetic and morphological heterogeneity within *Eucyclops serrulatus* (Fischer,1851) (Crustacea: Copepoda: Cyclopidae). Journal of Natural History 49: 2929–2953. DOI: 10.1080/00222933.2015.1056267

Timoshkin O.A. 2001. Lake Baikal: fauna diversity, problems of its immiscibility and origin, ecology and "exotic" communities. In: Timoshkin O.A. (Ed.), Index of animal species inhabiting Lake Baikal and its catchment area. Novosibirsk, pp. 16–74. (in Russian)

Ueda H., Yamaguchi A., Saitoh S. et al. 2011. Speciation of two salinity-associated size forms of *Oithona dissimilis* (Copepoda: Cyclopoida) in eustuaries. Journal of Natural History 45: 2069–2079. DOI: 10.1080/00222933.2011.574801

Wyngaard G.A., Hołyńska M., Schulte J.A. II. 2010. Phylogeny of the freshwater copepod *Mesocyclops* (Crustacea: Cyclopidae) based on combined molecular and morphological data, with notes on biogeography. Molecular Phylogenetics and Evolution 55: 753–764. DOI: 10.1016/j.ympev.2010.02.029

Zagoskin M.V., Lazareva V.I., Grishanin A.K. et al. 2014. Phylogenetic information content of Copepoda ribosomal DNA repeat units: ITS1 and ITS2 impact. BioMed Research International 2014. DOI: 10.1155/2014/926342

Zaidykov I.Yu., Naumova E.Yu. 2011. The fine morphology of mouth parts of *Epischura chankensis* Rylov, 1928 (Copepoda, Calanoida). Vladimir Ya. Levanidov's Biennial Memorial Meetings 5: 182–186.

Original Article

ISSN 2658-3518
LIMNOLOGY FRESHWATER BIOLOGY
www.limnolfwbiol.com

Sponges Lubomirskiidae as bioindicators of the state of Lake Baikal

Itskovich V.B.[1,*], Shigarova A.M.[2], Glyzina O.Y.[1], Kaluzhnaya O.V.[1], Borovskii G.B.[2], Selvin J.[3]

[1] *Limnological Institute of the Siberian Branch of the Russian Academy of Sciences, Ulan-Batorskaya 3, 664 033 Irkutsk, Russia.*
[2] *Siberian Institute of Plant Physiology and Biochemistry of Siberian Branch of Russian Academy of Sciences, Lermontova 132, P.O. Box 317, 664033, Irkutsk, Russia*
[3] *Department of Microbiology, School of Life Sciences, Pondicherry University, Puducherry, 605014, India*

ABSTRACT. Sponges are ideal bioindicators of the environmental state due to their simple body structure, filter-feeding lifestyle and widespread abundance.For marine sponges, stress response studies are conducted in the field of microbial composition, gene expression and transcriptome techniques. For freshwater sponges expression of the stress protein HSP70 was studied. In the Baikal sponges, the content of HSP70 is an indicator of the stress response to temperature increase. Transcriptomic studies of the endemic Baikal sponges are in progress.

Keywords: Porifera, bioindicators, Lake Baikal, Lubomirskiidae, HSP70, hyperthermia

1. Introduction

Sponges (Porifera) are the earliest multicellular animals and important component of marine and freshwater ecosystems (Diaz and Rützler, 2001; Bell, 2008; Van Soest et al., 2012; Webster et al., 2013). Sponges show remarkable ecological adaptability and they were able to inhabit all aquatic ecosystems of the Earth.

Sponges are ideal bioindicators of the environmental state, due to their simple body structure, species richness, filter-feeding life style and widespread abundance. Sponges pump large quantities of water and have ability to concentrate a wide range of chemicals from both the suspended and dissolved phases of the water (Orani et al., 2018). Additionally, sponges are highly tolerant of some pollutants and have detoxification systems, making them suitable model organisms for monitoring studies (Orani et al., 2018).

For all monitoring programs, it is important to identify monitoring parameters and to determine the most appropriate indicators. In particular, for sponge monitoring a focus on specific sponge populations with estimates of abundance and taxonomic composition at regular intervals should be a important part of the program (Bell et al., 2017). Sponge tissue can be sampled periodically for microbial community composition, metabolite production and stress protein expression, which will provide a large amount of data. The studies of the influence of changes in environmental conditions on these parameters are limited, although sponges have shown to be very sensitive to changes in surrounding conditions (López-Legentil et al., 2008; Pantile and Webster, 2011).

For marine sponges, stress response studies were conducted in the field of microbial composition, gene expression and transcriptome techniques. The understanding of molecular mechanisms of the sponge stress response is poor, since most studies focus on the effect of stress on the sponge-associated microbial community (Selvin et al., 2009; 2010; Kiran et al., 2018). However, the microbial composition has a large intraspecific and interspecific variability, as well as varies by depth and season (Selvin et al., 2009).

Changes in the gene expression patterns of stress proteins can serve as a biomarker to assess levels of acute stress and determine the environmental load on a sponge (Bell et al., 2017). Heat shock proteins (Hsps) play an important role in maintaining protein homeostasis during adaptation of organisms to variable environmental conditions (Parsell and Lindquist, 1993; Feder and Hofmann, 1999; Tomanek, 2010). Previous studies demonstrated enhanced transcription of HSP70 in marine sponges undergoing temperature stress, osmotic shock, pH stress, heavy metals and phenols stress (Schröder et al., 2006; López-Legentil et al., 2008; Webster et al., 2013).

The studies on the stress response of freshwater sponges are rare. HSP70 expression was first shown in the freshwater sponge *Ephydatia fluviatilis* (Müller

*Corresponding author.
E-mail address: itskovich@mail.ru (V.B. Itskovich)

et al., 1995). In thermally stressed *Spongilla lacustris* HSP70 level patterns resemble those of gene expression patterns and exhibit an even greater intensity and sensitivity (Schill et al., 2006). In gemmules (resting bodies that contain totipotent cells) of the freshwater sponge *S. lacustris*, increased levels of cellular HSP70 and hsp70 mRNA likely allow the gemmules to stabilize their proteins and membranes when the water temperature changes (Schill et al., 2006). Increased HSP70 level was detected in the Lake Baikal sponges *Lubomirskia abietina* and *Baikalospongia intermedia* after exposure at the elevated temperature of 20°C, waste water from the Baikal Pulp and Paper Mill, lead and zinc, while copper had no effect (Efremova et al., 2002; Schröder et al., 2006).

Lake Baikal is the oldest and deepest lake in the world. Its age is estimated at 35 million years, and its maximum depth has been recorded at 1,647 meters. Endemic species in the lake evolved into species flocks and form special mechanisms for adaptation. The Lake Baikal endemic sponge of the family Lubomirskiidae constitutes the bulk of benthic biomass and includes thirteen described species and two subspecies (Efremova, 2001; 2004; Itskovich et al., 2017). *Lubomirskia baicalensis* inhabits depths of 3-120 meters and dominates the littoral zone of the lake (Masuda, 2009). We analyzed the effect of increasing temperatures on the dynamics of the HSP70 level in Baikal endemic sponge *Lubomirskia baicalensis* to evaluate this marker as a possible bioindicator.

2. Materials and methods

Samples of *L. baicalensis* were collected by SCUBA diving in August 2013 in the Southern basin of Lake Baikal near the Bol'shye Koty settlement at a depth of 10 m. Immediately after transfer to the laboratory, sponge specimens (n = 3) were placed into an aquarium with Baikal water and were kept at 4°C with 12h/12h light-dark cycles and aeration for 14 days to achieve acclimatization (Fig. 1). One part (5 cm lengths) of each sponge was cultivated in a 6 L aquarium at 9°C and 13°C with daily water exchange. The controls were continuously kept at 4 °C for one month. Temperatures of 9°C and 13°C were chosen according to data on the variation of the fatty acid composition of total lipids in *L. baicalensis* during aquarium cultivation at these temperatures (Glyzina and Glyzin, 2014). Incubation times were 2 h, 15 h and 7 days. Subsequently, small parts (in triplicate samples) of each sponge were frozen in liquid nitrogen.

Total protein was extracted from three replicates of each sample frozen in liquid nitrogen immediately after the temperature treatment. Protein from the *L. baicalensis* sponge was extracted as described previously (Voinikov et al., 1986). Protein concentration in the samples was determined with Quant-iT™ Protein Assay Kit (Thermo Fisher Scientific). 30 μg of protein from each sample were separated by electrophoresis in 12% SDS-PAGE (Laemmli, 1970) then the protein was transferred onto a nitrocellulose membrane in a

Fig. 1. Endemic Baikal sponge *Lubomirskia baicalensis* (Pallas, 1773)

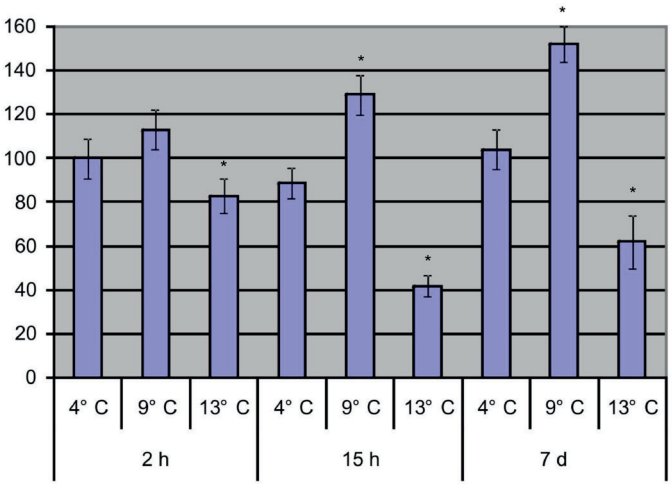

Fig. 2. The relative HSP70 levels in *L. baicalensis* exposed to thermal stress at 9 °C and 13 °C for 2 hours, 15 hours and 7 days. The HSP70 level of sponge kept at 4 °C for 2 hours was estimated as 100%. Means ± SD. Asterisks indicate significant difference ($p < 0.05$) from the control

mini–Protean III (Bio–Rad, USA) system following the manufacturers protocol.

HSP70 was detected with antibodies, as described previously (Timmons and Dunbar, 1990). Primary antibodies against HSP70 were used (Cat. No H5147 «Sigma», USA). The antibodies were visualized with secondary antibodies conjugated with alkaline phosphatase («Sigma», USA). The intensity of spot coloring was determined with Gel Analysis software and expressed as percentage of intensity to the spot coloring of the protein in the control (= 100%, left bar in figures) as previously described (Itskovich et al., 2018).

Statistical analysis included mean ± SD, normality test (Shapiro–Wilk), and one-way analysis of variance (ANOVA) with SigmaPlot (V12.0, SysStat Software Inc., Ca, USA). Statistical significance was tested by the Fisher LSD method.

3. Results and discussion

To study the effect of elevated temperatures on the dynamics of HSP70 accumulation in the Baikal endemic sponge *L. baicalensis* we used two elevated temperature. Constitutive synthesis of HSP70 was detected in samples immediately after sampling. After acclimatization and further keeping in the aquarium during 1 month at 4 ˚C we did not detect increased Hsp70 levels, which indicate appropriate cultivation conditions.

We have determined that after the temperature rise from 4˚C to 9˚C the HSP70 level increased in 2 hours to 110% compared to the control, and in 15 hours it further increased to 130% (Fig. 2). However, when the temperature rose to 13˚C, the HSP70 level decreased in 2 hours to 80% and in 15 hours − to 40% in comparison with the control. After 7 days of incubation at 9˚C the HSP70 level increased to 150% compared to the control (Fig. 2). Thus, the rising temperature to 9˚C increased the HSP70 level in *L. baicalensis*, but the temperature rise to 13˚C reduced the HSP70 , indicating the inhibition of metabolism.

Our experimental data have shown that the Baikal sponges respond to a rise in temperature by changing the content of HSP70. The detected temperature optimum of *L. baicalensis* associated with the environmental conditions of its natural habitat. *L. baicalensis* is a littoral species inhabiting the depths of 3-120 m (Efremova, 2001; Masuda, 2009). The water temperature in the lake at a depth below 250 m is a constant 3.3 - 4.3˚C, but during warming up periods in summer it can reach 12-13 ˚C in some places at 10 m depth (Shimaraev et al., 1994; Timoshkin et al., 2009). In bays and the Maloye More Strait (Central Baikal) temperature fluctuations are most significant, from 0.1 to 25˚C (Kozhova and Izmest'eva, 1998).

Along with the experimental data, the development of bioindicators and assessment of the state of the lake ecosystem requires research in natural conditions. The study of the stress response of the Baikal sponges is relevant in connection with a mass sponge bleaching event which has been detected recently (Kaluzhnaya and Itskovich, 2015; Timoshkin et al., 2016; Itskovich et al., 2018; Khanaev et al., 2018; Kulakova et al., 2018). In situ sponge surveys should be performed to estimate HSP70 level and gene expression and these data can be used to assess the health status of sponges in Baikal. In marine sponge *Xestospongia muta,* two types of bleaching have been described: cyclic bleaching, from which sponges can recover, and fatal bleaching, which usually results in sponge death (López-Legentil et al., 2008). Unlike cyclically bleached tissues, fatally bleached samples had higher hsp70 gene expression. At the same time both cyclic and fatally bleached tissues had lower chlorophyll a concentrations than unbleached tissue. Therefore hsp70 expression was a better indicator between fatal and cyclical bleaching, compared to chlorophyll a content (López-Legentil et al., 2008). Our preliminary study revealed the decreased HSP70 level of in *L. baicalensis* both in the case of bleaching after exposure to 13 ˚C, and in diseased individuals from Lake Baikal (Itskovich et al., 2018). At present, little is known about the HSP70 production in response to chronic stress, since most studies deal with acute stress of Porifera (Bell et al., 2017). Mass sponge disease in Lake Baikal indicates that sponges are subject to chronic stress in the lake. Longer observations of the HSP content and gene expression in diseased and healthy sponges from Lake Baikal can provide information about their ability to recover.

The complete information about changes in gene expression can be obtained by transcriptome-wide survey. Study of gene expression dynamics in the shallow-water sponge *Haliclona tubifera* by high-throughput transcriptome sequencing revealed activation of various processes that interact to maintain cellular homeostasis during stress response to elevated temperature (Guzman and Conaco, 2016). Heat shock proteins, antioxidants, and genes involved in signal transduction and innate immunity pathways were upregulated after short-term thermal stress whereas prolonged exposure resulted in higher expression of genes involved in cellular damage repair, apoptosis, signaling and transcription (Guzman and Conaco, 2016). While in *L. baicalensis* HSP70 level was decreased at sublethal temperature, in *H. tubifera* the relative expression of Hsp70 was strongly upregulated during exposure to sublethal temperature (Guzman and Conaco, 2016). This may indicate that *L. baicalensis* has greater sensitivity to thermal stress then *H. tubifera* due to living in more stable conditions. These results may also indicate differences in gene expression and protein content of HSP70 due to posttranscriptional regulation. Combining transcriptome data with those on protein content would provide important information about the stress response of sponges. Transcriptomic studies of the endemic Baikal sponges are in progress.

4. Conclusion

HSP70 is a molecular indicator which can provide early identification of environmental stress on aquatic communities. Our data have shown that the changes in HSP70 content accurately reflect the stress response to elevated temperature in *L. baicalensis* and, therefore, is indicative and can serve as an early marker of environmental stress. The in situ studying of chronic stress by evaluating gene expression and protein content would contribute to a better understanding of the potential mechanisms of adaptation, resilience and conservation of sponges.

Acknowledgements

This study was performed within the framework of the State project No. 0345-2019-0002 (AAAA-A16-116122110066-1) and partially supported by RFBR grant No. 17-04-01598 and RFBR and the Government of the Irkutsk region grant No. 17-44-388103. This work was conducted using unique scientific installation "Experimental freshwater aquarium complex of Baikal hydrobionts" (Limnological Institute SB RAS).

References

Bell J.J. 2008. The functional roles of marine sponges. Estuarine Coastal and Shelf Science 79: 341–352. DOI: 10.1007/s10750-013-1799-8

Bell J.J., Biggerstaff A., Bates T. et al. 2017. Sponge monitoring: moving beyond diversity and abundance measures. Ecological Indicators 78: 470–488. DOI: 10.1016/j.ecolind.2017.03.001

Cebrian E., Uriz M.J., Turon X. et al. 2007. Sponges as biomonitors of heavy metals in spatial and temporal surveys in northwestern mediterranean: multispecies comparison. Environmental Toxicology and Chemistry 26: 2430–2439. DOI: 10.1897/07-292.1

Cebrian E., Uriz M.J., Garrabou J. et al. 2011. Sponge mass mortalities in a warming mediterranean sea: are cyanobacteria-harboring species worse off? PLoS One 6. DOI: 10.1371/journal.pone.0020211.

Diaz M.C., Rutzler. K. 2001. Sponges: an essential component of Caribbean coral reefs. Bulletin of Marine Science 69: 535–546. DOI: 10.1371/journal.pone.0098181

Efremova S.M. 2001. Sponges (Porifera). In: Timoshkin O.A. (Ed.), Index of animal species inhabiting Lake Baikal and its catchment area. Novosibirsk, pp. 182–192. (in Russian).

Efremova S., Itskovich V., Parfenova V. et al. 2002. Lake Baikal: a unique place to study evolution of sponges and their stress response in an environment nearly unimpaired by anthropogenic perturbation. Cellular and Molecular Biology 48: 359–371.

Efremova S.M. 2004. New genus and new species of sponges from family Lubomirskiidae Rezvoj, 1936. In: Timoshkin O.A. (Ed.), Index of animal species inhabiting Lake Baikal and its catchment area. Novosibirsk, pp. 1261–1278. (in Russian).

Feder M.E., Hofmann G.E. 1999. Heat-shock proteins, molecular chaperones and the stress response: evolutionary and ecological physiology. Annual Reviews of Physiology 61: 243–282. DOI: 10.1146/annurev.physiol.61.1.243.

Glyzina O.Yu., Glyzin A.V. 2014. Biochemical adaptation of *Lubomirskia baicalensis* Baikal sponge to changes in temperature conditions of the environment. Water: Chemistry and Ecology 1: 71–79.

Guzman C., Conaco C. 2016. Gene expression dynamics accompanying the sponge thermal stress response. PLoS One 27: 11. DOI: 10.1371/journal.pone.0165368.

Itskovich V., Kaluzhnaya O., Veynberg Y. et al. 2017. Endemic Lake Baikal sponges from deep water. 2: Taxonomy and bathymetric distribution. Zootaxa 4236: 335–342. DOI: 10.11646/zootaxa.4236.2.8

Itskovich V.B., Shigarova A.M., Glyzina O.Y. et al. 2018. Heat shock protein 70 (Hsp70) response to elevated temperatures in the endemic Baikal sponge *Lubomirskia baicalensis*. Ecological Indicators 88: 1–7. DOI: 10.1016/j.ecolind.2017.12.055

Kaluzhnaya O.V., Itskovich V.B. 2015. Influence of Baikal sponge bleaching to taxonomic composition of symbiotic microorganisms. Russian Journal of Genetics 51: 1–6. DOI: 10.1134/S1022795415110071

Khanaev I.V., Kravtsova L.S., Maikova O.O. et al. 2018. Current state of the sponge fauna (Porifera: Lubomirskiidae) of Lake Baikal: sponge disease and the problem of conservation of diversity. Journal of Great Lakes Research 44: 77–85. DOI: 10.1016/j.jglr.2017.10.004

Kültz D. 2005. Molecular and evolutionary basis of the cellular stress response. Annual Review of Physiology 67: 225–257.

Kiran G.S., Sekar S., Ramasamy P. et al. 2018. Marine sponge microbial association: towards disclosing unique symbiotic interactions. Marine Environmental Research 140: 169–179. DOI: 10.1016/j.marenvres.2018.04.017.

Kozhova O.M., Izmest'eva L.R. 1998. Lake Baikal – evolution and biodiversity. Leiden: Backhuys Publishers.

Kulakova N.V., Sakirko M.V., Adelshin R.V. et al. 2018. Brown rot syndrome and changes in the bacterial community of the Baikal sponge *Lubomirskia baicalensis*. Microbial Ecology 75: 1024–1034. DOI: 10.1007/s00248-017-1097-5

López-Legentil S., Song B., McMurray S.E. et al. 2008. Bleaching and stress in coral reef ecosystems: Hsp70 expression by the giant barrel sponge Xestospongia muta. Molecular Ecology 17: 1840–1850. DOI: 10.1111/j.1365-294X.2008.03667.x.

Masuda Y. 2009. Studies on the taxonomy and distribution of freshwater sponges in Lake Baikal. Progress in Molecular and Subcellular Biology 47: 81–110. https://doi.org/10.1007/978-3-540-88552-8_4

Müller W.E.G., Koziol C., Kurelec B. et al. 1995. Combinatory effects of temperature stress and nonionic organic pollutants on stress protein (hsp70) gene expression in the fresh water sponge *Ephydatia fluviatilis*. Environmental Toxicology and Chemistry 14: 1203–1208. DOI: 10.1002/etc.5620140712

Orani A.M., Baratsa A., Vassileva E. et al. 2018. Marine sponges as a powerful tool for trace elements biomonitoring studies in coastal environment. Marine Pollution Bulletin 131: 633–645. DOI: 10.1016/j.marpolbul.2018.04.073

Pantile R., Webster N.S. 2011. Strict thermal threshold identified by quantitative PCR in the sponge *Rhopaloeides odorabile*. Marine Ecology Progress Series 431: 97–105. DOI: 10.3354/meps09128

Parsell D.A., Lindquist S. 1993. The function of heat-shock proteins in stress tolerance: degradation and reactivation of damaged proteins. Annual Review of Genetics 27: 437–496. DOI: 10.1146/annurev.ge.27.120193.002253

Schill R.O., Pfannkuchen M., Fritz G. et al. 2006. Quiescent gemmules of the freshwater sponge, *Spongilla lacustris* (Linnaeus, 1759), contain remarkably high levels of Hsp70 stress protein and hsp70 stress gene mRNA. Journal of Experimental Zoology. Part A. Comparative Experimental Biology 305: 449–457. DOI: 10.1002/jez.a.281

Selvin J., Priya S.S., Kiran G.S. et al. 2009. Sponge associated marine bacteria as indicators of heavy metal pollution. Microbiological Research 164: 352–363. DOI: 10.1016/j.micres.2007.05.005

Selvin J., Ninawe A.S., Kiran G.S. et al. 2010. Sponge-microbial interactions: ecological implications and bioprospecting avenues. Critical Reviews Microbiology 36: 82–90. DOI: 10.3109/10408410903397340

Shimaraev M.N., Verbolov V.I., Granin N.G. et al. 1994. Physical limnology of Lake Baikal: a review. Irkutsk and Okayama: BICER Publishers.

Schröder H.C., Efremova S.M., Margulis B.A. et al. 2006. Stress response in Baikalian sponges exposed to pollutants. Hydrobiologia 568: 277–287. DOI: 10.1007/s10750-006-0302-1

Timmons T.M., Dunbar B.S. 1990. Protein blotting and immunodetection. Methods in Enzymology 182: 679–688.

Timoshkin O.A., Ivanov V.G., Obolkin V.A. et al. 2009. Water temperature dynamics in the shallow zone of western coast of southern Baikal in the area of interdisciplinary test site Berezovy as revealed from non-stop measurements by onset StowAway TidbiT loggers. In: Timoshkin O.A. (Ed.), Index of animal species inhabiting Lake Baikal and its catchment area. Novosibirsk, pp. 727–731. (in Russian)

Timoshkin O.A., Samsonov D.P., Yamamuro M. et al. 2016. Rapid ecological change in the coastal zone of Lake Baikal (East Siberia): is the site of the world's greatest freshwater biodiversity in danger? Journal of Great Lakes Research 42: 487–497. DOI: 10.1016/j.jglr.2016.02.011

Tomanek L. 2010. Variation in the heat shock response and its implication for predicting the effect of global climate change on species' biogeographical distribution ranges and metabolic costs. Journal of Experimental Biolology 213: 971–979. DOI: 10.1242/jeb.038034

Van Soest R.W.M., Boury-Esnault N., Vacelet J. et al. 2012. Global diversity of sponges (Porifera). PLoS One 7. DOI: 10.1371/journal.pone.0035105

Voinikov V.K., Ivanova G.G., Korytov M.V. 1986. Protein synthesis in plants at low temperature. Physiology and Biochemistry of Cultivated Plants 18: 211–222.

Webster N., Pantile R., Botté E. et al. 2013. Complex life cycle in a warming planet: gene expression in thermally stressed sponges. Molecular Ecology 22: 1854–1868. DOI: 10.1111/mec.12213

Limnology and Freshwater Biology 2019 (1): 177-180 DOI:10.31951/2658-3518-2019-A-1-177

Original Article

ISSN 2658-3518
LIMNOLOGY FRESHWATER BIOLOGY
www.limnolfwbiol.com

Vertical distribution of zooplankton after rapid change in temperature and chlorophyll concentration

Makarov M.M.*, Kucher K.M., Naumova E.Yu.

Limnological Institute, Siberian Branch of the Russian Academy of Sciences, Ulan-Batorskaya Str., 3, Irkutsk, 664033, Russia

ABSTRACT. In October 2018, after the change in the temperature profile and chlorophyll concentration, we recorded the changes in the distribution parameters of mesozooplankton in the surface 100 m layer at the station located in the pelagic zone of Lake Baikal. The study was carried out on horizons of 0-50 and 50-100 m. Measurements were performed using an AAQ-Rinko water quality probe (JFE, Japan), a SBE-25 CTD probe (SeaBirdElectronics, USA) and a Furuno FCV-1100 sonar (Furuno, Japan). We found a deepening of zooplankton after the immersion of the chlorophyll and temperature maximum.

Keywords: Lake Baikal, chlorophyll, zooplankton, contemporary approaches, water quality probe, sonar

Introduction

Plankton is a complex three-dimensional system, which rapidly changes with time. The changes depend on physical and chemical factors that are daily, seasonal, etc. The vertical distribution of zooplankton is associated with the changes in biological parameters: the food volume and the presence of predators. Zooplankton itself affects the environment, consuming algae and returning nutrients to the environment, as well as changes the existence conditions of phyto- and bacterioplankton. Many aspects of this issue have not been yet understood for Lake Baikal: the formation of the zooplankton microlayers, environmental implication of stratification and turbulent mixing (Melnik et al., 2008; Hampton et al., 2014). Due to global climate change, ecological monitoring programs for large lakes should combine high spatial and temporal resolution of data collection, which requires innovative instruments and contemporary approaches (Hampton, 2013; Izmest'eva et al., 2016).

Instrumental methods for studying zooplankton allow almost real-time tracking of the changes in the vertical and horizontal distribution and state. Additionally, conventional net and bathometer sampling followed by laboratory processing can supplement the accurate data on the quality and quantity of planktonic organisms. Thus, it is possible to create an accurate picture in almost real time scale.

The aim of this study was to correlate the rapidly changing environmental factors with the behaviour of zooplankton.

Material and methods

The study was carried out near Cape Berezovy, Southern Baikal, at a depth of 1338 m on October 11 and 19, 2018 (51,7849°N; 104,9329°E). Time was 17:00-19:00. Water temperature, chlorophyll, photosynthetically active radiation and other parameters were measured with a AAQ-Rinko probe. The Table 1 shows the probe specifications in detail.

In addition to the AAQ-Rinko data, we had access to the data from SBE-25 CTD-probe, which was used at the same stations with a delay of 5-10 minutes. The hydroacoustic survey was performed with an upgraded FCV-1100 sonar. The sonar was configured as follows: signal frequency – 28 kHz, the pulse repetition rate – 5 Hz and the pulse duration – 0.3 ms. The 3 dB beam width of the single beam hydroacoustic transducer was 12°. Mesozooplankton were sampled with Juday net of 88 μm mesh size (open diameter 35,7 cm) at 0 – 50, 50 – 100 m, fixed in 4% formalin and counted under a light microscope after concentration by sedimentation.

Results and discussion

The temperature profile obtained using the SBE-25 probe correlates well with the hydroacoustic survey data. Within the depth range of 100-150 m, there are sound scattering layers (SLs) resulted from an abrupt decrease in temperature by 3°C, from 7.5 to 4.5°C.

Figure 1 shows the data on the hydroacoustic survey and CTD profiling up to a depth of 110 m, which

*Corresponding author.
E-mail address: mmmsoft@hlserver.lin.irk.ru (M.M. Makarov)

Table 1. AAQ-Rinko probe instrument specifications

Measured parameter	Measurement range	Resolution	Accuracy	Response time
Depth	0 - 100 m	0.002 m	±0.3% of full scale	0.2 s.
Water temperature	-3 - 45 °C	0.001 °C	±0.01 °C (0 - 35 °C)	0.2 s.
Electrical conductivity	0 – 2000μS cm^{-1}	0.1μS cm^{-1}	±2 μS cm^{-1} (0 to 200μS cm^{-1})	0.2 s.
Suspended matter	0 - 1,000 FTU	0.03 FTU	±0.3 FTU or ±2%	0.2 s.
Chlorophyll	0 – 400 mgm^{-3}	0.01 mgm^{-3}	±1% of full scale	0.2 s.
Dissolved oxygen	0 – 20 mgL^{-1} (0 - 200%)	0.001- 0.004 mg L^{-1}	±0.4mg L^{-1} (±2% of full scale)	0.4 s.
Photosynthetically active radiation in water	0 - 5,000 μ$molm^{-2}s^{-1}$	0.1 μ$molm^{-2}s^{-1}$	±4%	0.2 s.
pH value	2 - 14 pH	0.01 pH	±0.2 pH	10 s.
Oxidation / reduction potential	0 - ±1,000 mV	0.1 mV	-	10 s.

were performed on October 11, 2018. A week later (October 19, 2018), we performed a second survey at this site. There was windy weather for several days, which caused the intense mixing of the upper 100-meter water layer (see Fig. 2). The temperature rise remained at the same depth. There were no significant SLs.

The average temperature of the surface 20-meter layer was 8-8.5°C, which decreased to 7.5°C at a depth of 100 m. After the mixing, we observed (Fig. 1) the immersion of the layer with a temperature of approximately 8°C up to 70 m. Below, the temperature of approximately 7.5°C remained.

In oligotrophic water bodies and in Baikal Lake, there is a high correlation between the vertical distribution of chlorophyll and temperature (Hampton et al., 2008; Watkins et al., 2015; Shimaraeva et al., 2017) In the surface layer, chlorophyll a varied significantly (0.58–5.3 mg/m^3) in July 2018 (Churilova et al., 2018). We could observe a maximum of chlorophyll in the 0-20 m layer with a concentration of 1.2 mg/m^3. Below 50 m, we observed an abrupt decrease in the concentration to 0.7 mg/m^3 and an increase in the concentration to 0.8 mg/m^3 at a depth of 90 m. After mixing, the picture changed, and the concentration gradually decreased from 1.1 mg/m^3 in the surface layer to 0.8 mg/m^3 in the layer below 70 m.

Normally, in autumn three groups play the main role in zooplankton of the Baikal pelagic zone: Copepoda, Cladocera and Rotifera. The copepods *Epischura baikalensis* Sars and *Cyclops kolensis* Lilljeborg are almost constant habitants here (Mazepova, 1998; Melnik et al., 1998). The fauna of rotifers in open waters is mostly based on paleo- and Holarctic species, which are widespread in lakes of northern latitudes. They form two ecological groups of rotifers, all-season and summer-autumn ones. The first group includes *Keratella quadrata* (Müller), *K. cochlearis* (Gosse), *Kellicottia longispina* (Kellicott) and *Filinia terminalis* Plate. The second group includes 19 species and has a very variable species composition in different years. Endemic species form the third ecological group, spring rotifers, which occur only from December to June-July.

In our samples, there were *E. baikalensis* and *C. kolensis* from the Copepoda group. *Bosmina longirostris* (O.F.Müller) was the only representative of Cladocera in the pelagic plankton. All-season rotifers were found

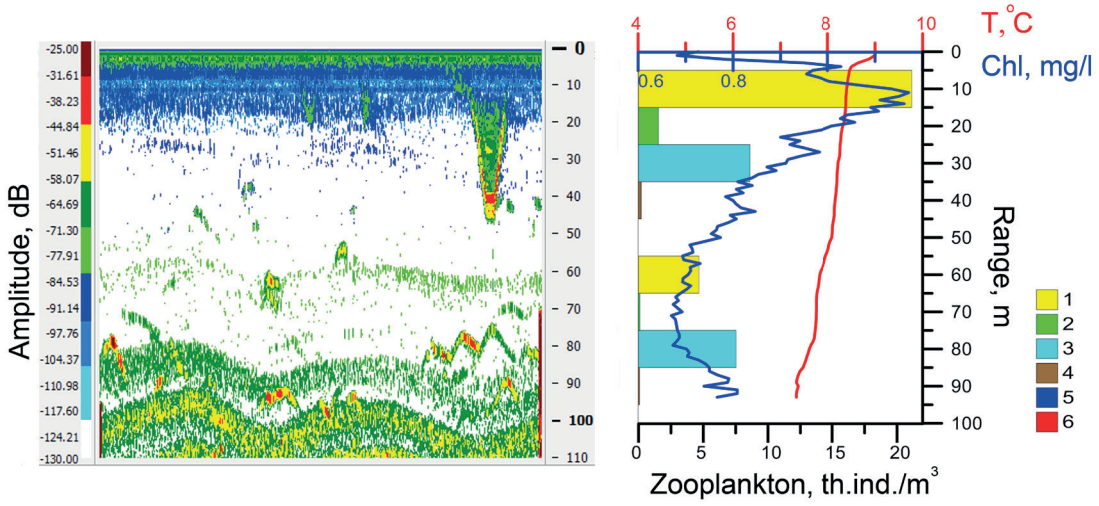

Fig. 1. Echogram, temperature and chlorophyll profile, zooplankton concentration obtained in 3 km from Cape Berezovy on October 11, 2018. 1- All-season Rotifera; 2- Summer Rotifera; 3- Copepoda; 4- Cladocera; 5- Chlorophyll; 6- Temperature

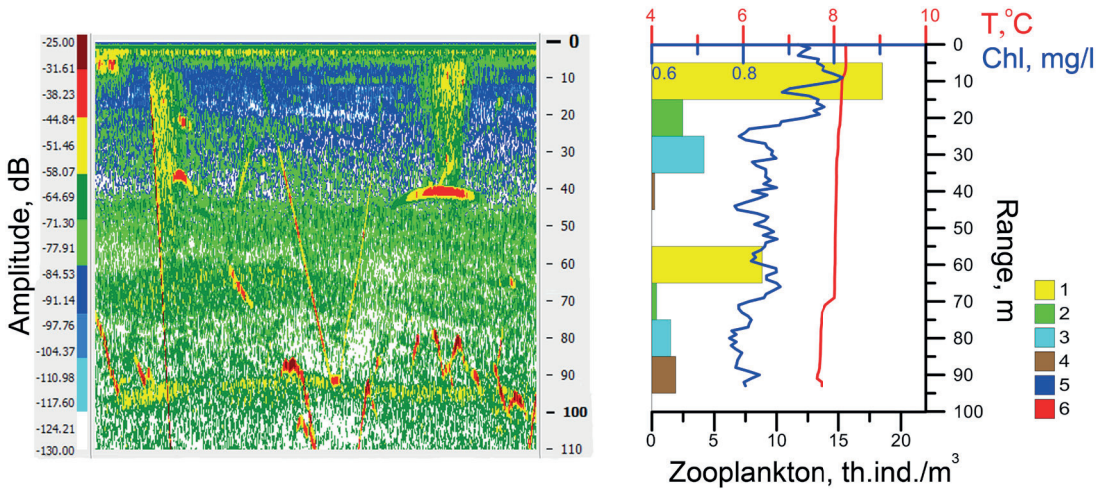

Fig. 2. Echogram, temperature and chlorophyll profile, zooplankton concentration obtained in 3 km from Cape Berezovy on October 19, 2018

in all samples. The number and species composition of summer-autumn rotifers were higher on October 11. Thus, the samples contained: *Bipalpus hudsoni* (Imhof), *Synchaeta stylata* Wierzejski, *Synchaeta grandis* Zacharias, *Collotheca sp.sp., Lecane(M) lunaris* (Ehrenberg), *Asplanchna priodonta* Gosse, *Polyarthra dolichoptera* Idelson, and *Trichocerca capucina* (Wierzejski et Zacharias).

On October 11, in the upper 50 m layer epishura dominated mesozooplankton (Table 2). The plankton contained all age stages, but copepodite stages 4 and 5, as well as nauplius stages 4 and 5 prevailed. The number of *Bosmina longirostris* reached 0.2 thousand ind./m^3 in the surface layer and 0.09 thousand ind./m^3 in the layer below 50 m. *Keratella quadrata* and *Filinia terminalis* dominated rotifers. The total number of *C. kolensis* was up to 0.4 thousand ind./m^3 in the surface layer, where rotifers and cladocerans concentrated. Below 50 m, the zooplankton concentration decreased. The age structure of epishura changed. In this layer, nauplius stages 3 and 4 prevailed. Therefore, most of the copepodite stages of epishura and *C. kolensis* were in the layer of the maximum chlorophyll. The surface layer also contained 74% of the total number of all-season rotifers and 91% of the total number of summer-autumn ones.

After wind mixing, on October 19 the zooplankton concentration in the surface layer decreased. Epishura nauplius stages 3 - 5 and copepodite stages 4 and 5 predominated near the surface. *Bosmina longirostris* was 0.2 thousand ind./m^3 in the surface layer and 0.2 thousand ind./m^3 below 50 m. The number of rotifers remained almost the same near the surface. They were represented by all-season complex and *S. stylata* together with *S. grandis* (2.5 thousand ind./m^3). Below 50 m, epishura nauplius stages 3 and 4 and copepodite stages 1 and 2 predominated. The composition of rotifers was the same as in the surface layer. In the distribution of epishura, adult specimens and copepodites deepen in the layer of 50-100 m. At the same time, they are very likely to be found in a significant number below 100 m from the surface. This may explain the overall decrease in zooplankton biomass in the surface layers after mixing and immersion of the high temperature and chlorophyll layer. During the autumn overturn the chlorophyll *a* reached depths 200 m (Fietz et al., 2005).

The total zooplankton number in the layer of 0-100 m before and after mixing was almost the same (19.7 and 19.1 thousand ind./m^3, respectively). At the same time, the biomass decreased by 42 %. We assume that this was due to the deepening of the crustaceans to a layer below 100 m.

Table 2. Abundance and biomass of zooplankton at the station 3 km from Cape Berezovy

	October 11, 2018		October 19, 2018	
	0-50 m	50-100 m	0-50 m	50-100 m
Zooplankton number, thousand ind./m^3	31.5	12.5	25.47	13.1
Zooplankton biomass, mg/m^3	225.5	84.4	102.0	61.3
Epishura nauplii number, thousand ind./m^3	2.1	6.0	1.3	1.5
Epishura nauplii biomass, mg/m^3	8.9	23.9	5.5	5.8
Number of epishura copepodite stages 1-6, thousand ind./m^3	6.2	1.5	2.6	2.0
Biomass of epishura copepodite stages 1-6, mg/m^3	198.8	55.2	77.9	47.6
Total number of rotifers, thousand ind./m^3	22.7	4.8	21.0	9.2

A high chlorophyll concentration below 50 m creates an active layer for the formation of primary and secondary products (Twiss et al., 2012). This explains the decrease in the number of zooplankton in the surface 50 m layer, which takes place in autumn at high chlorophyll concentrations (Kiprushina, 2009; Pislegina, 2013).

Summary

The preliminary results of complex investigations carried out at Lake Baikal in October 2018 showed that the wind mixing causes an immersion of the layer with a high chlorophyll concentration and a deeper distribution of zooplankton. Temperature can be a marker of the plankton distribution depth. Disregarding the change in patterns of the spatial distribution may lead to an incorrect estimate of the total number of zooplankton and its individual groups. This work allows developing a system for operative (real-time) ecological monitoring.

Acknowledgments

The study was carried out within the project 0345–2019–0008 (AAAA-A16-116122110065-4) “Assessment and forecast of ecological status of Lake Baikal and adjacent areas under the anthropogenic stress and the global climate change”.

References

Churilova T.Ya., Moiseeva N.A., Latushkin A.A. et al. 2018. Preliminary results of bio-optical investigations at Lake Baikal. Limnology and Freshwater Biology 1: 58–61. DOI: 10.31951/2658-3518-2018-A-1-58

Fietz S., Kobanova G., Izmest’eva L. et al. 2005. Regional, vertical and seasonal distribution of phytoplankton and photosynthetic pigments in Lake Baikal. Journal of Plankton Research 27: 793–810. DOI: 10.1093/plankt/fbi054

Hampton S.E. 2013. Understanding lakes near and far. Science 342: 815–816.

Hampton S.E., Gray D.K., Izmest’eva L.R. et al. 2014. The rise and fall of plankton: long-term changes in the vertical distribution of algae and grazers in Lake Baikal, Siberia. PLoS ONE 9. DOI: 10.1371/journal.pone.0088920

Hampton S.E., Izmest’eva L.R., Moore M.V. et al. 2008. Sixty years of environmental change in the in the world’s largest freshwater lake—Lake Baikal, Siberia. Global Change Biology 14: 1947–1958. DOI: 10.1111/j.1365-2486.2008.01616.x

Izmest’eva L.R., Moore M.V., Hampton S.E. et al. 2016. Lake-wide physical and biological trends associated with warming in Lake Baikal. Journal of Great Lakes Research 42: 6–17. DOI: 10.1016/j.jglr.2015.11.006

Kiprushina K.N. 2009. Seasonal dynamics of the zooplankton vertical distribution in the open part of Southern Baikal (near the Bolshiye Koty settlement). The Bulletin of Irkutsk State University. Series “Biology. Ecology” 2: 39–44. (in Russian)

Mazepova G.F. 1998. The role of copepods in the Baikal ecosystem. Journal of Marine System 15: 113–120. DOI: 10.1016/S0924-7963(97)00065-1

Melnik N.G., Dzyuba E.V., Degtyarev V.A. et al. 2008. Life strategy of pelagic animals in Lake Baikal. Verhandlungen des Internationalen Verein Limnologie [Negotiations of the International Limnology Association] 30: 291–294. DOI: 10.1080/03680770.2008.11902129

Melnik N.G., Sheveleva N.G., Pomazkova G.I. 1998. Distribution of planktonic copepods of Lake Baikal. Journal of Marine System 15: 149–153. DOI: 10.1016/S0924-7963(97)00074-2

Pislegina E.V. 2013. Biomass dynamics of phytoplankton, epishura and copepods in the years of their maximum abundance in the pelagic zone of Southern Baikal. Izvestiya Irkutskogo Gosudarstvennogo Universiteta. Seriya “Biologiya, Ecologiya” [The Bulletin of Irkutsk State University. Series “Biology. Ecology”] 6: 100–104. (in Russian)

Shimaraeva S.V., Pislegina E.V., Krashchuk L.S. et al. 2017. Dynamics of chlorophyll *a* concentration in the South Baikal pelagic during the direct temperature stratification period. Inland Water Biology 10: 59–63. DOI: 10.1134/S1995082917010163

Twiss M.R., Ulrich C., Zastepa A. et al. 2012. On phytoplankton growth and loss rates to microzooplankton in the epilimnion and metalimnion of Lake Ontario in mid-summer. Journal of Great Lakes Research 38: 146–153. DOI: 10.1016/j.jglr.2012.05.002

Watkins J.M., Weidel B.C., Rudstam L.G. et al. 2015. Spatial extent and dissipation of the deep chlorophyll layer in Lake Ontario during the Lake Ontario lower food web assessment, 2003 and 2008. Aquatic Ecosystem Health & Management 18:18–27. DOI: 10.1080/14634988.2014.937316

Limnology and Freshwater Biology 2019 (1): 181-198 DOI:10.31951/2658-3518-2019-A-1-181

Original Article

ISSN 2658-3518
LIMNOLOGY FRESHWATER BIOLOGY
www.limnolfwbiol.com

Validation of 123 names of new diatom taxa from Lake Baikal

Pomazkina G.V., Rodionova E.V., Sherbakova T.A.*

Limnological Institute of the Siberian Branch of the Russian Academy of Sciences, Ulan-Batorskaya 3, 664 033 Irkutsk, Russia.

ABSTRACT. The monograph "Benthic diatom algae of the family Naviculaceae of Lake Baikal: Atlas and Key" by Pomazkina et al., published in 2018, in Russian, included 123 diatom taxa new to science along with well-known species. The new names were lacking descriptions in English or Latin and thus not in line with ICN. Herein English descriptions for 123 new species and intraspecific taxa are presented to validate new names for baikalian diatom algae.

Keywords: names, new benthic Bacillariophyta, validation, Lake Baikal

Introduction

The book "Benthic diatom algae of the family Naviculaceae of Lake Baikal: Atlas and Key" by G.V.Pomazkina, E.V.Rodionova & T.A. Sherbakova (in Russian), pp. 315, released in 2018 by "Nauka" (Novosibirsk, Russia), extends the series of "Guides and Keys to Identification of Fauna and Flora of Lake Baikal". The monograph is documenting the diversity of five genera within the family Naviculaceae – the key group of Lake Baikal benthic diatoms. The first part includes a brief history and biogeography of the genera as well as ecological characteristics of areas of Lake Baikal littoral zone with increased diversity of Bacillariophyta especially Naviculaceae. The systematic sections include descriptions for 79 taxa of the genus *Navicula*, 30 of *Hippodonta*, 48 of *Placoneis*, 2 species of *Petroplacus* and 21 of *Paraplaconeis* of which 123 species are new to science including two new genera, *Irkutia* and *Polygonaria*. The name of each taxon is accompanied by synonyms (if available), complete description, location, and electron microscopic images. Since the descriptions for new species were not provided in Latin or English they were not valid according to regulations of the International Code of Nomenclature for algae, fungi, and plants (International code…, 2018). Herein English descriptions and associated information for 123 new taxa are included to validate their names.

Validation

Genus Hippodonta Lange-Bertalot, Witkowski & Metzeltin

Hippodonta acris Pomazkina & Sherbakova sp. nov. (Pomazkina et al., 2018, p. 25, Table 2)

Valves narrowly-rhombic with sharply rounded protracted ends. Length 21.0–21.5 μm, width 4.9–5.0 μm. Axial area narrow, linear. Central area forming the incomplete fascia in a form of a butterfly with 1–2 shortened central striae. Raphe filiform, straight, proximal endings with small pores weakly deflected oppositely, terminal raphe fissures elongated straight. Transapical striae in the middle of the valve slightly radiate, towards the apices becoming parallel then slightly convergent, 12–14 in 10 μm.

Type :—Russia. Lake Baikal, the Olkhon Gates Strait, epilithon, st. 7, 20 m depth, 27 June 1997, collector V. Votyakov (holotype: slide 0017-BK collection "Darwin initiative" housed at the Limnological Institute SB RAS, Irkutsk, Russia; isotype: slide 0017a-BK *ibid.*).

Hippodonta anglica Pomazkina & Rodionova sp. nov. (Pomazkina et al., 2018, p. 27, Table 5)

Valves elliptic with sharply rounded protracted ends. Length 32.0–33.0 μm, width 9.0–10.0 μm. Axial area narrow, linear. Central area transapically widened with shortened striae. Raphe filiform, straight with prominent central and terminal pores. Transapical striae radiate, becoming slightly convergent towards the apices, 9–10 in 10 μm. Interstriae broader than striae.

*Corresponding author.
E-mail address: tsherb@lin.irk.ru (T.A. Sherbakova)

Type :—Russia, Lake Baikal, the Olkhon Gates Strait, epilithon, st. 7, 20 m depth, 27 June 1997, collector V. Votyakov (holotype: slide 0017-BK collection "Darwin initiative" housed at the Limnological Institute SB RAS, Irkutsk, Russia; isotype: slide 0018-BK *ibid.*).

Hippodonta cryptocephala Pomazkina & Rodionova sp. nov. (Pomazkina et al., 2018, p. 28, Table 8).

Valves narrowly-lanceolate with protracted rostrate ends. Length 24.0–25.0 μm, width 6–7 μm. Axial area narrow, linear. Central area slightly transapically widened with shortened striae. Raphe filiform, straight. Proximal raphe endings linear closely positioned, terminal fissures deflected unilaterally. Striae in the middle moderately radiate, towards the apices becoming slightly convergent, 13–14 in 10 μm.

Type :—Russia, Lake Baikal, near Baikalsk sity, silt, st. 40, 20 m depth, 23 June 1998, collector V. Votyakov (holotype: slide 0145-BK collection "Darwin initiative" housed at the Limnological Institute SB RAS, Irkutsk, Russia; isotype: slide 0145a-BK, *ibid.*).

Hippodonta dissimilis Pomazkina & Rodionova sp. nov. (Pomazkina et al., 2018, p. 28, Table 9)

Valve elliptic-lanceolate with rounded protracted ends. Length 25.0 μm, width 5.0 μm. Axial area narrow, linear widening towards the center. Central area small elliptic with shortened striae bordering the central area. Raphe filiform, straight with small proximal pores, distal widening endings deflected to the same side. Transapical striae in the middle of the valve radiate multiseriate 10 in 10 μm, becoming biseriate, convergent and more denser at the apices, 14 in 10 μm. Terminal hyaline areas wide, convex.

Type :—Russia. Lake Baikal, southern basin, near the settlement B. Koty, epilithon, st. 1, 20 m depth, 22 June 1997, collector V. Votyakov (holotype: slide 0001-BK collection "Darwin initiative" housed at the Limnological Institute SB RAS, Irkutsk, Russia; isotype: slide 0001c-BK, *ibid.*).

Hippodonta elliptica Pomazkina & Sherbakova sp. nov. (Pomazkina et al., 2018, p. 29, Table 11)

Valve lanceolate with broadly rounded ends. Length 14.9 μm, width 4.1 μm. Axial area linear continuously widening into the central area forming the incomplete fascia with two shortened striae. Raphe filiform, straight. Proximal and distal raphe endings weakly curved, slightly widened and insignificantly deflected unilaterally. Striae radiate at middle of the valve, slightly convergent near the apices,14 in 10 μm. Interstriae broader than striae.

Type :—Russia. Lake Baikal, the Cape Rytiy, epilithon, st. 10, 20 m depth, 28 June 1997, collector V. Votyakov (holotype: slide 0033-BK collection "Darwin initiative" housed at the Limnological Institute SB RAS, Irkutsk, Russia; isotype: slide 0033c-BK, *ibid.*).

Hippodonta ignita Pomazkina sp. nov. (Pomazkina et al., 2018, p. 29, Table 12)

Valve rombic-lanceolate with sharply-rounded protracted ends. Valve length 18–19 μm, width 4–5 μm. Axial area linear wide. Central area forming the butterfly–shaped fascia continued on the margin. Raphe filiform, straight. Proximal and distal raphe endings direct with teardrop-shaped pores. Striae radiate, spaced, 11–12 in 10 μm. Interstriae broader than striae.

Type :—Russia. Lake Baikal, southern basin, near the settlement B. Koty, epilithon, st. 1, 20 m depth, 22 June 1997, collector V. Votyakov (holotype: slide 0001-BK collection "Darwin initiative" housed at the Limnological Institute SB RAS, Irkutsk, Russia; isotype: slide 0001a-BK, *ibid.*).

Hippodonta incrustata Pomazkina & Rodionova sp. nov. (Pomazkina et al., 2018, p. 29, Table 13)

Valves rhombic-lanceolate with protracted ends. Valve length 10.4–12.1 μm, width 3.5–3.6 μm. Axial area narrow, linear. Central area forming the incomplete fascia with 2 shortened striae bordering the central area. Raphe filiform. Proximal raphe endings with pores weakly one-sided deflected, distal endings with larger pores. Transapical striae in the central part spaced, radiate, towards the apices becoming slightly convergent, 15 in 10 μm.

Type :—Russia. Lake Baikal, southern basin, near the settlement Kultuk, epilithon, st. 42, 13 m depth, 22 June 1998, collector V. Votyakov (holotype: slide 0132-BK collection "Darwin initiative" housed at the Limnological Institute SB RAS, Irkutsk, Russia; isotype: slide 0132a-BK, *ibid.*).

Hippodonta interrupta Pomazkina & Sherbakova sp. nov. (Pomazkina et al., 2018, p. 30, Table 15)

Valve rombic-lanceolate with narrow cuneal rounded ends. Valve length 38–39 μm, valve width 7–8 μm. Axial area narrow, linear. Central area forming the incomplete fascia with two shortened striae bordering the central area. Raphe filiform, straight with widened proximal and distal endings. Striae coarse, radiate, slightly spaced at middle, becoming slightly convergent at apices, 9 –10 in 10 μm. Terminal hyaline areas broad.

Type :—Russia. Lake Baikal, Anga bay, silt and sand, st. 6, 17 m depth, 27 June 1997, collector V. Votyakov (holotype: slide 0114-BK collection "Darwin initiative" housed at the Limnological Institute SB RAS, Irkutsk, Russia; isotype: slide 0115-BK, *ibid.*).

Hippodonta lepida Pomazkina & Rodionova sp. nov. (Pomazkina et al., 2018, p. 31, Table 16)

Valve narrow elliptically-lanceolate with sharp cuneal protracted ends. Valve length 26.4 μm, width 4 μm. Axial area narrow, linear. Central area forming the wide complete fascia. Raphe filiform, straight with closely positioned proximal raphe endings, terminal fissures deflected in one side. Striae radiate, becoming slightly convergent near the apices, 6–7in 10 μm.

Type :—Russia. Lake Baikal, Anga bay, silt and sand, st. 6, 17 m depth, 27 June 1997, collector V. Votyakov (holotype: slide 0114-BK collection "Darwin initiative" housed at the Limnological Institute SB RAS, Irkutsk, Russia; isotype: slide 0115-BK, *ibid.*).

Hippodonta luculenta Pomazkina & Rodionova sp. nov. (Pomazkina et al., 2018, p. 31, Table 17)

Valve linear-lanceolate with broadly rounded protracted ends. Valve length 13.7 μm, width 3.7 μm. Axial area narrow, the central area nearly indistinct. Raphe filiform, straight with widened proximal and distal endings. Striae radiate, becoming convergent towards apices, 6–7 in 10 μm.

Type :—Russia. Lake Baikal, Peschanaya bay, epilithon, st. 3, 17 m depth, 27 June 1997, collector V. Votyakov (holotype: slide 0007-BK collection "Darwin initiative" housed at the Limnological Institute SB RAS, Irkutsk, Russia; isotype: slide 0007a-BK, *ibid.*).

Hippodonta navicula* var. *baicalensis Pomazkina & Sherbakova var. nov. (Pomazkina et al., 2018, p. 33, Table 21)

Valves lanceolate with obtusely rounded ends. Valve length 16–17 μm, width 3–4 μm. Axial area narrow, the central area small rounded with shortened striae. Raphe filiform Straight. Proximal raphe endings with teardrop-shaped pores, distally the raphe ends with long fissures. Both endings slightly deflected into the same side. Striae strongly radiate in the middle of the valve, becoming convergent towards apices, 11–12 in 10 μm. Interstriae in the center broader than striae, closer to apices becoming narrower.

Type :—Russia. Lake Baikal, near the settlement M. Goloustnoe, epilithon, st. 2, 20 m depth, 26 June1997, collector V. Votyakov (holotype: slide 0003-BK collection "Darwin initiative" housed at the Limnological Institute SB RAS, Irkutsk, Russia; isotype: slide 0003c-BK, *ibid.*).

Hippodonta parva Pomazkina & Sherbakova sp. nov. (Pomazkina et al., 2018, p. 33, Table 22)

Valve lanceolate with broadly rounded ends. Valve length 10 μm, width 4.3 μm. Axial area narrow gradually turns into the central area forming the butterfly –shaped fascia continued on the margin. Raphe filiform, straight. Proximal and distal raphe endings slightly widened subtly deflected to the same side. Striae radiate becoming convergent at the apices, 10 in 10 μm.

Type :—Russia. Lake Baikal, the Cape Krestovskiy, stones and silt, st. 5, 20 m depth, 27 June1997, collector V. Votyakov (holotype: slide 0012-BK collection "Darwin initiative" housed at the Limnological Institute SB RAS, Irkutsk, Russia; isotype: slide 0013-BK, *ibid.*).

Hippodonta peculiaris Pomazkina & Rodionova sp. nov. (Pomazkina et al., 2018, p. 34, Table 23)

Valve lanceolate with protracted cuneal ends. Valve length 41.0 μm, width 10.7 μm. Axial area linear gradually turns into the oval central area forming broad fascia with shortened striae. Raphe filiform, straight. Proximal and distal raphe endings direct with elongated teardrop-shaped fissures. Proximal raphe ends very distant. Striae radiate, convergent at the apices, 12 in 10 μm.

Type :—Russia. Lake Baikal, the Cape Krestovskij, stones and silt, st. 5, 20 m depth, 27 June1997, collector V. Votyakov (holotype: slide 0012-BK collection "Darwin initiative" housed at the Limnological Institute SB RAS, Irkutsk, Russia; isotype: slide 0012c-BK, *ibid.*).

Hippodonta rostellata Pomazkina & Rodionova sp. nov. (Pomazkina et al., 2018, p. 34, Table 24)

Valve lanceolate with protracted sharply rounded ends. Valve length 52.4 μm, width 9.0 μm. Axial area linear gradually widening turns into the apically elongated oval central area. Raphe broad, straight. Proximal raphe endings elongated widened direct, distal ends teardrop-shaped subtly deflected to the same side. Striae radiate in the center, spaced, 10 in 10 μm, becoming convergent and denser towards apices, 12 in 10 μm.

Type :—Russia, Lake Baikal, the northern basin, near the Cape Kabanij, epilithon, st. 22, 20 m depth, 04 July 1997, collector V. Votyakov (holotype: slide 0073-BK collection "Darwin initiative" housed at the Limnological Institute SB RAS, Irkutsk, Russia; isotype: slide 0073a-BK, *ibid.*).

Hippodonta scalpelliformis Pomazkina & Sherbakova sp. nov. (Pomazkina et al., 2018, p. 34, Table 25)

Valve lanceolate with broadly rounded ends. Valve length 10.9 μm, width 3.2 μm. Axial area linear gradually widening and turns into the small central area with 2 shortened striae. Raphe filiform, straight with teardrop-shaped widenings of proximal and distal raphe endings. Striae radiate biseriate, becoming slightly convergent at apices, 7–8 in 10 μm.

Type :— Lake Baikal, the Cape Rytyi, epilithon, st. 10, 20 m depth, 28 June 1997, collector V. Votyakov (holotype: slide 0033-BK collection "Darwin initiative" housed at the Limnological Institute SB RAS, Irkutsk, Russia; isotype: slide 0034-BK, *ibid.*).

Hippodonta subsalsa (Grunow) Pomazkina & Rodionova comb. nov. & stat. nov. (Pomazkina et al., 2018, p. 35, Table 27)

Basionym: *Navicula tumida* var. *subsalsa* Grunow 1860: 537, pl. 2: figs 43 b, c

Synonym: *Navicula anglica* var. *subsalsa* (Grunow) Cleve 1895: 22

Valve elliptically-lanceolate with cuneal broadly rounded ends. Valve length 34.0 μm, width 7.5 μm. Axial area linear, central area oval with shortened striae. Raphe filiform, straight with widening proximal and distal raphe endings. Striae radiate, becoming parallel then slightly convergent at apices, 11–12 in 10 μm.

Hippodonta tenuis Pomazkina & Sherbakova sp. nov. (Pomazkina et al., 2018, p. 36, Table 28)

Valve rhombic-lanceolate with protracted sharply rounded ends. Valve length 30.0 μm, width 4.8 μm. Axial area broad , the central area transapically widening forming incomplete fascia with shortened striae. Raphe filiform, straight with small widening of proximal and distal raphe endings. Striae radiate becoming slightly parallel at apices, 13 in 10 μm.

Type :— Lake Baikal, south basin, near the settlement Mangutaj, stones and silt, st. 41, 20 m depth, 22 June 1998, collector V. Votyakov (holotype: slide 0139-BK collection "Darwin initiative" housed at the Limnological Institute SB RAS, Irkutsk, Russia; isotype: slide 0138-BK, *ibid.*).

Hippodonta vadosa Pomazkina & Sherbakova sp. nov. (Pomazkina et al., 2018, p. 36, Table 29)

Valve rhombic-lanceolate with narrow protracted cuneal ends. Valve length 17.8 μm, width 4.7 μm. Axial area narrow, linear , the central area transapically widening forming incomplete fascia with two shortened striae. Raphe filiform, straight with small widening of proximal and distal raphe endings. Striae nearly radiate, spaced in the middle of the valve becoming

slightly convergent at apices, 14 in 10 μm.

Type :— Lake Baikal, Anga bay, silt and sand, st. 6, 17 m depth, 27 June 1997, collector V. Votyakov (holotype: slide 0114-BK collection "Darwin initiative" housed at the Limnological Institute SB RAS, Irkutsk, Russia; isotype: slide 0115-BK, *ibid.*).

Hippodonta ventricosa Pomazkina & Sherbakova sp. nov. (Pomazkina et al., 2018, p. 37, Table 30)

Valves elliptically-lanceolate with broadly-rounded weakly protracted ends. Valve length 13.0–19.0 μm, width 4.0–4.5 μm. Axial area narrow, linear, the central area small, rounded. Raphe filiform, straight with wide teardrop-shaped proximal and distal raphe endings deflected into the same side. Striae nearly radiate in the middle of the valve becoming parallel and slightly convergent at apices, 15–16 in 10 μm.

Type :— Lake Baikal, southern basin, near the settlement B. Koty, epilithon, st. 1, 20 m depth, 22 June 1997, collector V. Votyakov (holotype: slide 0001-BK collection "Darwin initiative" housed at the Limnological Institute SB RAS, Irkutsk, Russia; isotype: slide 0001a-BK, *ibid.*).

Genus Irkutia Pomazkina, Rodionova & Sherbakova gen. nov.

Type generic: *Irkutia dispersepunctata* (Skabitchevsky) Pomazkina & Rodionova comb. nov. (Pomazkina et al., 2018, p. 37)

Cells biraphid, valves isopolar, "naviculoid". Characters of the chloroplast is not yet known. Valves linear to linear–elliptic. Ends slightly protracted, cuneate and obtusely rounded. Raphe filiform, weakly lateral, with fine central endings and long widely rounded to the same side terminal fissures. Striae slightly radiate, punctate.

Central raphe endings slit-like with small pores slightly deflected to the primary side (with an exception of *Irkutia baicalensis* Pomazkina, Rodionova & Sherbakova with short proximal endings abruptly bent contrary). Terminal raphe fissures hooked, both bent in the direction opposite to proximal endings. Striae punctate, slightly radiate, composed of irregular large transapically widened oval areolae. Axial area broad, linear; central area slightly asymmetrically expanded. Axial and central areas are encircled by a row or rows of larger rounded or oval areolae. Internal proximal raphe endings slit-like, short, bent in the same side; distally, the raphe ends with helictoglossae.

Irkutia baicalensis Pomazkina, Rodionova & Sherbakova sp. nov. (Pomazkina et al., 2018, p. 39, Table 31)

Valves linear–elliptic with parallel margins. Length 22–43 μm, width 5.3–6.7 μm. Raphe slightly lateral, filiform with fine central endings that deflected oppositely, terminal fissures widely rounded in the same side. Axial area broad, linear; central area slightly expanded and asymmetric. Striae coarsely punctuate, radiate, 15–16 in 10 μm. Areolae in striae irregular.

Type :— Lake Baikal, the Cape Rytyi, epilithon, st. 10, 20 m depth, 28 June 1997, collector V. Votyakov (holotype: slide 0033-BK collection "Darwin initiative" housed at the Limnological Institute SB RAS, Irkutsk, Russia; isotype: slide 0034-BK, *ibid.*).

Irkutia dispersepunctata (Skabitchevsky) Pomazkina & Rodionova comb. nov. (Pomazkina et al., 2018, p. 39, Table 32)

Basionym: *Navicula dispersepunctata* Skabitchevsky 1936, p. 712, pl. 2, fig. 16.

Valves broadly linear with parallel margins. Ends cuneate, slightly protracted. Length 54–60 μm, width 13.5–14.0 μm. Raphe slightly lateral, filiform with small central pores, terminal fissures long widely rounded oppositely. Axial area broad, linear; central area slightly expanded. Striae coarse, unevenly punctuate, parallel, 13–15 in 10 μm, becoming radiate towards apices, 15–17 in 10 μm.

Irkutia memorabilis Rodionova & Pomazkina sp. nov. (Pomazkina et al., 2018, p. 39, Table 33)

Valves linear-elliptic with parallel margins. Ends cuneate obtusely rounded. Length 36–40 μm, width 9.2–9.8 μm. Raphe slightly lateral, filiform with fine central endings, terminal fissures bent to the same side. Axial area broad, linear; central area slightly expanded. Striae coarse, unevenly punctate, parallel, 13–15 in 10 μm, becoming radiate towards apices, 15–17 in 10 μm.

Type :—Russia, Lake Baikal, the Cape Rytyi, epilithon, st. 10, 20 m depth, 28 June 1997, collector V. Votyakov (holotype: slide 0032-BK collection "Darwin initiative" housed at the Limnological Institute SB RAS, Irkutsk, Russia; isotype: slide 0033-BK, *ibid.*).

Genus Navicula Bory

Navicula admiranda Pomazkina, Rodionova & Sherbakova sp. nov. (Pomazkina et al., 2018, p. 41, Table 34)

Valves lanceolate with strongly protracted rostrate ends. Length 50–67 μm, width 5.3–6.7 μm. Raphe filiform, straight. Axial area narrow; linear; central area transapically widened. Striae lineolate, radiate in the middle of the valve, 8–10 in 10 μm, convergent at the apices, 10–12 in 10 μm. Areolae comparatively dense.

Type :—Russia, Lake Baikal, the Olkhon Gates Strait, the Cape Khara-khulun, epilithon, st. 51, 20 m depth, 25 June 1998, collector V. Votyakov (holotype: slide 0177-BK collection "Darwin initiative" housed at the Limnological Institute SB RAS, Irkutsk, Russia; isotype: slides 0173-BK, 0176- BK, *ibid*).

Navicula affinibaicalensis Pomazkina, Rodionova & Sherbakova sp. nov. (Pomazkina et al., 2018, p. 42, Table 36)

Valves linear-lanceolate with protracted rounded ends. Length 118–140 μm, width 16–20 μm. Raphe filiform, straight, slightly lateral. Axial area narrow becoming wider towards the center; central area indistinct. Striae lineolate, radiate in the middle of the valve, convergent at the apices, 10–12 in 10 μm. Proximal raphe endings with pores, terminal fissures thin, bent.

Type :—Russia. Lake Baikal, Olkhon Island, the Cape Ukhan, epilithon and algae, st. 8, 15 m depth,

28 June 1997, collector V. Votyakov (holotype: slide 0022-BK collection "Darwin initiative" housed at the Limnological Institute SB RAS, Irkutsk, Russia; isotype: slide 0023-BK, *ibid.*).

Navicula angensis Rodionova & Pomazkina sp. nov. (Pomazkina et al., 2018, p. 43, Table 38**)**

Valves lanceolate with strongly protracted sharply rounded ends. Length 43–66 μm, width 11–13 μm. Raphe Straight, slightly lateral. Axial area moderately broad, lanceolate; central area small, oval. Striae lineolate, uneven in length, radiate in the middle of the valve, 8–10 in 10 μm, parallel or convergent at the apices, 12–13 in 10 μm. Proximal raphe endings with pores, terminal fissures widened, then fine and rounded.

Type :—Russia, Lake Baikal, Anga Bay, silt and sand, st. 6, 17 m depth, 27 June 1997, collector V. Votyakov (holotype: slide 0014-BK collection "Darwin initiative" housed at the Limnological Institute SB RAS, Irkutsk, Russia; isotype: slides 0015-BK, 0016-BK, *ibid.*).

Navicula baicaloblonga Pomazkina, Rodionova & Sherbakova sp. nov. (Pomazkina et al., 2018, p. 44, Table 41)

Valves linear-lanceolate with broadly rounded ends. Length 85–115 μm, width 13.8–17.5 μm. Raphe filiform, slightly lateral. Axial area narrow; linear; central area rounded. Striae lineolate, radiate, in the middle of the valve, 7–8 in 10 μm, at the apices, 9–10 in 10 μm. Proximal raphe endings with pores, terminal fissures widened, then fine and bent to one side.

Type :—Russia, Lake Baikal, near Baikalsk sity, silt, st. 40, 20 m depth, 23 June 1998, collector V. Votyakov (holotype: slide 0145-BK collection "Darwin initiative" housed at the Limnological Institute SB RAS, Irkutsk, Russia; isotype: slide 0146-BK, *ibid.*).

Navicula baicalocylindrata Rodionova & Pomazkina sp. nov. (Pomazkina et al., 2018, p. 45, Table 43)

Valves linear-elliptic with broadly rounded slightly protracted ends. Length 15–19 μm, width 4.0–4.2 μm. Raphe filiform, curved. Axial area narrow; linear; central rhombic, widened transapically. Striae lineolate, strongly radiate in the middle of the valve, then abruptly parallel, l6–18 in 10 μm. Proximal raphe endings thing, terminal fissures hooked, bent to one side.

Type :—Russia, Lake Baikal, near Baikalsk sity, silt, st. 47, 20 m depth, 23 June 1998, collector V. Votyakov (holotype: slide 0165-BK collection "Darwin initiative" housed at the Limnological Institute SB RAS, Irkutsk, Russia; isotype: slide 0166-BK, *ibid.*).

Navicula baicalogregaria Pomazkina, Rodionova & Sherbakova sp. nov. (Pomazkina et al., 2018, p. 45, Table 44)

Valves linear-lanceolate with protracted cuneate ends. Length 21–22 μm, width 3.7–3.8 μm. Raphe filiform, uneven. Axial area narrow; linear; central area transapically oval. Striae lineolate, strongly radiate in the middle of the valve, then parallel, 10–11 in 10 μm. Proximal raphe endings thing, terminal fissures hooked, bent to the secondary side.

Type :—Russia, Lake Baikal, the Olkhon Gates Strait, cape Khara-khulun, epilithon, st. 51, 20 m depth, 25 June 1998, collector V. Votyakov (holotype: slide 0177-BK collection "Darwin initiative" housed at the Limnological Institute SB RAS, Irkutsk, Russia; isotype: slide 0176-BK, *ibid.*).

Navicula caudata* var. *austrolacustris Rodionova & Pomazkina var. nov. (Pomazkina et al., 2018, p. 45, Table 48)

Valves linear-elliptic with protracted cuneate ends. Length 45–46 μm, width 15.0–16.0 μm. Raphe weakly lateral, straight. Axial area moderate; central area small, rounded. Striae lineolate, radiate, 7–8 in 10 μm, weakly convergent at apices, 9–10 in 10 μm. Proximal raphe endings with pores, terminal fissures widened, then fine, rounded. Hyaline uneven bands parallel to the edge of the valve.

Type :—Russia, Lake Baikal, near Baikalsk city, silt, st. 40, 20 m depth, 23 June 1998, collector V. Votyakov (holotype: slide 0145-BK collection "Darwin initiative" housed at the Limnological Institute SB RAS, Irkutsk, Russia; isotype: slide 0146-BK, *ibid.*).

Navicula caudata* var. *elliptica Pomazkina, Rodionova & Sherbakova var. nov. (Pomazkina et al., 2018, p. 47, Table 49)

Valves elliptic with cuneate ends. Length 47–54 μm, width 17.0–21.0 μm. Raphe weakly lateral, straight. Axial area broad; central area transapically oval. Striae lineolate, radiate, 8–9 in 10 μm, becoming parallel at the apices, 9–10 in 10 μm. In the middle of the valve long striae alternate short. Proximal raphe endings with pores, terminal fissures widened, then thin and rounded. Hyaline uneven discontinuous bands parallel to the edge of the valve.

Type :—Russia, Lake Baikal, island Olkhon, the Khoboj cape, epilithon and algae, st. 9, 20 m depth, 28 June 1997, collector V. Votyakov (holotype: slide 0027-BK collection "Darwin initiative" housed at the Limnological Institute SB RAS, Irkutsk, Russia; isotype: slide 0028-BK, *ibid.*).

Navicula caudata* var. *romboidea Pomazkina, Rodionova & Sherbakova var. nov. (Pomazkina et al., 2018, p. 48, Table 50)

Valves elliptically-rhombic with cuneate ends. Length 47–50 μm, width 19.0–20.0 μm. Raphe weakly lateral, straight. Axial area narrow; central area transapically widened. Striae lineolate, radiate, 8–9 in 10 μm, becoming parallel or slightly convergent at the apices, 9–10 in 10 μm. In the middle of the valve striae shortened. Proximal raphe endings with pores, terminal fissures widened, then thin and rounded. Hyaline patches irregular on the valve.

Type :—Russia, Lake Baikal, the Olkhon Gates Strait, Antikhai bay, epilithon, st. 50, 5 m depth, 25 June 1998, collector V. Votyakov (holotype: slide 0173-BK collection "Darwin initiative" housed at the Limnological Institute SB RAS, Irkutsk, Russia; isotype: slide 0174-BK, *ibid.*).

Navicula caudata* var. *skvortzowii Rodionova & Pomazkina var. nov. (Pomazkina et al., 2018, p. 48, Table 51)

Valve elliptic with cuneate slightly protracted

ends. Length 41.8–50 μm, width 17.3 μm. Raphe weakly lateral, straight. Axial area moderately broad; central area rounded, transapically widened. Striae lineolate, radiate, becoming parallel at the apices, 9–10 in 10 μm. In the middle of the valve long striae alternate short. Distinct striae interrupted with hyaline patches. Proximal raphe endings with pores, terminal fissures rounded.

Type :—Russia, Lake Baikal, south basin, near the settlement Mangutaj, stones and silt, st. 41, 20 m depth, 22 June 1998, collector V. Votyakov (holotype: slide 0138-BK collection "Darwin initiative" housed at the Limnological Institute SB RAS, Irkutsk, Russia; isotype: slide 0140-BK, *ibid.*).

Navicula cryptocephala* var. *baicalensis Rodionova & Pomazkina var. nov. (Pomazkina et al., 2018, p. 49, Table 53)

Valves lanceolate with slightly protracted capitates ends. Length 20.1–25.6 μm, width 4.5–5.6 μm. Raphe filiform, weakly uneven, lateral. Axial area narrow; central area small, rhombic-rounded, asymmetric. Striae lineolate, slightly radiate, convergent at the apices, 18–20 in 10 μm. Proximal raphe endings straight with pores, terminal fissures long, bent to one side.

Type :—Russia, Lake Baikal, south basin, near the settlement Mangutaj, stones and silt, st. 41, 20 m depth, 22 June 1998, collector V. Votyakov (holotype: slide 0138-BK collection "Darwin initiative" housed at the Limnological Institute SB RAS, Irkutsk, Russia; isotype: slide 0139-BK, *ibid.*).

Navicula hasta* var. *austrolacustris Rodionova & Pomazkina var. nov. (Pomazkina et al., 2018, p. 51, Table 57)

Valves lanceolate with protracted rostrate ends. Length 53–54 μm, width 11.0–11.7μm. Raphe filiform, weakly lateral. Axial area narrow, lineal; central area transapically widened. Striae lineolate, radiate, in the center 8–9 in 10 μm, at the apices 11–12 in 10 μm. Proximal raphe endings with pores, terminal fissures long, bent to one side.

Type :—Russia, Lake Baikal, south basin, near the settlement Mangutaj, stones and silt, st. 41, 20 m depth, 22 June 1998, collector V. Votyakov (holotype: slide 0138-BK collection "Darwin initiative" housed at the Limnological Institute SB RAS, Irkutsk, Russia; isotype: slides 0139-BK, 0140-BK, 0141-BK, *ibid.*).

Navicula hasta* var. *baicalensis Rodionova & Pomazkina var. nov. (Pomazkina et al., 2018, p. 51, Table 58)

Valves lanceolate with sharply rounded ends. Length 93–104 μm, width 16.0–17.1 μm. Raphe filiform, weakly lateral. Axial area moderate, lineal; central area small rounded. Striae lineolate, radiate, in the center 5–6 in 10 μm, at the apices 9–10 in 10 μm. Proximal raphe endings with pores, terminal fissures long, bent to one side.

Type :—Russia, Lake Baikal, near the settlement south basin, stones and silt, st. 41, 20 m depth, 22 June 1998, collector V. Votyakov (holotype: slide 0138-BK collection "Darwin initiative" housed at the Limnological Institute SB RAS, Irkutsk, Russia; isotype: slides 0139-BK, 0140-BK, 0141-BK, *ibid.*).

Navicula lacusbaicali* var. *ottochuschinica Pomazkina, Rodionova & Sherbakova var. nov. (Pomazkina et al., 2018, p. 53, Table 63)

Valves elliptically-lanceolate with cuneate ends. Length 23–37 μm, width 9.7–13.5 μm. Raphe weakly lateral, straight. Axial area broad; central area small, transapically widened, asymmetric. Striae lineolate, weakly radiate, 9–10 in 10 μm, becoming parallel or slightly convergent at the apices, 10–12 in 10 μm. In the middle of the valve striae shortened. Distinct hyaline patches on one half of the valve. Proximal raphe endings with pores, terminal fissures long, fine.

Type :—Russia, Lake Baikal, the Olkhon Gates Strait, the Cape Otto-Khushin, epilithon, st. 53, 20 m depth, 25 June 1998, collector V. Votyakov (holotype: slide 0183-BK collection "Darwin initiative" housed at the Limnological Institute SB RAS, Irkutsk, Russia; isotype: slide 0184-BK, *ibid*).

Navicula latilanceolata Rodionova & Pomazkina sp. nov. (Pomazkina et al., 2018, p. 54, Table 64)

Valves broadly lanceolate with weakly protracted narrowly rounded ends. Length 22–23 μm, width 7.6–8.0 μm. Raphe filiform. Axial area narrow, linear; central area small, rounded. Striae lineolate, radiate, becoming slightly convergent at the apices, 14 in 10 μm. Proximal raphe endings with pores, terminal fissures short hooked.

Type :—Russia, Lake Baikal, Anga Bay, silt and sand, st. 6, 17 m depth, 27 June 1997, collector V. Votyakov (holotype: slide 0014-BK collection "Darwin initiative" housed at the Limnological Institute SB RAS, Irkutsk, Russia; isotype: slides 0015-BK, 0016-BK, *ibid.*).

Navicula menisculus* var. *baicalensis Rodionova & Pomazkina var. nov. (Pomazkina et al., 2018, p. 56, Table 69**)**

Valves elliptical-lanceolate with weakly protracted narrowly rounded ends. Length 18.7–26.2 μm, width 8.4–10.5 μm. Raphe filiform. Axial area narrow, linear; central area small, rounded. Striae lineolate, slightly radiate in the center, becoming almost parallel at the apices, 12–14 in 10 μm. Proximal raphe endings with pores, terminal fissures short hooked.

Type :—Russia, Lake Baikal, northern basin, the Cape Elokhin, sand, st. 12.3, 4 m depth, 29 June 1997, collector V. Votyakov (holotype: slide 0043-BK collection "Darwin initiative" housed at the Limnological Institute SB RAS, Irkutsk, Russia; isotype: slide 0043b-BK, *ibid.*).

Navicula meridielacum Rodionova & Pomazkina sp. nov. (Pomazkina et al., 2018, p. 56, Table 70)

Valves lanceolate with obtusely rounded elongated ends. Length 68–79 μm, width 14.4–15.8 μm. Raphe slightly lateral. Axial area narrow, linear; central area transapically widened. Striae lineolate, radiate, in the center 8–9 in 10 μm, denser at the apices, 10–11 in 10 μm. Proximal raphe endings with pores, terminal fissures widened then fine and rounded.

Type :—Russia, Lake Baikal, near the city of Baikalsk, silt, st. 40, 20 m depth, 23 June 1998, collector V. Votyakov (holotype: slide 0145-BK collection "Darwin initiative" housed at the Limnological Institute

SB RAS, Irkutsk, Russia; isotype: slide 0145a-BK, *ibid.*).

Navicula meridielacum* var. *skvortzowii Pomazkina, Rodionova & Sherbakova var. nov. (Pomazkina et al., 2018, p. 57, Table 71)

Valves lanceolate with weakly protracted rounded ends. Length 91–108 μm, width 17.4–19.2 μm. Raphe slightly lateral. Axial area moderate; central area transapically widened, asymmetric. Striae lineolate, radiate, in the middle of the valve long striae alternate short, 6–8 in 10 μm. Striae slightly denser at the apices, 9–10 in 10 μm. Proximal raphe endings with marked pores, terminal fissures widened then fine and rounded.

Type :—Russia, Lake Baikal, south basin, near the settlement Mangutaj, stones and silt, st. 41, 20 m depth, 22 June 1998, collector V. Votyakov (holotype: slide 0138-BK collection "Darwin initiative" housed at the Limnological Institute SB RAS, Irkutsk, Russia; isotype: slide 0139-BK, *ibid.*).

Navicula neooppugnata Rodionova & Pomazkina sp. nov. (Pomazkina et al., 2018, p. 58, Table 73)

Valves lanceolate with weakly protracted cuneate ends. Length 37–60 μm, width 7.8–11.6 μm. Raphe slightly lateral. Axial area narrow, linear; central area transapically elliptic. Striae lineolate, radiate in the middle of the valve, 8–10 in 10 μm, becoming almost convergent towards the apices, 10–12 in 10 μm. Proximal raphe endings with pores, terminal fissures widened then fine and rounded.

Type :—Russia, Lake Baikal, near the city of Baikalsk, silt, st. 40, 20 m depth, 23 June 1998, collector V. Votyakov (holotype: slide 0145-BK collection "Darwin initiative" housed at the Limnological Institute SB RAS, Irkutsk, Russia; isotype: slide 0145b-BK, *ibid.*).

Navicula picea* var. *paucimarensis Rodionova & Pomazkina var. nov. (Pomazkina et al., 2018, p. 60, Table 79)

Valves lanceolate with weakly protracted sharply rounded ends. Length 31–32 μm, width 6.1–6.3 μm. Raphe slightly lateral. Axial area narrow; central area lanceolate, small. Striae lineolate, radiate, becoming convergent towards the apices, 16–18 in 10 μm. Proximal raphe endings with pores, terminal fissures broadly rounded.

Type :—Russia, Lake Baikal, the Olkhon Gates Strait, the Cape Khara-Khulun, epilithon, st. 51, 20 m depth, 25 June 1998, collector V. Votyakov (holotype: slide 0176-BK collection "Darwin initiative" housed at the Limnological Institute SB RAS, Irkutsk, Russia; isotype: slide 0177-BK, *ibid*).

Navicula pseudoajajensis Pomazkina, Rodionova & Sherbakova sp. nov. (Pomazkina et al., 2018, p. 61, Table 81)

Valves lanceolate with obtusely rounded ends. Length 56–58 μm, width 13–15 μm. Raphe slightly lateral. Axial area wide, linear; central area small, rounded. Striae lineolate, in the middle of the valve long striae alternate short, radiate, becoming parallel then slightly convergent at the apices, 11–12 in 10 μm. Proximal raphe endings with wide pores, terminal fissures widened, then thin and rounded.

Type :—Russia, Lake Baikal, the Olkhon Gates Strait, M. Mujgin bay, epilithon, st. 52, 20 m depth, 25 June 1998, collector V. Votyakov (holotype: slide 0179-BK collection "Darwin initiative" housed at the Limnological Institute SB RAS, Irkutsk, Russia; isotype: slide 0179a-BK, *ibid*).

Navicula pseudobaicalensis Pomazkina, Rodionova & Sherbakova sp. nov. (Pomazkina et al., 2018, p. 62, Table 82)

Valves lanceolate with long narrowly-rounded ends. Length 67–72 μm, width 9.3–10.4 μm. Raphe filiform. Axial area narrow; central area small, oval or rounded. Striae lineolate, radiate in the middle of the valve, 9–10 in 10 μm, becoming convergent at the apices, 16–18 in 10 μm. Proximal raphe endings hooked, terminal fissures long bent to the primary valve side.

Type :—Russia. Lake Baikal, the Olkhon Gates Strait, epilithon, st. 7, 20 m depth, 27 June 1997, collector V. Votyakov (holotype: slide 0017-BK collection "Darwin initiative" housed at the Limnological Institute SB RAS, Irkutsk, Russia; isotype: slides 0018-BK, 0019-BK, *ibid.*).

Navicula pseudosemenicula Rodionova & Pomazkina sp. nov. (Pomazkina et al., 2018, p. 62, Table 84)

Valves lanceolate with slightly protracted obtusely-rounded ends. Length 67–72 μm, width 9.3–10.4 μm. Raphe filiform. Axial area narrow; central area small, oval or rouneded. Striae lineolate, in the middle of the valve radiate, 9–10 in 10 μm, becoming convergent at the apices, 16–18 in 10 μm. Proximal raphe endings hooked, terminal fissures long bent to the primary valve side.

Type :—Russia. Lake Baikal, the Olkhon Gates Strait, epilithon, st. 7, 20 m depth, 27 June 1997, collector V. Votyakov (holotype: slide 0017-BK collection "Darwin initiative" housed at the Limnological Institute SB RAS, Irkutsk, Russia; isotype: slides 0018-BK, 0019-BK, 0020-BK , 0021-BK, *ibid.*).

Navicula quasibaicalensis Pomazkina, Rodionova & Sherbakova sp. nov. (Pomazkina et al., 2018, p. 63, Table 85)

Valves narrowly-lanceolate with long protracted narrowly-rounded ends. Length 101–115 μm, width 14.3–19.0 μm. Raphe slightly lateral. Axial area narrow; central area small, rounded. Striae lineolate, radiate, in the middle of the valve, 7–10 in 10 μm, at the apices, 11–13 in 10 μm. Proximal raphe endings with pores, terminal fissures hooked, bent to the primary valve side.

Type :—Russia, Lake Baikal, southern basin, near the settlement Kultuk, epilithon, st. 42, 20 m depth, 22 June 1998, collector V. Votyakov (holotype: slide 0132-BK collection "Darwin initiative" housed at the Limnological Institute SB RAS, Irkutsk, Russia; isotype: slide 0132a-BK, *ibid.*).

Navicula quasibaicalensis* var. *inflata Rodionova & Pomazkina var. nov. (Pomazkina et al., 2018, p. 64, Table 86)

Valves broadly-lanceolate with long protracted narrowly-rounded ends. Length 105–114 μm, width 20.4–21.0 μm. Raphe slightly lateral. Axial area narrow; central area small, rounded. Striae lineolate,

radiate, in the middle of the valve, 7–8 in 10 μm, at the apices, 10–11 in 10 μm. Proximal raphe endings with pores, terminal fissures hooked, bent to the primary valve side.

Type :—Russia, Lake Baikal, south basin, near the settlement Mangutaj, stones and silt, st. 41, 20 m depth, 22 June 1998, collector V. Votyakov (holotype: slide 0138-BK collection "Darwin initiative" housed at the Limnological Institute SB RAS, Irkutsk, Russia; isotype: slide 0139-BK, slides 0140-BK, slide 0141-BK, *ibid.*).

Navicula quasibaicalensis* var. *paucimarensis Pomazkina, Rodionova & Sherbakova var. nov. (Pomazkina et al., 2018, p. 64, Table 87)

Valves lanceolate with long protracted narrowly-rounded ends. Length 53–68 μm, width 10.0–11.9 μm. Raphe filiform. Axial area narrow; central area large, rounded. Striae lineolate, radiate in the middle of the valve, 8–9 in 10 μm, becoming almost parallel at the apices, 10–13 in 10 μm. Proximal raphe endings with pores, terminal fissures widened, then thin and rounded to the same side.

Type :—Russia, Lake Baikal, the Olkhon Gates Strait, the Cape Khara-Khulun, epilithon, st. 51, 20 m depth, 25 June 1998, collector V. Votyakov (holotype: slide 0177-BK, collection "Darwin initiative" housed at the Limnological Institute SB RAS, Irkutsk, Russia; isotype: slides 0176-BK, 0173-BK *ibid*).

Navicula reinchardtiana* var. *baicalensis Rodionova & Pomazkina var. nov. (Pomazkina et al., 2018, p. 66, Table 91)

Valves broadly-lanceolate with protracted obtusely-rounded ends. Length 24–27 μm, width 7.5–8.5 μm. Raphe filiform. Axial area narrow; central area almost round, asymmetric. Striae lineolate, radiate, shortened in the middle of the valve becoming slightly convergent or parallel towards the apices, 13–16 in 10 μm. Proximal raphe endings with pores, terminal fissures weakly widened and slightly bent.

Type :—Russia, Lake Baikal, the Olkhon Gates Strait, the Cape Khara-Khulun, epilithon, st. 51, 20 m depth, 25 June 1998, collector V. Votyakov (holotype: slide 0176-BK, collection "Darwin initiative" housed at the Limnological Institute SB RAS, Irkutsk, Russia; isotype: slides 0177-BK, 0178-BK, *ibid*).

Navicula rhombicinsolitum Pomazkina, Rodionova & Sherbakova sp. nov. (Pomazkina et al., 2018, p.67, Table 95)

Valves elliptic-lanceolate or rhombic-lanceolate with protracted sharply-rounded ends. Length 69–77 μm, width 16.7–19.4 μm. Raphe slightly lateral, straight. Axial area wide; central area rounded. Striae lineolate, weakly radiate in the middle of the valve, 7–8 in 10 μm, becoming parallel, then convergent towards the apices, 9–10 in 10 μm. Hyaline uneven areas one each half of the valve. Proximal raphe endings with pores, terminal ends short, widened, bent to the secondary valve side.

Type :—Russia, Lake Baikal, the Olkhon Gates Strait, the Cape Khara-Khulun, epilithon, st. 51, 20 m depth, 25 June 1998, collector V. Votyakov (holotype: slide 0176-BK, collection "Darwin initiative" housed at the Limnological Institute SB RAS, Irkutsk, Russia; isotype: slides 0177-BK, 0178-BK, *ibid*).

Navicula subajajensis* var. *skvortzowii Rodionova & Pomazkina var. nov. (Pomazkina et al., 2018, p. 69, Table 98)

Valves linear-lanceolate with cuneate slightly protracted ends. Length 60–68 μm, width 12.8–13.0 μm. Raphe slightly lateral, curved proximally. Axial area wide, linear; central area small, transapically widened. Striae lineolate, radiate, in the middle of the valve long striae alternate short. Striae becoming parallel or slightly convergent towards the apices, 10–12 in 10 μm. Proximal raphe endings short forked, terminal endings short hooked.

Type :—Russia, Lake Baikal, the Olkhon Gates Strait, the Cape Otto-Khushin, epilithon, st. 53, 20 m depth, 25 June 1998, collector V. Votyakov (holotype: slide 0183-BK collection "Darwin initiative" housed at the Limnological Institute SB RAS, Irkutsk, Russia; isotype: slide 0184-BK, *ibid*).

***Navicula subelongata* var. *meyeri* Pomazkina, Rodionova & Sherbakova var. nov.** (Pomazkina et al., 2018, p. 70, Table 100)

Valves linear-lanceolate with cuneate slightly protracted rounded ends. Length 73–76.9 μm, width 11.7–13.2 μm. Raphe slightly lateral. Axial area wide, lanceolate; central area indistinct. Striae lineolate, radiate, 8–9 in 10 μm, in the middle of the valve long striae alternate short. Proximal raphe endings with wide pores, terminal fissures long, bent.

Type :—Russia, Lake Baikal, south basin, near the settlement Mangutaj, stones and silt, st. 41, 20 m depth, 22 June 1998, collector V. Votyakov (holotype: slide 0138-BK collection "Darwin initiative" housed at the Limnological Institute SB RAS, Irkutsk, Russia; isotype: slide 0140-BK, *ibid.*).

Navicula vadosa Pomazkina, Rodionova & Sherbakova sp. nov. (Pomazkina et al., 2018, p. 71, Table 104)

Valve broad lanceolate with protracted rostrate ends. Length 39 μm, width 11.7 μm. Raphe filiform. Axial area narrow; central area small, oval. Striae lineolate, radiate in the middle of the valve becoming slightly convergent towards the apices, 10–11 in 10 μm. Proximal raphe endings with large pores, terminal fissures long, bent to the same side.

Type :—Russia, Lake Baikal, the central basin, the River Selenga delta, silt, st. 32, 15 m depth, 06 July 1997, collector V. Votyakov (holotype: slide 0109-BK collection "Darwin initiative" housed at the Limnological Institute SB RAS, Irkutsk, Russia; isotype: slide 0109a-BK, *ibid.*).

Navicula vasilii Rodionova sp. nov. (Pomazkina et al., 2018, p. 71, Table 105)

Valve lanceolate with slightly protracted rounded ends. Length 16.6 μm, width 5.1 μm. Raphe filiform. Axial area narrow; central area small, transapically widened. Striae irregular: uniseriate, occasionally biseriate, lineolate, punctuate, radiate in the middle of the valve, 16 in 10 μm, becoming parallel at the apices, 18 in 10 μm. Proximal raphe endings with large pores, terminal fissures long, bent to the secondary side.

Type :—Russia, Lake Baikal, near the city of

Baikalsk, silt, st. 40, 20 m depth, 23 June 1998, collector V. Votyakov (holotype: slide 0145-BK collection "Darwin initiative" housed at the Limnological Institute SB RAS, Irkutsk, Russia; isotype: slide 0145a-BK, *ibid.*).

Navicula viridula* var. *baicalensis Rodionova & Pomazkina var. nov. (Pomazkina et al., 2018, p. 72, Table 106)

Valves linear-lanceolate with obtuse-rounded ends. Length 56–57 μm, width 8.6–9.0 μm. Raphe filiform. Axial area narrow, straight; central area rectangular transapically widened. Striae lineolate, strongly radiate, in the middle of the valve, convergent at the apices, 10–11 in 10 μm. Proximal raphe endings with pores, terminal fissures widened then thin and rounded.

Type :—Russia, Lake Baikal, the River Selenga delta, silt, st. 32, 15 m depth, 06 July 1997, collector V. Votyakov (holotype: slide 0109-BK collection "Darwin initiative" housed at the Limnological Institute SB RAS, Irkutsk, Russia; isotype: slide 0109a-BK, *ibid.*).

Navicula visenda Pomazkina, Rodionova & Sherbakova sp. nov. (Pomazkina et al., 2018, p. 73, Table 108)

Valves broad lanceolate with slightly protracted rounded ends. Length 35–45 μm, width 9.7–10.9 μm. Raphe slightly lateral. Axial area narrow; central area rounded. Striae lineolate, radiate in the middle of the valve, 8–9 in 10 μm, becoming slightly convergent at the apices, 10–11 in 10 μm. Proximal raphe endings with large pores, terminal fissures long, bent to the same side. Proximal raphe endings with pores, terminal fissures broadly bent to the same side.

Type :—Russia, Lake Baikal, the central basin, the River Selenga delta, silt, st. 32, 15 m depth, 06 July 1997, collector V. Votyakov (holotype: slide 0109-BK collection "Darwin initiative" housed at the Limnological Institute SB RAS, Irkutsk, Russia; isotype: slide 0109c-BK, *ibid.*).

Navicula vivata Rodionova & Pomazkina sp. nov. (Pomazkina et al., 2018, p. 73, Table 109)

Valve elliptic-lanceolate with protracted obtusely-rounded ends. Length 26 μm, width 7 μm. Raphe slightly lateral and bent. Axial area narrow; central area large, transapically widened. Striae lineolate, strongly radiate in the middle of the valve, becoming slightly convergent towards the apices, 18–20 in 10 μm. Proximal raphe endings with pores, terminal endings angular, bent to the same valve side.

Type :—Russia, Lake Baikal, the central basin, the River Selenga delta, silt, st. 32, 15 m depth, 06 July 1997, collector V. Votyakov (holotype: slide 0109-BK collection "Darwin initiative" housed at the Limnological Institute SB RAS, Irkutsk, Russia; isotype: slide 0109c-BK, *ibid.*).

Navicula witkowskii Pomazkina, Rodionova & Sherbakova sp. nov. (Pomazkina et al., 2018, p. 74, Table 111)

Valve lanceolate with long narrowly-rounded ends. Length 96.4 μm, width 16.4 μm. Raphe filiform. Axial area narrow; central area small, rounded. Striae lineolate, slightly radiate in the middle of the valve, 8 in 10 μm, becoming strongly radiate at the apices, 10 in 10 μm. Proximal raphe endings with pores, terminal fissures fine, weakly bent to the same side.

Type :—Russia, Lake Baikal, the northern basin, near the Cape Kabanij, epilithon, st. 22, 20 m depth, 04 July 1997, collector V. Votyakov (holotype: slide 0073-BK collection "Darwin initiative" housed at the Limnological Institute SB RAS, Irkutsk, Russia; isotype: slide 0073a-BK, *ibid.*).

Navicula xenium Rodionova & Pomazkina sp. nov. (Pomazkina et al., 2018, p. 75, Table 113)

Valve lanceolate with protracted rounded ends. Length 41 μm, width 9.4 μm. Raphe filiform. Axial area narrow; central area small, transapically widened. Striae lineolate, slightly radiate, shortened in the middle of the valve, becoming radiate at the apices, 10–12 in 10 μm. Proximal raphe endings with pores, terminal fissures widened, then thin and rounded.

Type :—Russia, Lake Baikal, near the city of Baikalsk, silt, st. 40, 20 m depth, 23 June 1998, collector V. Votyakov (holotype: slide 0145-BK collection "Darwin initiative" housed at the Limnological Institute SB RAS, Irkutsk, Russia; isotype: slide 0145c-BK, *ibid.*).

Genus Paraplaconeis Kulikovskiy, Lange-Bertalot & Metzeltin

Paraplaconeis ampla Pomazkina & Rodionova sp. nov. (Pomazkina et al., 2018, p. 78, Table 114)

Valve elliptic-lanceolate with slightly attenuated rostrate ends. Length 81.4 μm, width 20.7 μm. Axial area linear, narrow at the apices, widening to the center; central area oval transapically widened. Striae biseriate, radiate, 8–9 in 10 μm. Raphe filiform, lateral. Proximal raphe endings with pores, terminal thin broadly rounded to the same side.

Type :—Russia, Lake Baikal, the northern basin, near the Cape Kabanij, epilithon, st. 22, 20 m depth, 04 July 1997, collector V. Votyakov (holotype: slide 0073-BK collection "Darwin initiative" housed at the Limnological Institute SB RAS, Irkutsk, Russia; isotype: slide 0074-BK, *ibid.*).

Paraplaconeis anfracta Pomazkina sp. nov. (Pomazkina et al., 2018, p. 78, Table 115)

Valves elliptic-lanceolate with slightly attenuated rostrate ends. Length 27.7–31.0 μm, width 12.6–15.5 μm. Axial area linear, narrow; central area small transapically widened. Striae biseriate, radiate, 10–11 in 10 μm. Raphe filiform, linear is contoured on either side by wide sinuous depression. Proximal raphe endings with pores, terminal thin broadly rounded to the same side.

Type :—Russia, Lake Baikal, the northern basin, the Cape Orlovij, sand, st. 25, 12 m depth, 05 July 1997, collector V. Votyakov (holotype: slide 0083-BK collection "Darwin initiative" housed at the Limnological Institute SB RAS, Irkutsk, Russia; isotype: slide 0083a-BK, *ibid.*).

Paraplaconeis arcuata Pomazkina & Rodionova sp. nov. (Pomazkina et al., 2018, p. 78, Table 116)

Valve elliptic-lanceolate with slightly attenuated

rostrate ends. Length 25,6 μm, width 12.2 μm. Axial area linear, narrow; central area small rectangular. Striae biseriate, radiate, 10 in 10 μm, becoming denser at apices, 20 in 10 μm. Raphe filiform. Raphe sternum is contoured on either side by wide sinuous depression adjoining to striae. Proximal raphe endings with pores, terminal fissures differently curved to the same side.

Type :—Russia, Lake Baikal, south basin, near the settlement Mangutaj, stones and silt, st. 41, 20 m depth, 22 June 1998, collector V. Votyakov (holotype: slide 0139-BK collection "Darwin initiative" housed at the Limnological Institute SB RAS, Irkutsk, Russia; isotype: slide 0139a-BK, *ibid.*).

Paraplaconeis australis Pomazkina & Rodionova sp. nov. (Pomazkina et al., 2018, p. 79, Table 117)

Valves elliptic-lanceolate with attenuated rostrate ends. Length 38.5–40.8 μm, width 12.0–15.7 μm. Axial area linear, narrow; central area small slightly transapically widened with shortened central striae. Striae biseriate, radiate, 10–11 in 10 μm, becoming strongly radiate and denser at the apices, 13 in 10 μm. Raphe filiform, proximal endings with pores, terminal fissures rounded to the same side.

Type :—Russia, Lake Baikal, near the city of Baikalsk, silt, st. 40, 20 m depth, 23 June 1998, collector V. Votyakov (holotype: slide 0145-BK collection "Darwin initiative" housed at the Limnological Institute SB RAS, Irkutsk, Russia; isotype: slide 0146-BK, *ibid*.).

Paraplaconeis baicalensis Pomazkina & Sherbakova sp. nov. (Pomazkina et al., 2018, p. 79, Table 118)

Valves broad elliptic-lanceolate to rhombic with weakly attenuated rostrate ends. Length 28.4 μm, width 13.2 μm. Axial area narrow at the apices widening to the middle of the valve; central area small slightly transapically widened with shortened central striae. Striae biseriate, radiate, 11–12 in 10 μm, becoming strongly radiate and closer at the apices, 12–13 in 10 μm. Raphe filiform, proximal raphe endings with pores, terminal fissures differently rounded to the same side. Raphe sternum is contoured on either side except for the apices by wide undulated depression adjoining to striae.

Type :—Russia, Lake Baikal, near the city of Baikalsk, silt, st. 40, 20 m depth, 23 June 1998, collector V. Votyakov (holotype: slide 0145-BK collection "Darwin initiative" housed at the Limnological Institute SB RAS, Irkutsk, Russia; isotype: slide 0145a-BK, *ibid.*).

Paraplaconeis decorata Pomazkina sp. nov. (Pomazkina et al., 2018, p. 80, Table 120)

Valves elliptic-lanceolate with shortly attenuated rostrate ends. Length 30.3–31.0 μm, width 13.0–14.0 μm. Axial area narrow, linear; central area small transapically elongate oval. Striae radiate, 10 in 10 μm, becoming closer at the apices, 11–12 in 10 μm. Raphe filiform, distal endings differently bent to the same side, central raphe pores slightly undulating.

Type :—Russia, Lake Baikal, the northern basin, near the Cape Kabanij, epilithon, st. 22, 20 m depth, 04 July 1997, collector V. Votyakov (holotype: slide 0073-BK collection "Darwin initiative" housed at the Limnological Institute SB RAS, Irkutsk, Russia; isotype: slide 0074-BK, *ibid.*).

Paraplaconeis dimidia Pomazkina & Sherbakova sp. nov. (Pomazkina et al., 2018, p. 81, Table 121)

Valve broad elliptic rhombic-lanceolate with shortly attenuated rostrate ends. Length 46.2 μm, width 14.6 μm. Axial area narrow at the apices widening to the middle of the valve; central area small slightly transapically widened with shortened central striae. Striae radiate, biseriate, 10–11 in 10 μm, becoming closer at the apices, 11–12 in 10 μm. Raphe filiform, distal endings differently bent to the same side, central raphe endings slightly undulating with small pores.

Type :—Russia, Lake Baikal, the southern basin, the Cape Polovinnyj, epilithon, st. 44, 9 m depth, 22 June 1998, collector V. Votyakov (holotype: slide 0126-BK collection "Darwin initiative" housed at the Limnological Institute SB RAS, Irkutsk, Russia; isotype: slide 0125-BK, *ibid.*).

Paraplaconeis dissimilis Pomazkina & Rodionova sp. nov. (Pomazkina et al., 2018, p. 81, Table 122)

Valve elliptic-lanceolate with shortly attenuated rostrate ends. Length 52.5 μm, width 20.0 μm. Axial area narrow, linear; central area small transapically widened. Striae radiate, becoming biseriate at the apices, 8–9 in 10 μm. Raphe filiform, linear with proximal pores and weakly undulating distal endings. Raphe sternum is contoured on either side except for the apices by wide undulated depression adjoining to striae.

Type :—Russia, Lake Baikal, the northern basin, near the Cape Kabanij, epilithon, st. 22, 20 m depth, 04 July 1997, collector V. Votyakov (holotype: slide 0073-BK collection "Darwin initiative" housed at the Limnological Institute SB RAS, Irkutsk, Russia; isotype: slide 0074-BK, *ibid.*).

Paraplaconeis elongata Pomazkina & Sherbakova sp. nov. (Pomazkina et al., 2018, p. 82, Table 123)

Valves elliptic-lanceolate with weakly attenuated rostrate ends. Length 62.0–62.8 μm, width 19.1–20 μm. Axial area narrow, linear; central area almost indistinct. Striae radiate, biseriate, strongly radiate to the apices, 9–10 in 10 μm. Raphe filiform, proximal endings linear with small pores, distal endings differently curved to the same side. Raphe sternum is contoured on either side by narrow undulated depression adjoining to striae.

Type :—Russia, Lake Baikal, the southern basin, the Cape Polovinnyj, epilithon, st. 44, 9 m depth, 22 June 1998, collector V. Votyakov (holotype: slide 0127-BK collection "Darwin initiative" housed at the Limnological Institute SB RAS, Irkutsk, Russia; isotype: slide 0125-BK, *ibid.*).

Paraplaconeis foliaris Pomazkina & Sherbakova sp. nov. (Pomazkina et al., 2018, p. 82, Table 124)

Valves elliptic-lanceolate with rostrate ends. Length 52.7–61.8 μm, width 19.1–23.6 μm. Axial area narrow at the apices widening to the middle of the valve; central area small weakly transapically widened with shortened central striae. Striae radiate, biseriate, strongly radiate to the apices, 9–10 in 10 μm. Raphe filiform, proximal endings linear with small pores, distal endings differently curved to the same side.

Raphe sternum is contoured on either side by narrow undulated depression adjoining to striae.

Type :—Russia, Lake Baikal, the southern basin, the Cape Polovinnyj, epilithon, st. 44, 9 m depth, 22 June 1998, collector V. Votyakov (holotype: slide 0127-BK collection "Darwin initiative" housed at the Limnological Institute SB RAS, Irkutsk, Russia; isotype: slide 0127a-BK, *ibid.*).

Paraplaconeis interrupta Pomazkina & Sherbakova sp. nov. (Pomazkina et al., 2018, p. 83, Table 125)

Valves wide, elliptic-lanceolate with attenuated rostrate ends. Length 36.6–41.1 μm, width 17.3–18.0 μm. Axial area wide, linear; central area small weakly transapically widened with shortened central striae. Striae radiate, biseriate, 9–10 in 10 μm. Raphe filiform, undulate, proximal endings with small pores slightly deflected oppositely, distal endings differently curved to the same side. Raphe sternum is contoured on either side by wide undulated depression adjoining to striae.

Type :—Russia, Lake Baikal, the northern basin, near the Cape Kabanij, epilithon, st. 22, 20 m depth, 04 July 1997, collector V. Votyakov (holotype: slide 0073-BK collection "Darwin initiative" housed at the Limnological Institute SB RAS, Irkutsk, Russia; isotype: slide 0074-BK, *ibid.*).

Paraplaconeis lacustris Pomazkina & Sherbakova sp. nov. (Pomazkina et al., 2018, p. 83, Table 126)

Valves elliptic-lanceolate with weakly attenuated rostrate ends. Length 69.5–80.6 μm, width 17.8–22.6 μm. Axial area narrow at the apices widening to the middle of the valve; central area small, oval with shortened central striae. Striae radiate, biseriate, strongly radiate at the apices, 8–10 in 10 μm. Raphe filiform, proximal endings with pores slightly deflected to the same side, distal endings differently bent. Raphe sternum is contoured on either side by wide undulated depression adjoining to striae.

Type :—Russia, Lake Baikal, the southern basin, the Cape Polovinnyj, epilithon, st. 44, 9 m depth, 22 June 1998, collector V. Votyakov (holotype: slide 0127-BK collection "Darwin initiative" housed at the Limnological Institute SB RAS, Irkutsk, Russia; isotype: slide 0127a-BK, *ibid.*).

Paraplaconeis litoralis Pomazkina sp. nov. (Pomazkina et al., 2018, p. 84, Table 123)

Valve elliptic-lanceolate with attenuated rostrate ends. Length 93.6–101.0 μm, width 33.6–41.1 μm. Axial area narrow, linear; central area small oval transapically widened with shortened central striae. Striae radiate, uniseriate, becoming biseriate towards valve ends and the margin, 8–9 in 10 μm, at the apices 10 in 10 μm. Raphe filiform, linear with proximal pores, distal endings widely curved to the same side. Raphe sternum is contoured on either side by narrow depression adjoining to striae.

Type :—Russia, Lake Baikal, near the city of Baikalsk, silt, st. 40, 20 m depth, 23 June 1998, collector V. Votyakov (holotype: slide 0145-BK collection "Darwin initiative" housed at the Limnological Institute SB RAS, Irkutsk, Russia; isotype: slide 0146-BK, *ibid.*).

Paraplaconeis maculata Pomazkina & Sherbakova sp. nov. (Pomazkina et al., 2018, p. 85, Table 128)

Valve elliptic-lanceolate with attenuated rostrate ends. Length 44.0 μm, width 16.8 μm. Axial area narrow, linear widening to the middle of the valve; central area small transapically extended. Striae radiate, biseriate, 13–14 in 10 μm. Raphe filiform with narrow linear endings proximally, terminal fissures differently curved to the same side. Raphe sternum is contoured on either side by narrow depression adjoining to striae.

Type :—Russia, Lake Baikal, the northern basin, the Cape Orlovij, sand, st. 25, 12 m depth, 05 July 1997, collector V. Votyakov (holotype: slide 0083-BK collection "Darwin initiative" housed at the Limnological Institute SB RAS, Irkutsk, Russia; isotype: slide 0084-BK, *ibid.*).

Paraplaconeis magna Pomazkina & Sherbakova sp. nov. (Pomazkina et al., 2018, p. 85, Table 129)

Valve elliptic-lanceolate with shortly attenuated rostrate ends. Length 62.5 μm, width 26.0 μm. Axial area narrow, linear gradually wider to the middle of the valve; central area small, oval, transapically extended with shortened central striae. Striae radiate, 8 in 10 μm becoming denser at the apices, 10 in 10 μm. Raphe filiform narrow, proximal endings with pores, terminal fissures differently bent to the same side. Raphe sternum is contoured on either side by depression adjoining to striae.

Type :—Russia, Lake Baikal, south basin, near the settlement Mangutaj, stones and silt, st. 41, 20 m depth, 22 June 1998, collector V. Votyakov (holotype: slide 0139-BK collection "Darwin initiative" housed at the Limnological Institute SB RAS, Irkutsk, Russia; isotype: slide 0139a-BK, *ibid.*).

Paraplaconeis propria Pomazkina sp. nov. (Pomazkina et al., 2018, p. 86, Table 130)

Valves elliptic-lanceolate with slightly attenuated rostrate ends. Length 40.4–44.0 μm, width 14–17.3 μm. Axial area narrow, linear; central area small, oval, transapically extended with shortened central striae. Striae biseriate, radiate, 9–10 in 10 μm becoming closer at the apices, 14–15 in 10 μm. Raphe filiform linear, proximal endings slightly expanded, terminal fissures curved to the same side. Raphe sternum is contoured on either side by depression wide undulated in the center, becoming narrow towards the apices.

Type :—Russia, Lake Baikal, the northern basin, near the Cape Kabanij, epilithon, st. 22, 20 m depth, 04 July 1997, collector V. Votyakov (holotype: slide 0073-BK collection "Darwin initiative" housed at the Limnological Institute SB RAS, Irkutsk, Russia; isotype: slide 0074-BK, *ibid.*).

Paraplaconeis recta Pomazkina & Rodionova sp. nov. (Pomazkina et al., 2018, p. 86, Table 131)

Valve elliptic-lanceolate with attenuated capitate ends. Length 22.2 μm, width 6.7 μm. Axial area narrow, becoming gradually wider to the middle of the valve; central area small, rounded with shortened central striae. Striae biseriate, radiate, 14–15 in 10 μm becoming closer at the apices, 18–19 in 10 μm. Raphe filiform linear, proximal endings slightly expanded, terminal fissures bent to the same side.

Type :—Russia, Lake Baikal, the northern basin, near the Cape Kabanij, epilithon, st. 22, 20 m depth, 04 July 1997, collector V. Votyakov (holotype: slide 0073-BK collection “Darwin initiative” housed at the Limnological Institute SB RAS, Irkutsk, Russia; isotype: slide 0074-BK, *ibid.*).

Paraplaconeis signum Pomazkina & Rodionova sp. nov. (Pomazkina et al., 2018, p. 87, Table 132

Valve broad elliptic-lanceolate with weakly attenuated rostrate ends. Length 45.6 μm, width 18.3 μm. Axial area narrow at the apices, slightly widening to the middle of the valve; central area slightly transapically extended with shortened central striae. Striae biseriate, radiate, 10–11 in 10 μm becoming closer near the apices, 12–13 in 10 μm. Raphe filiform linear, proximal endings with pores, endings slightly expanded, terminal fissures differently bent to the same side.

Type :—Russia, Lake Baikal, the southern basin, the Cape Polovinnyj, epilithon, st. 44, 9 m depth, 22 June 1998, collector V. Votyakov (holotype: slide 0127-BK collection “Darwin initiative” housed at the Limnological Institute SB RAS, Irkutsk, Russia; isotype: slide 0127a-BK, *ibid.*).

Paraplaconeis undulata Pomazkina & Sherbakova sp. nov. (Pomazkina et al., 2018, p. 87, Table 133)

Valve broad elliptic-lanceolate with cuneate ends. Length 55.6 μm, width 23.0 μm. Axial area narrow near the apices becoming slightly wider towards the middle of the valve; central area almost indistinct weakly transapically extended with shortened central striae. Striae biseriate, radiate, 7–8 in 10 μm. Raphe filiform, proximal endings with oppositely bent pores, terminal fissures differently bent to the same side. Raphe sternum is contoured on either side by narrow depression adjoining to striae.

Type :—Russia, Lake Baikal, the southern basin, the Cape Polovinnyj, epilithon, st. 44, 9 m depth, 22 June 1998, collector V. Votyakov (holotype: slide 0127-BK collection “Darwin initiative” housed at the Limnological Institute SB RAS, Irkutsk, Russia; isotype: slide 0127c-BK, *ibid.*).

Paraplaconeis vernalis Pomazkina & Sherbakova sp. nov. (Pomazkina et al., 2018, p. 88, Table 134)

Valves broad elliptic-lanceolate with shortly protracted cuneate ends. Length 69.9 μm, width 31.1 μm. Axial area narrow near the apices becoming wider towards the middle of the valve; central area small transapically extended with shortened central striae. Striae biseriate, radiate, 7–8 in 10 μm, becoming closer towards the apices, 12–13 in 10 μm. Raphe filiform, proximal endings with oppositely bent pores, terminal fissures differently undulate to the same side.

Type :—Russia, Lake Baikal, the southern basin, the Cape Polovinnyj, epilithon, st. 44, 9 m depth, 22 June 1998, collector V. Votyakov (holotype: slide 0127-BK collection “Darwin initiative” housed at the Limnological Institute SB RAS, Irkutsk, Russia; isotype: slide 0127a-BK, *ibid.*).

Genus Placoneis Mereschkowsky

Placoneis abundans* var. *australis Pomazkina & Rodionova var. nov. (Pomazkina et al., 2018, p. 91, Table 137)

Valves elliptic-lanceolate with protracted capitate ends. Length 27.9–32.0 μm, width 10.7–12.0 μm. Axial area narrow near the apices becoming slightly wider towards the small transversally extended central area with alternating short and long striae. One or more (up to four) round stigmata in the central area. Striae radiate, 12–13 in 10 μm, becoming closer towards the apices, 16–17 in 10 μm. Raphe filiform, proximal endings slightly expanded, terminal raphe fissures differently undulated.

Type :—Russia, Lake Baikal, the southern basin, near the settlement Kultuk, epilithon, st. 42, 20 m depth, 22 June 1998, collector V. Votyakov (holotype: slide 0132-BK collection “Darwin initiative” housed at the Limnological Institute SB RAS, Irkutsk, Russia; isotype: slide 0133-BK, *ibid.*).

Placoneis abundans* var. *baicalensis Pomazkina & Rodionova sp. nov. (Pomazkina et al., 2018, p. 92, Table 138)

Valves elliptic-lanceolate with protracted rostrate ends. Length 22.0–24.1 μm, width 9.1–10.0 μm. Axial area becoming gradually wider to the transapically extended central area with alternating short and long striae. Striae radiate, 13–14 in 10 μm, becoming closer towards the apices, 15–16 in 10 μm. Raphe filiform, proximal endings with pores, terminal raphe fissures arcuated. Two round stigmata in the central area.

Type :—Russia, Lake Baikal, the southern basin, near the settlement Kultuk, epilithon, st. 42, 20 m depth, 22 June 1998, collector V. Votyakov (holotype: slide 0132-BK collection “Darwin initiative” housed at the Limnological Institute SB RAS, Irkutsk, Russia; isotype: slide 0133-BK, *ibid.*).

Placoneis abyssalis Pomazkina & Sherbakova sp. nov. (Pomazkina et al., 2018, p. 92, Table 139)

Valve elliptic-lanceolate with slightly protracted rounded ends. Length 23.3 μm, width 10.8 μm. Axial area narrow slightly widening to the small rounded central area with alternating short and long striae. Striae radiate, 14–15 in 10 μm, becoming closer near the apices, 30 in 10 μm. Raphe filiform, proximal endings straight with pores, terminal raphe fissures widely curved to the same side. Isolated stigma absent.

Type :—Russia, Lake Baikal, south basin, near the settlement Mangutaj, stones and silt, st. 41, 20 m depth, 22 June 1998, collector V. Votyakov (holotype: slide 0138-BK collection “Darwin initiative” housed at the Limnological Institute SB RAS, Irkutsk, Russia; isotype: slide 0139-BK, *ibid.*).

Placoneis acuta Pomazkina & Rodionova sp. nov. **(**Pomazkina et al., 2018, p. 93, Table 140)

Valves elliptic-lanceolate with cuneate ends. Length 45.8–47.1 μm, width 16.2–17.1 μm. Axial area narrow; central area small, insignificantly transapically widened with shortened central striae. Striae radiate, 5–6 in 10 μm. Raphe filiform, proximal endings with pores bent oppositely, terminal raphe fissures

differently widely curved. Raphe sternum is contoured on either side by narrow depression adjoining to striae. Isolated stigma absent.

Type :—Russia. Lake Baikal, the Olkhon Gates Strait, epilithon, st. 7, 20 m depth, 27 June 1997, collector V. Votyakov (holotype: slide 0017-BK collection "Darwin initiative" housed at the Limnological Institute SB RAS, Irkutsk, Russia; isotype: slide 0018-BK *ibid.*).

Placoneis argentata Pomazkina & Sherbakova sp. nov. (Pomazkina et al., 2018, p. 93, Table 141)

Valves elliptic-lanceolate with protracted rostrate ends. Length 30.0–58.0 μm, width 12.9–23.2 μm. Axial area narrow, slightly widening to the small transapically extended central area with shortened central striae. Striae broad, slightly radiate in the center, strongly radiate near the apices, 6–11 in 10 μm. Raphe filiform, curved distally. Proximal raphe endings with pores bent oppositely, terminal fissures differently widely-curved. Raphe sternum is contoured on either side by narrow undulating depression adjoining to striae.

Type :—Russia, Lake Baikal, the northern basin, the Cape Velikan, epilithon, st. 23, 20 m depth, 04 July 1997, collector V. Votyakov (holotype: slide 0075-BK collection "Darwin initiative" housed at the Limnological Institute SB RAS, Irkutsk, Russia; isotype: slide 0076-BK, *ibid.*).

Placoneis attenuata Pomazkina & Rodionova sp. nov. (Pomazkina et al., 2018, 94, Table 142)

Valve elliptic with cuneate rounded ends. Length 27.2 μm, width 17.4 μm. Axial area gradually widening to the small rounded central area with alternating short and long striae. Striae radiate, 10 in 10 μm, becoming closer towards the apices, 11 in 10 μm.

Raphe filiform, proximal raphe endings with pores bent oppositely, terminal fissures extending at the very raphe ends, widely-curved unilaterally. Isolated stigma absent.

Type :—Russia, Lake Baikal, the Olkhon Gates Strait, the Cape Otto-Khushin, epilithon, st. 53, 20 m depth, 25 June 1998, collector V. Votyakov (holotype: slide 0182-BK collection "Darwin initiative" housed at the Limnological Institute SB RAS, Irkutsk, Russia; isotype: slide 0182a-BK, *ibid*)

Placoneis betulina Pomazkina & Rodionova sp. nov. (Pomazkina et al., 2018, 94, Table 143)

Valves elliptic-lanceolate with cuneate ends. Length 78.7–82.5 μm, width 20.7–21.3 μm. Axial area gradually widening to the rhombic insignificantly transversely extended central area with shortened striae. Striae weakly radiate in the center, 8-11 in 10 μm, becoming closer towards the apices, 11–13 in 10 μm. Raphe filiform, proximal endings with pores bent unilaterally, terminal fissures extending at the very raphe ends, widely-curved to the same side. Isolated stigma absent.

Type :—Russia, Lake Baikal, southern basin, near the settlement B. Koty, epilithon, st. 1, 20 m depth, 22 June 1997, collector V. Votyakov (holotype: slide 0001-BK collection "Darwin initiative" housed at the Limnological Institute SB RAS, Irkutsk, Russia; isotype: slide 0001a-BK *ibid.*).

Placoneis bona Pomazkina & Sherbakova sp. nov. (Pomazkina et al., 2018, p. 95, Table 144)

Valves elliptic-lanceolate with attenuate rostrate ends. Length 25.8–27.0 μm, width 10.5–11.0 μm. Axial area narrow; central area small oval with alternating short and long striae. Striae strongly radiate, 16-19 in 10 μm. Raphe filiform, proximal endings with pores, terminal fissures widely-curved to the same direction as the central ends. Single stigma at the very end of one of the central striae.

Type :—Russia, Lake Baikal, the southern basin, near the settlement Kultuk, epilithon, st. 42, 20 m depth, 22 June 1998, collector V. Votyakov (holotype: slide 0132-BK collection "Darwin initiative" housed at the Limnological Institute SB RAS, Irkutsk, Russia; isotype: slide 0133-BK, *ibid.*).

Placoneis composita Pomazkina & Sherbakova sp. nov. (Pomazkina et al., 2018, p. 95, Table 145)

Valves elliptic-lanceolate with sharp cuneate ends. Length 35.9–42.4 μm, width 15.1–16.0 μm. Axial area moderate; central area transversely extended with shortened striae. Striae radiate, 10–11 in 10 μm, becoming closer towards the apices, 12 in 10 μm. Raphe filiform, undulate distally. Proximal raphe endings with pores, terminal fissures long bent oppositely. Distinct raphe branch including the central pore is encircled on either side with the straight depression, excluding near the apices areas and not adjoined the striae. Isolated stigma absent.

Type :—Russia, Lake Baikal, near the city of Baikalsk, silt, st. 40, 20 m depth, 23 June 1998, collector V. Votyakov (holotype: slide 0145-BK collection "Darwin initiative" housed at the Limnological Institute SB RAS, Irkutsk, Russia; isotype: slide 0146-BK, *ibid.*).

Placoneis cruciata Pomazkina & Rodionova sp. nov. (Pomazkina et al., 2018, p. 96, Table 146)

Valve elliptic with wide slightly protracted capitate ends. Length 13.9 μm, width 5.5 μm. Axial area narrow, linear; central area elliptic, transversely extended with shortened striae. Striae radiate, 18 in 10 μm. Raphe filiform, linear. Proximal raphe endings straight weakly expanded, terminal fissures widely-curved unilaterally.

Type :—Russia, Lake Baikal, Peschanaya Bay, small stones, st. 3, 20 m depth, 26 June1997, collector V. Votyakov (holotype: slide 0007-BK collection "Darwin initiative" housed at the Limnological Institute SB RAS, Irkutsk, Russia; isotype: slide 0008-BK *ibid.*).

Placoneis dahurica (Skvortzow) Pomazkina & Rodionova comb. nov. (Pomazkina et al., 2018, p. 96, Table 147)

Basionym: *Navicula dahurica* Skvortzow 1937, p. 337, pl. 7, fig. 35, pl. 8, fig. 7.

Valves elliptic-lanceolate with slightly protracted rostrate ends. Length 48.0–49.1 μm, width 20.0–21.0 μm. Axial area narrow, linear; central area small, transversely extended with alternating short and long striae. Striae radiate, becoming strongly radiate towards the apices, 7–8 in 10 μm. Raphe filiform, linear. Proximal raphe endings with pores, terminal fissures differently curved unilaterally end with a small depression at the very raphe ending.

Placoneis diaphana Pomazkina & Rodionova sp. nov. (Pomazkina et al., 2018, p. 96, Table 148)

Valve elliptic-lanceolate with cuneate ends. Length 20.9 μm, width 9.6 μm. Axial area narrow near the apices becoming gradually wider towards the small rounded central area with alternating short and long striae. Striae radiate, 14 in 10 μm becoming closer towards the apices, 18 in 10 μm. Raphe filiform, linear. Proximal raphe endings with pores, terminal fissures fine, differently curved unilaterally. One rounded stigma in the central area.

Type :—Russia, Lake Baikal, the northern basin, the Cape Velikan, stones, st. 23, 20 m depth, 04 July 1997, collector V. Votyakov (holotype: slide 0075 collection "Darwin initiative" housed at the Limnological Institute SB RAS, Irkutsk, Russia; isotype: slide 0076, *ibid.*).

Placoneis distincta Pomazkina & Sherbakova sp. nov. (Pomazkina et al., 2018, p. 97, Table 149)

Valve elliptic-lanceolate with slightly protracted rostrate ends. Length 43.3 μm, width 13.8 μm. Axial area narrow, becoming gradually wider towards the transversely elliptical central area with some shortened striae. Striae radiate, 14 in 10 μm, becoming closer towards the apices, 18 in 10 μm. Raphe filiform, uneven. Proximal raphe endings with pores bent oppositely to the curved terminal fissures.

Type :—Russia, Lake Baikal, Anga Bay, silt and sand, st. 6, 17 m depth, 27 June 1997, collector V. Votyakov (holotype: slide 0014-BK collection "Darwin initiative" housed at the Limnological Institute SB RAS, Irkutsk, Russia; isotype: slide 0015-BK *ibid.*).

Placoneis elenae Pomazkina & Sherbakova sp. nov. (Pomazkina et al., 2018, p. 97, Table 150)

Valve elliptic-lanceolate with cuneate ends. Length 41.1 μm, width 20.0 μm. Axial area narrow, gradually widening towards the transversely extended central area with alternating short and long striae. Striae wide, radiate, 17 in 10 μm, becoming closer near the apices, 18 in 10 μm. Raphe filiform, linear, then curved closer to the apices. Proximal raphe endings with pores bent oppositely; terminal fissures fine, differently curved unilaterally. One rounded stigma in the central area.

Type :—Russia, Lake Baikal, the southern basin, near the settlement Kultuk, epilithon, st. 42, 20 m depth, 22 June 1998, collector V. Votyakov (holotype: slide 0132-BK collection "Darwin initiative" housed at the Limnological Institute SB RAS, Irkutsk, Russia; isotype: slide 0133-BK, *ibid.*).

Placoneis elenae* var. *undata Pomazkina & Sherbakova var. nov. (Pomazkina et al., 2018, p. 98, Table 151)

Valve elliptic-lanceolate with cuneate ends. Length 33.6 μm, width 18.0 μm. Axial area narrow gradually widening towards the transversely elliptical central area with alternating short and long striae. Striae wide, radiate, 8 in 10 μm, becoming closer near the apices, 9 in 10 μm. Raphe filiform, closer to the apices uneven. Proximal raphe endings with pores, terminal fissures differently curved to the same side. Isolated stigma absent.

Type :—Russia, Lake Baikal, the southern basin, near the settlement Kultuk, epilithon, st. 42, 20 m depth, 22 June 1998, collector V. Votyakov (holotype: slide 0132-BK collection "Darwin initiative" housed at the Limnological Institute SB RAS, Irkutsk, Russia; isotype: slide 0133-BK, *ibid.*).

Placoneis eugeniae Sherbakova sp. nov. (Pomazkina et al., 2018, p. 98, Table 152)

Valves wide elliptic-lanceolate with cuneate rounded ends. Length 35.0–44.4 μm, width 20.7–25.4 μm. Axial area narrow at the apices widening towards the transversely elliptical central area with alternating short and long striae. Striae radiate, 7–8 in 10 μm, becoming closer near the apices, 10–11 in 10 μm. Raphe filiform, becoming curved closer to the apices. Proximal raphe endings with pores, terminal fissures differently bent to the same side. Isolated stigma absent. Distinct raphe branch including the central pore is encircled on either side with the straight depression, excluding near the apices areas, and not adjoined the striae.

Type :—Russia. Lake Baikal, the Olkhon Gates Strait, epilithon, st. 7, 20 m depth, 27 June 1997, collector V. Votyakov (holotype: slide 0017-BK collection "Darwin initiative" housed at the Limnological Institute SB RAS, Irkutsk, Russia; isotype: slide 0017a-BK *ibid.*).

Placoneis extraordinaris Pomazkina & Rodionova sp. nov. (Pomazkina et al., 2018, p. 99, Table 153)

Valves elliptic-lanceolate with cuneate rounded ends. Length 15.3–17.5 μm, width 6.8–7.5 μm. Axial area narrow linear continuously widening into the small transversely extended central area with shortened central striae. Striae radiate, 14–15 in 10 μm. Raphe filiform, linear. Proximal raphe endings with pores, terminal fissures differently curved unilaterally. Isolated stigma absent

Type :—Russia, Lake Baikal, the southern basin, near the settlement Kultuk, epilithon, st. 42, 20 m depth, 22 June 1998, collector V. Votyakov (holotype: slide 0132-BK collection "Darwin initiative" housed at the Limnological Institute SB RAS, Irkutsk, Russia; isotype: slide 0133-BK, *ibid.*).

Placoneis gelegma* var. *baicalensis Pomazkina & Rodionova var. nov. (Pomazkina et al., 2018, p. 100, Table 155)

Valves elliptic-lanceolate with cuneate ends. Length 21.2–33.2 μm, width 8.6–13.2 μm. Axial area narrow linear continuously widening towards the small oval slightly transversely extended central area with alternating short and long striae. Striae wide, radiate, 10 in 10 μm, becoming closer near the apices, 18–20 in 10 μm. Raphe filiform, linear. Proximal raphe endings with pores, terminal fissures differently curved unilaterally. Isolated stigma absent.

Type :—Russia, Lake Baikal, the southern basin, near the settlement Kultuk, epilithon, st. 42, 20 m depth, 22 June 1998, collector V. Votyakov (holotype: slide 0132-BK collection "Darwin initiative" housed at the Limnological Institute SB RAS, Irkutsk, Russia; isotype: slide 0133-BK, *ibid.*).

Placoneis granum Pomazkina & Sherbakova sp. nov. (Pomazkina et al., 2018, p. 100, Table 156)

Valve narrow elliptic-lanceolate with attenuate rostrate ends. Length 46.2 μm, width 16.2 μm. Axial area narrow continuously widening towards the small transversely extended central area with alternating short and long striae. Striae radiate, 10 in 10 μm, becoming closer and strongly radiate near the apices, 14 in 10 μm. Raphe filiform, linear. Proximal raphe endings with pores, terminal fissures differently curved unilaterally. Three round stigmata in the central area.

Type :—Russia, Lake Baikal, the southern basin, near the settlement Kultuk, epilithon, st. 42, 20 m depth, 22 June 1998, collector V. Votyakov (holotype: slide 0132-BK collection "Darwin initiative" housed at the Limnological Institute SB RAS, Irkutsk, Russia; isotype: slide 0132a-BK, *ibid.*).

Placoneis grata Pomazkina sp. nov. (Pomazkina et al., 2018, p. 101, Table 157)

Valves elliptic with rounded ends. Length 22.1–23.0 μm, width 10.7–11.0 μm. Axial area narrow linear; central area small oval, the central stria more distant from neighboring striae. Striae radiate, 10–12 in 10 μm, becoming closer near the apices, 15–16 in 10 μm. Raphe filiform, linear. Proximal raphe endings with pores, terminal fissures bent unilaterally. One elongated stigmoid at the end of one of central striae.

Type :—Russia, Lake Baikal, the southern basin, near the settlement Kultuk, epilithon, st. 42, 20 m depth, 22 June 1998, collector V. Votyakov (holotype: slide 0132-BK collection "Darwin initiative" housed at the Limnological Institute SB RAS, Irkutsk, Russia; isotype: slide 0132a-BK, *ibid.*).

Placoneis ignita Pomazkina & Sherbakova sp. nov. (Pomazkina et al., 2018, p. 101, Table 158)

Valves elliptic-lanceolate with protracted capitate ends. Length 26.0–28.4 μm, width 10.3–11.0 μm. Axial area narrow slightly widening towards the small insignificantly transversely extended central area with alternating short and long striae. Striae radiate, 13–15 in 10 μm. Raphe filiform. Proximal raphe endings with pores, terminal fissures differently curved unilaterally. One round stigma in the central area.

Type :—Russia, Lake Baikal, the southern basin, near the settlement Kultuk, epilithon, st. 42, 20 m depth, 22 June 1998, collector V. Votyakov (holotype: slide 0132-BK collection "Darwin initiative" housed at the Limnological Institute SB RAS, Irkutsk, Russia; isotype: slide 0132a-BK, *ibid.*).

Placoneis insularis Sherbakova & Pomazkina sp. nov. (Pomazkina et al., 2018, p. 102, Table 159)

Valves elliptic-lanceolate with slightly protracted rostrate ends. Length 35.5–36.2 μm, width 14.5–15.0 μm. Axial area narrow slightly widening towards the transversely extended central area with alternating short and long striae. Striae radiate, 9–10 in 10 μm, becoming weakly radiate and closer near the apices, 12–13 in 10 μm. Raphe filiform. Proximal raphe endings with pores, terminal fissures curved unilaterally. One small round stigma in the central area.

Type :—Russia, Lake Baikal, the Olkhon Gates Strait, epilithon, st. 7, 20 m depth, 27 June 1997, collector V. Votyakov (holotype: slide 0017-BK collection "Darwin initiative" housed at the Limnological Institute SB RAS, Irkutsk, Russia; isotype: slide 0017a-BK *ibid.*).

Placoneis ivanii Pomazkina & Rodionova sp. nov. (Pomazkina et al., 2018, p. 102, Table 160)

Valves elliptic-lanceolate with rounded cuneate ends. Length 17.3–19.6 μm, width 10.3–10.4 μm. Axial area narrow slightly widening towards the transversely extended central area with alternating short and long striae. Striae radiate, 13–14 in 10 μm. Raphe filiform. Proximal raphe endings with pores, terminal fissures differently bent unilaterally. One small round stigma is present in the central area.

Type :—Russia, Lake Baikal, Anga Bay, silt and sand, st. 6, 17 m depth, 27 June 1997, collector V. Votyakov (holotype: slide 0014-BK collection "Darwin initiative" housed at the Limnological Institute SB RAS, Irkutsk, Russia; isotype: slide 0015-BK *ibid.*).

Placoneis linearis Pomazkina & Sherbakova sp. nov. (Pomazkina et al., 2018, p. 103, Table 161)

Valves linear-lanceolate with protracted rostrate ends. Length 37.2–38.0 μm, width 13.0–13.5 μm. Axial area narrow near apices, widening towards the transversely extended central area with shortened central striae. Striae radiate, 13–14 in 10 μm, becoming closer near the apices, 15–16 in 10 μm. Raphe filiform, straight. Proximal raphe endings with pores, terminal fissures curved unilaterally. Isolated stigma absent.

Type :—Russia, Lake Baikal, the southern basin, near the settlement Kultuk, epilithon, st. 42, 20 m depth, 22 June 1998, collector V. Votyakov (holotype: slide 0132-BK collection "Darwin initiative" housed at the Limnological Institute SB RAS, Irkutsk, Russia; isotype: slide 0146-BK, *ibid.*).

Placoneis ludmilae Pomazkina & Sherbakova sp. nov. (Pomazkina et al., 2018, p. 103, Table 162)

Valves elliptic-lanceolate with rounded ends. Length 46.0–50.0 μm, width 23.1–22.6 μm. Axial area moderate near apices, widening towards the rounded transversely extended central area with shortened central striae. Striae radiate to strongly radiate, in the center 7–9 in 10 μm, becoming closer near the apices, 9–10 in 10 μm. Raphe filiform, straight. Proximal raphe endings slit-like or with very small pores, terminal fissures fine differently bent to the same side then completed with little triangle depression. Isolated stigma absent.

Type :—Russia, Lake Baikal, south basin, near the settlement Mangutaj, stones and silt, st. 41, 20 m depth, 22 June 1998, collector V. Votyakov (holotype: slide 0138-BK collection "Darwin initiative" housed at the Limnological Institute SB RAS, Irkutsk, Russia; isotype: slide 0139-BK, *ibid.*).

Placoneis magna Pomazkina & Sherbakova sp. nov. (Pomazkina et al., 2018, p. 104, Table 163)

Valve elliptic-lanceolate with protracted rostrate ends. Length 67.7 μm, width 30.6 μm. Axial area narrow slightly becoming wider towards the rounded transversely extended central area with alternating short and long striae. Striae radiate, spaced, 6–7 in 10 μm. Raphe filiform, uneven. Proximal raphe endings with T-shaped pores, terminal fissures differently bent unilaterally. Isolated stigma absent.

Type :—Russia, Lake Baikal, the southern basin,

near the settlement Kultuk, epilithon, st. 42, 20 m depth, 22 June 1998, collector V. Votyakov (holotype: slide 0132-BK collection "Darwin initiative" housed at the Limnological Institute SB RAS, Irkutsk, Russia; isotype: slide 0132c-BK, *ibid.*).

Placoneis mira Pomazkina & Rodionova sp. nov. (Pomazkina et al., 2018, p. 104, Table 165)

Valves elliptic-lanceolate with protracted capitate ends. Length 25.0–27.0 μm, width 9.0–9.7 μm. Axial area narrow; central area small transversely extended with alternating short and long striae. Striae strongly radiate, 15–16 in 10 μm, becoming closer near the apices, 18 in 10 μm. Raphe filiform, linear. Proximal raphe endings with pores, terminal fissures differently bent unilaterally. Isolated stigma absent.

Type :—Russia, Lake Baikal, the southern basin, near the settlement Kultuk, epilithon, st. 42, 20 m depth, 22 June 1998, collector V. Votyakov (holotype: slide 0132-BK collection "Darwin initiative" housed at the Limnological Institute SB RAS, Irkutsk, Russia; isotype: slide 0132c-BK, *ibid.*).

Placoneis mollis Pomazkina & Rodionova sp. nov. (Pomazkina et al., 2018, p. 105, Table 167)

Valves elliptic-lanceolate with slightly protracted cuneate ends. Length 23.0–24.0 μm, width 7.0–9.0 μm. Axial area narrow; central area small insignificantly transversely extended with alternating short and long striae. Striae radiate, 14–15 in 10 μm, becoming closer near the apices, 19–20 in 10 μm. Raphe filiform, linear. Proximal raphe endings with pores, terminal fissures differently bent unilaterally. One stigma in the central area.

Type :—Russia, Lake Baikal, the southern basin, near the settlement Kultuk, epilithon, st. 42, 20 m depth, 22 June 1998, collector V. Votyakov (holotype: slide 0132-BK collection "Darwin initiative" housed at the Limnological Institute SB RAS, Irkutsk, Russia; isotype: slide 0132c-BK, *ibid.*).

Placoneis navicula Pomazkina & Sherbakova sp. nov. (Pomazkina et al., 2018, p. 106, Table 168)

Valve elliptic-lanceolate with protracted rostrate ends. Length 46.9 μm, width 19.1 μm. Axial area narrow; central area small transversely extended with shortened central striae. Striae radiate, 7–8 in 10 μm. Raphe filiform, linear. Proximal raphe endings slightly widened, terminal fissures differently curved unilaterally. Isolated stigma absent.

Type :—Russia, Lake Baikal, the Cape Krestovskij, stones and silt, st. 5, 20 m depth, 27 June1997, collector V. Votyakov (holotype: slide 0011-BK collection "Darwin initiative" housed at the Limnological Institute SB RAS, Irkutsk, Russia; isotype: slide 0012-BK *ibid.*).

Placoneis paragelegma Pomazkina & Rodionova sp. nov. (Pomazkina et al., 2018, p. 106, Table 169)

Valves elliptic-lanceolate with slightly protracted rostrate ends. Length 21.4–23.0 μm, width 7.8–8.0 μm. Axial area narrow slightly widening to the small insignificantly transversely extended central area with alternating short and long striae. Striae radiate, 12–13 in 10 μm, becoming closer near the apices, 15–16 in 10 μm. Raphe filiform, linear. Proximal raphe endings with pores, terminal fissures differently curved unilaterally. One stigma in the central area.

Type :—Russia, Lake Baikal, the Olkhon Gates Strait, the Cape Otto-Khushin, epilithon, st. 53, 20 m depth, 25 June 1998, collector V. Votyakov (holotype: slide 0183-BK collection "Darwin initiative" housed at the Limnological Institute SB RAS, Irkutsk, Russia; isotype: slide 0182-BK, *ibid*).

Placoneis parvula Pomazkina & Rodionova sp. nov. (Pomazkina et al., 2018, p. 107, Table 171)

Valves elliptic with protracted capitate ends. Length 16.6–18.0 μm, width 6.3–6.5 μm. Axial area narrow linear slightly widening to the small insignificantly transversely extended central area with alternating short and long striae. Striae radiate, 16 in 10 μm. Raphe filiform, linear. Proximal raphe endings with pores, terminal fissures differently curved unilaterally. One stigma inon the central area.

Type :—Russia, Lake Baikal, the southern basin, near the settlement Kultuk, epilithon, st. 42, 20 m depth, 22 June 1998, collector V. Votyakov (holotype: slide 0132-BK collection "Darwin initiative" housed at the Limnological Institute SB RAS, Irkutsk, Russia; isotype: slide 0132a-BK, *ibid.*).

Placoneis paucimarensis Rodionova & Pomazkina sp. nov. (Pomazkina et al., 2018, p. 108, Table 172)

Valves elliptic-lanceolate with slightly protracted rostrate ends. Length 24.1–27.0 μm, width 10.0–11.0 μm. Axial area narrow linear; the central area small, oval insignificantly transversely extended central area with alternating short and long striae. Striae strongly radiate, 12–13 in 10 μm. Raphe filiform, linear. Proximal raphe endings with pores, terminal fissures differently curved unilaterally. An elongated stigmoid at the end of the central shortened stria.

Type :—Russia, Lake Baikal, the Olkhon Gates Strait, the Cape Khara-Khulun, epilithon, st. 51, 20 m depth, 25 June 1998, collector V. Votyakov (holotype: slide 0176-BK collection "Darwin initiative" housed at the Limnological Institute SB RAS, Irkutsk, Russia; isotype: slide 0177-BK, *ibid*).

Placoneis radialis Pomazkina & Rodionova sp. nov. (Pomazkina et al., 2018, p. 108, Table 173)

Valves elliptic-lanceolate with slightly protracted rostrate ends. Length 24.2–27.6 μm, width 9.3–10.0 μm. Axial area narrow slightly widening to the small transversely extended central area with alternating short and long striae. Striae radiate, 13–15 in 10 μm, becoming strongly radiate and closer near the apices, 18–24 in 10 μm. Raphe filiform, undulated near the apices. Proximal raphe endings with pores, terminal fissures differently rounded to the same side. Two or more (up to 5) of small round stigmata in the central area.

Type :—Russia, Lake Baikal, the southern basin, near the settlement Kultuk, epilithon, st. 42, 20 m depth, 22 June 1998, collector V. Votyakov (holotype: slide 0132-BK collection "Darwin initiative" housed at the Limnological Institute SB RAS, Irkutsk, Russia; isotype: slide 0132a-BK, *ibid.*).

Placoneis radialis* var. *producta Pomazkina &

Rodionova var. nov. (Pomazkina et al., 2018, p. 109, Table 174)

Valves elliptic-lanceolate with protracted rostrate ends. Length 29.8–38.4 μm, width 8.3–12.3 μm. Axial area narrow slightly widening to the small transversely extended central area with alternating short and long striae. Striae radiate, 12–17 in 10 μm, becoming strongly radiate and closer near the apices, 20–25 in 10 μm. Raphe filiform, undulated near the apices. Proximal raphe endings straight with pores, terminal fissures differently curved to the same side. Two or more stigmata (up to 7) of small round stigmata in the central area.

Type :—Russia, Lake Baikal, the southern basin, near the settlement Kultuk, epilithon, st. 42, 20 m depth, 22 June 1998, collector V. Votyakov (holotype: slide 0132-BK collection "Darwin initiative" housed at the Limnological Institute SB RAS, Irkutsk, Russia; isotype: slide 0132a-BK, *ibid.*).

Placoneis regionalis Pomazkina & Sherbakova sp. nov. (Pomazkina et al., 2018, p. 109, Table 175)

Valve elliptic-lanceolate with cuneate rounded ends. Length 31.9 μm, width 19.3 μm. Axial area narrow; the central area small oval, transversely extended with shortened striae. Striae radiate, 9–10 in 10 μm. Raphe filiform, linear. Proximal raphe endings with elongated teardrop-shaped pores, terminal fissures differently curved unilaterally. Raphe sternum is contoured on either side by narrow deep depression interrupted near the central and apical areas, adjoining to striae.

Type :—Russia, Lake Baikal, the Olkhon Gates Strait, epilithon, st. 7, 20 m depth, 27 June 1997, collector V. Votyakov (holotype: slide 0017-BK collection "Darwin initiative" housed at the Limnological Institute SB RAS, Irkutsk, Russia; isotype: slide 0017a-BK *ibid.*).

Placoneis rhombea Pomazkina & Rodionova sp. nov. (Pomazkina et al., 2018, p. 110, Table 176)

Valve rhombic with cuneate rounded ends. Length 16.6 μm, width 8.2 μm. Axial area narrow, linear; the central area small, transversely extended with alternating short and long striae. Striae radiate, 14 in 10 μm. Raphe filiform, linear. Proximal raphe endings straihgt, terminal fissures differently curved unilaterally.

Type :—Russia, Lake Baikal, Peschanaya Bay, small stones, st. 3, 20 m depth, 26 June1997, collector V. Votyakov (holotype: slide 0007-BK collection "Darwin initiative" housed at the Limnological Institute SB RAS, Irkutsk, Russia; isotype: slide 0007a-BK *ibid.*).

Placoneis septentrionalis Pomazkina & Rodionova sp. nov. (Pomazkina et al., 2018, p. 110, Table 178)

Valve wide elliptic-lanceolate with shortly protracted rostrate ends. Length 40.7 μm, width 18.6 μm. Axial area broad; the central area small nearly indistinct with shortened striae. Striae radiate, 8–9 in 10 μm, becoming closer near the apices, 14–15 in 10 μm. Raphe filiform, slightly undulate. Proximal raphe endings with pores, terminal fissures differently curved unilaterally.

Type :—Russia, Lake Baikal, northern basin, near the Cape Elokhin, epilithon, st. 12, 20 m depth, 29 June 1997, collector V. Votyakov (holotype: slide 0040-BK collection "Darwin initiative" housed at the Limnological Institute SB RAS, Irkutsk, Russia; isotype: slide 0041-BK, *ibid.*).

Placoneis simplex Pomazkina & Rodionova sp. nov. (Pomazkina et al., 2018, p. 111, Table 179)

Valves elliptic with cuneate widely rounded ends. Length 16.9–18.0 μm, width 8.2–9.0 μm. Axial area narrow, linear; the central area small transversely extended with alternating short and long striae. Striae radiate, 14–15 in 10 μm. Raphe filiform, linear. Proximal raphe endings with elongated teardrop-shaped pores, terminal fissures differently curved unilaterally.

Type :—Russia, Lake Baikal, Peschanaya Bay, small stones, st. 3, 20 m depth, 26 June1997, collector V. Votyakov (holotype: slide 0007-BK collection "Darwin initiative" housed at the Limnological Institute SB RAS, Irkutsk, Russia; isotype: slide 0007a-BK *ibid.*).

Placoneis solaris Pomazkina, Rodionova & Sherbakova sp. nov. (c. 111, Table 180)

Valves elliptic-lanceolate with more or less protracted rostrate ends. Length 23.1–25.0 μm, width 8.1–9.0 μm. Axial area narrow slightly widening to the small nearly transversely extended central area with alternating short and long striae. Striae radiate, in the center12 in 10 μm, becoming closer near the apices, 20 in 10 μm. Raphe filiform, linear. Proximal raphe endings with pores slightly bent in the same direction as the differently curved terminal fissures. Round small stigma in the central area.

Type :—Russia, Lake Baikal, Anga Bay, silt and sand, st. 6, 17 m depth, 27 June 1997, collector V. Votyakov (holotype: slide 0014-BK collection "Darwin initiative" housed at the Limnological Institute SB RAS, Irkutsk, Russia; isotype: slide 0015-BK *ibid.*).

Placoneis vadosa Pomazkina & Rodionova sp. nov. (Pomazkina et al., 2018, p. 112, Table 181)

Valves elliptic-lanceolate with protracted capitate ends. Length 15.6–17.8 μm, width 7.2–8.0 μm. Axial area narrow; the central area small, weakly transversely extended with alternating short and long striae. Striae radiate, 14–16 in 10 μm. Raphe filiform, linear. Proximal raphe endings with pores, terminal fissures widely rounded unilaterally.

Type :—Russia, Lake Baikal, the Olkhon Gates Strait, the Cape Otto-Khushin, epilithon, st. 53, 20 m depth, 25 June 1998, collector V. Votyakov (holotype: slide 0183-BK collection "Darwin initiative" housed at the Limnological Institute SB RAS, Irkutsk, Russia; isotype: slide 0182-BK, *ibid*)

Placoneis vladimiri Pomazkina sp. nov. (Pomazkina et al., 2018, p. 112, Table 182)

Valve elliptic-lanceolate with cuneate ends. Length 45.0 μm, width 19.7 μm. Axial area narrow; the central area small, transversely extended with shortened striae. Striae radiate, 8–9 in 10 μm. Raphe filiform, linear at the center, becoming uneven closer to apices. Proximal raphe endings with pores, terminal fissures differently curved unilaterally.

Type :—Russia, Lake Baikal, Anga Bay, silt and sand, st. 6, 17 m depth, 27 June 1997, collector V. Votyakov (holotype: slide 0014-BK collection "Darwin

initiative" housed at the Limnological Institute SB RAS, Irkutsk, Russia; isotype: slide 0015-BK *ibid.*).

Placoneis vladimiri* var. *diminuta Pomazkina var. nov. (Pomazkina et al., 2018, p. 113, Table 183)

Valves elliptic-lanceolate with cuneate ends. Length 35.0–37.0 μm, width 19.0–19.7 μm. Axial area wide; the central area rounded, transversely extended with alternating short and long striae. Striae radiate, 8–9 in 10 μm. Raphe filiform, uneven. Proximal raphe endings with pores, terminal fissures differently curved unilaterally.

Type :—Russia, Lake Baikal, Anga Bay, silt and sand, st. 6, 17 m depth, 27 June 1997, collector V. Votyakov (holotype: slide 0014-BK collection "Darwin initiative" housed at the Limnological Institute SB RAS, Irkutsk, Russia; isotype: slide 0015-BK *ibid.*).

Placoneis witkowskii* var. *baicalensis Pomazkina & Sherbakova var. nov. (Pomazkina et al., 2018, p. 113, Table 184)

Valves elliptic-lanceolate with protracted capitate ends. Length 16.1–18.0 μm, width 4.2–7.0 μm. Axial area narrow; the central area nearly transversely extended with alternating short and long striae. Striae radiate, 16–17 in 10 μm. Raphe filiform, uneven. Proximal raphe endings with pores, terminal fissures differently curved unilaterally.

Type :—Russia, Lake Baikal, the Olkhon Gates Strait, the Cape Otto-Khushin, epilithon, st. 53, 20 m depth, 25 June 1998, collector V. Votyakov (holotype: slide 0183-BK collection "Darwin initiative" housed at the Limnological Institute SB RAS, Irkutsk, Russia; isotype: slide 0184-BK, *ibid.*).

Genus Polygonaria Rodionova, Pomazkina & Sherbakova gen.nov.

Type generic: ***Polygonaria wislouchii*** (Skvortzow & Meyer) Rodionova, Pomazkina & Sherbakova comb. nov. (Pomazkina et al., 2018, p. 115, Table 186)

Cells biraphid, "naviculoid". Characters of the chloroplast is not yet known. Valves isopolar, widely-linear. Valve ends slightly protracted, cuneate. External axial area wide; the central area oval, asymmetrically expended. Raphe filiform, weakly lateral. Proximal raphe endings with hooks bent in one direction. Terminal fissures rounded unilaterally. Striae punctated, parallel in the center, becoming slightly radial towards apices, composed of rounded to transapically widened oval areolae, irregularly arranged in the striae. Internally, proximal raphe endings slit-like, subtly bent unilaterally, distal raphe endings with helictoglossae. Areolae in striae also irregular, rounded to oval, open.

Polygonaria wislouchii (Skvortzow & Meyer) Rodionova, Pomazkina & Sherbakova comb. nov. (Pomazkina et al., 2018, p. 115, Table 186)

Basionym: *Navicula wislouchii* Skvortzow & Meyer 1928, p. 20, pl. 1, fig.72.

Valves widely-linear with slightly protracted, cuneate ends. Length 61.0–81.0 μm, width 16.8–20.7μm. Axial area wide; the central area nearly indistinct, asymmetrically expended. Raphe filiform, weakly lateral. Proximal raphe endings hooked, bent in one direction. Terminal fissures both rounded in the side opposite to the side the proximal endings bent. Areolae irregular in striae forming uneven hyaline lines on the valve surface. Striae punctated, parallel in the valve center, becoming radial towards apices, 11–13 in 10 μm.

Acknowledgements

We are very grateful to Wolf-Henning Kusber for his valuable help in preparing this article. This work was supported by the project 345-2019-0001 FASO Russia.

References

Cleve P.T. 1895. Synopsis of the naviculoid diatoms. Kongliga Svenska Vetenskaps-Akademiens Handlingar [Royal Swedish Academy of Sciences Documents] 27: 1–219.

Grunow A. 1860. Über neue oder ungenügend gekannte Algen. Erste Folge, Diatomeen, Familie Naviculaceen. Verhandlungen der Kaiserlich-Königlichen Zoologisch-Botanischen Gesellschaft [Negotiations of the Imperial-Royal Zoological-Botanical Society] 10: 503 – 582. (In German)

Pomazkina G.V., Rodionova E.V., Sherbakova T.A. 2018. Benthic diatom algae of the family Naviculaceae of Lake Baikal. Novosibirsk: Nauka. (In Russian)

Skabitchevsky A.P. 1936. New and interesting diatoms from the Northern Baikal. Botanicheskiy Zhurnal SSSR [Botanical Journal of the USSR] 21: 705 – 719. (In Russian)

Skvortzow B.W. 1937. Bottom diatoms from Olhon Gate of Baikal Lake, Siberia. Philippine Journal of Science 62: 293–377.

Skvortzow B.W., Meyer C.I. 1928. A contribution to the diatoms of Lake Baikal. Proceedings of the Sungaree River Biological Station 1: 1–55.

International code of nomenclature for algae, fungi, and plants (Shenzhen Code) adopted by the Nineteenth International Botanical Congress Shenzhen, China, July 2017. Regnum Vegetabile 159. 2018. In: Turland N.J., Wiersema J.H., Barrie F.R., Greuter W., Hawksworth D.L., Herendeen P.S., Knapp S., Kusber W.-H., Li D.-Z., Marhold K., May T.W., McNeill J., Monro A.M., Prado J., Price M.J., Smith G.F. (Eds.). Glashütten: Koeltz Botanical Books. DOI: doi.org/10.12705/Code.2018